NAVAL SHIP RESEARCH AND DEVELOPMENT CENTER
Bethesda, Maryland 20034

DYNAMIC ANALYSIS OF FRAME AND PLATE STRUCTURES WITH GEOMETRIC AND MATERIAL NONLINEARITIES

by

Theodore G. Toridis

APPROVED FOR PUBLIC RELEASE: DISTRIBUTION UNLIMITED

STRUCTURES DEPARTMENT
RESEARCH AND DEVELOPMENT REPORT

May 1973 Report 3988

DYNAMIC ANALYSIS OF FRAME AND PLATE STRUCTURES
WITH GEOMETRIC AND MATERIAL NONLINEARITIES

The Naval Ship Research and Development Center is a U. S. Navy center for laboratory effort directed at achieving improved sea and air vehicles. It was formed in March 1967 by merging the David Taylor Model Basin at Carderock, Maryland with the Marine Engineering Laboratory at Annapolis, Maryland.

Naval Ship Research and Development Center

Bethesda, Md. 20034

MAJOR NSRDC ORGANIZATIONAL COMPONENTS

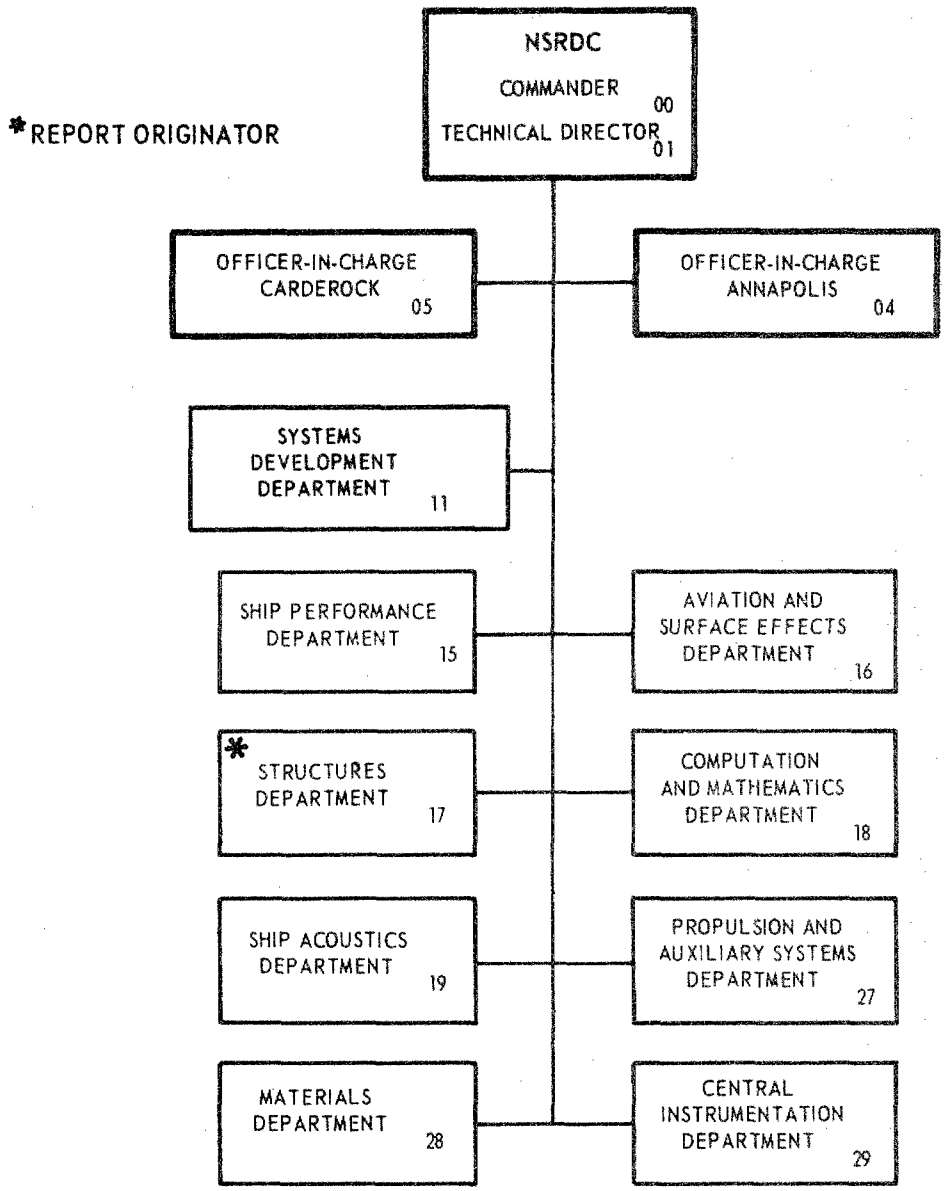

NDW-NSRDC 3960/44 (REV. 8/71)

GPO 917-872

DEPARTMENT OF THE NAVY

NAVAL SHIP RESEARCH AND DEVELOPMENT CENTER

BETHESDA, MD. 20034

DYNAMIC ANALYSIS OF FRAME AND PLATE STRUCTURES WITH GEOMETRIC AND MATERIAL NONLINEARITIES

by

Theodore G. Toridis

May 1973

Report 3988

TABLE OF CONTENTS

		Page
ABSTRACT		1
ADMINISTRATIVE INFORMATION		2
I.	INTRODUCTION	3
1.1	General and Review of Literature	3
1.2	Object and Scope	6
II.	BRIEF REVIEW OF BASIC CONCEPTS	8
2.1	Brief Review of Basic Concepts	8
2.2	Stiffness and Inertial Properties of Elements	10
2.3	Effect of Geometric and Material Nonlinearities	12
2.4	Transformation Matrices	13
2.5	The Basic Dynamical Equation	14
III.	THE BEAM ELEMENT	17
3.1	Strain Energy Expression for a Beam Element	17
3.2	Stiffness and Mass Matrices for a Beam Element	21
IV.	THE RECTANGULAR PLATE ELEMENT	24
4.1	The General Strain Energy Expression	24
4.2	Coordinate Systems and Degrees of Freedom	29
4.3	Stiffness Matrix for In-Plane Action	30
4.4	Mass Matrix for In-Plane Action	35
4.5	Stiffness Matrix for Bending Action	36
4.6	Mass Matrix for Bending Action	39
4.7	The Complete Form of Stiffness and Mass Matrices	41
4.8	Geometrical Stiffness Matrix	44
4.9	Transformation to the Global Coordinate System	49
V.	PROCEDURE OF NUMERICAL ANALYSIS AND THE SOFTWARE	51
5.1	General Procedure of Numerical Analysis	51
5.2	General Remarks	59
5.3	Plastic Behavior of In-Plane Stressed Plate Element	62
5.4	The Software Package	65

VI. COMPUTER ANALYSIS OF TYPICAL STRUCTURES--SUMMARY OF NUMERICAL RESULTS ..... Page 69

6.1 First Order Static Analysis of a Plate 69
6.2 Free Vibration Analysis of a Simply Supported Plate 70
6.3 Second Order Static Analysis of a Square Plate 73
6.4 First and Second Order Static and Elastic Dynamic Analysis of a Beam-Plate Assemblage. 75
6.5 Square Plate Subjected to a Lateral Load and In-Plane Compressive Forces 79

6.6 First Order Elastic and Plastic Dynamic Analysis of a Plate Structure 84
6.7 Elastic and Plastic Dynamic Analysis of a Plane Frame 86
6.8 Elastic and Plastic Dynamic Analysis of a Three-Dimensional Str cture Consisting of In-Plane Stressed Plate Elements 88

VII. SUMMARY AND CONCLUSIONS 91

ACKNOWLEDGMENTS 93

APPENDIX A--Strain and Stress Components due to In-Plane Action 111

APPENDIX B--Simplified Flowchart of the Modified GWU-FAP Program 117

APPENDIX C--Typical Input Format 120

REFERENCES 123

LIST OF FIGURES

Figure 1 - Typical Beam Element 94

Figure 2 - Plate Element with In-Plane and Bending Actions 95

Figure 3 - Plate Element with In-Plane Action Only 95

Figure 4 - Plate Element with Bending Action Only 96

Figure 5 - Element Displacements Corresponding to In-Plane Action 96

Page

Figure 6 - Element Displacements Corresponding to Bending Action 97

Figure 7 - General Stress-Strain Curve 97

Figure 8 - Trilinear Stress-Strain Curve 98

Figure 9 - In-Plane Stressed Plate Element with 8 D.O.F. 98

Figure 10 - Comparison of Central Deflections for a Clamped Plate with Concentrated Load P at Center 99

Figure 11 - Force-Deformation Relationships for Clamped and Simply Supported Square Plates 100

Figure 12 - Force-Deformation Curves for First and Second Order Static Analysis of a Plate Supported by Edge Beams 101

Figure 13 - First and Second Order Elastic Dynamic Analysis of a Plate Supported by Edge Beams--Time-History of Center Deflection for Load Intensities of 1 and 10 lb/in^2 102

Figure 14 - Second Order Elastic Dynamic Analysis of a Plate Supported by Edge Beams--Time-History of Center Deflection for Load Intensities of 1,2,5 and 10 lb/in^2 103

Figure 15 - First Order Elastic Dynamic Analysis of Simply Supported Square Plate with Lateral and In-Plane Compressive Forces--Time History of Center Deflection 104

Figure 16 - Plate Structure Subject to In-Plane Action ... 105

Figure 17 - Elastic and Plastic Dynamic Analysis of Plate Structure--Time-History at Deflection of Node C 106

Figure 18 - Plane Frame Subjected to Dynamic Loads 107

Figure 19 - Elastic and Plastic Dynamic Analysis of Plane Frame--Time-History of Deflection in the Direction of F_V 108

Figure 20 - Three-Dimensional Structure Consisting of In-Plane Stressed Plate Elements 109

Page

Figure 21 - Elastic and Plastic Dynamic Analysis of 3-D Structure Composed of In-Plane Stressed Plate Elements--Time-History of Deflection in the Direction of F 110

LIST OF TABLES

Table 1 Definition of Symbols Appearing in Equation (54) 34

Table 2 Definition of Symbols Appearing in Equations (60) - (62) 39

Table 3 Static Analysis of Simply Supported Plate--Comparison of Central Deflection Between Finite Element and Exact Methods .. 70

Table 4 Free Vibration of Simply Supported Square Plate--Comparison of Fundamental Frequencies Between Finite Element and Exact Methods 71

Table 5 Free Vibration of Simply Supported Square Plate--Comparison of Fundamental Normal Mode Shapes Between Finite Element and Exact Methods 72

Table 6 Free Vibration of Simply Supported Square Plate--Comparison of Higher Frequencies of Vibration Between Finite Element and Exact Methods 73

Table 7 Comparison of Methods Used in Solving the Nonlinear Problem of a Square Plate Clamped at Four Edges with a Concentrated Load at the Center 74

Table 8 First Order Static Analysis of a Square Plate with Four Edge Beams--Comparison of Results with Known Solutions 76

Table 9 First Order Static Analysis of a Simply Supported Square Plate Under a 1000 lb. Load at Center and Uniform Compressive Forces in the X-Direction--Comparison of Central Deflection Between Finite Element and Exact Methods 81

Page

Table 10 - Second Order Static Analysis of a Simply Supported Square Plate with P = 1000 lb at the Center and Uniform Compressive Forces N_x = 1000 lb/in--Comparison of Central Deflection for 4 and 16 Element Idealizations 82

Table 11 - Second Order Static Analysis of a Simply Supported Square Plate with Varying Lateral and Compressive Forces--Comparison of Central Deflections 83

ABSTRACT

The objective of this study is the development of a procedure for determining the large dynamic response of structural systems consisting of beam and rectangular plate elements. The analysis takes into account both geometrical and material nonlinearities. The general approach to the problem is based on the finite element method and the use of displacement interpolation functions. The energy expressions for both the beam and plate elements are obtained and are used to generate the stiffness and mass matrices of the elements. Also, the geometric stiffness matrices are derived which account for the effect of geometric nonlinearities. Plastic deformations are taken into account by means of an incremental theory of plasticity coupled with the concept of initial strain.

A computer program is developed for the analysis of structures which consist of beam and rectangular plate elements. This program may be used to perform an elastic static, elastic dynamic, or plastic dynamic analysis with or without the inclusion of geometric nonlinearity effects. It can also be used to perform a free vibration analysis of a structure, leading to the natural frequencies and modes of vibration. The computer program is used in this study to obtain the solution to several example structures

subjected to static or dynamic loads. Results indicate that both geometric and material nonlinearities have an important effect in the deformation of structures composed of beam and plate elements.

ADMINISTRATIVE INFORMATION

The work reported herein was funded by the Naval Ship Research and Development Center Independent Research Program administered under the direction of Dr. A. Powell, Technical Director, Naval Ship Research and Development Center.

I. INTRODUCTION

1.1 General and Review of Literature

Large deformations of a structural system give rise to a nonlinear phenomenon. This leads to nonlinear equations which immediately render classical methods of analysis inapplicable. Among many approaches to the solution of the problem, the finite element method has been the one most commonly used in recent years. The structure is first idealized as an assembly of discrete structural elements, and some assumptions on the displacement distribution with respect to these elements are then made. The complete formulation is obtained by combining these individual approximate displacement distributions in a manner which satisfies the force-equilibrium and displacement compatibility relations at the junctions of these elements. Numerical methods of analysis may then be used to solve the equations. In such a formulation of the problem, matrix algebra is appropriately utilized and conveniently lends itself to solution by means of a digital computer.

In dealing with large deformations of structures two types of nonlinearities have to be taken into account, i.e., geometrical and material nonlinearities. The concept of using the finite element approach in solving geometrically nonlinear structures was initially advanced by Turner et al (1). Martin (2) reviewed the work on geometrically nonlinear problems and presented geometric stiffness matrices for a number of structural elements,

while Oden (3) gave special attention to incremental formulations of these problems. Oden also studied the problem from dual viewpoints: first, the approach in which nonlinear stiffness relations with complete generality were generated and solved by the Newton-Raphson method. Secondly, the approach in which the structural problem was viewed as one of minimizing a scalar-valued function defining the total potential energy of the system of n-variables.

The behavior of geometrically nonlinear frames was the subject of several investigations, such as (4-7). The problem of large deformation of plate structures was previously investigated by Timoshenko (8), who considered the interaction of bending and in-plane (membrane) action. Greene (9), and Kapur (10) derived separately the stiffness properties for a rectangular plate for various static loading conditions. Murray and Wilson (11) studied the large deflection of plates by using triangular elements in which in-plane as well as out-of-plane displacements were permissible. Brebbia and Connor (12) investigated the same problem by initially setting up the stiffness matrix for the structure and then solving the system of force-displacement equations using a limited number of load steps, and followed by corrections based on the Newton-Raphson method.

Zienkiewicz and Cheung (13) analyzed a plate with edge beams subjected to static loading of relatively small magnitude, and compared the finite element solution to the classical solution given by Timoshenko (8). The elastic-plastic analysis of plates with edge beams was considered by McNeice (14). Weaver et.al. (15)

considered a rectangular plate with in-plane and torsional action. Timoshenko (16) studied the problem of the small deformation of a rectangular plate subject to a concentrated lateral load at center and uniformly compressed in the in-plane directions.

In recent years, there have been other significant contributions, for example (17,18). Furthermore, the problem of material nonlinearity as related to structural systems has received increased attention by several investigators, such as (19-21). In most of these investigations, plastic behavior beyond the elastic range has been determined by the use of the Prandtl-Reuss equations (22) of the classical plasticity theory. Concurrently, two distinct methods of incorporating plastic behavior into a finite element analysis have been developed, and are referred to in the literature as the "initial strain" and the "tangent modulus" methods (20). Such techniques are very suitable in dealing with problems that involve both geometric and material nonlinearities.

Very few solutions to structural dynamics problems have been reported in the literature which aim at determining the complete response of a structural system, including the elastic and inelastic deformations, as well as the effect of geometric nonlinearities. In this connection Farhoomand, Iverson, and Wen (23) developed a method of dynamic analysis of space frames considering the combined effect of material and geometric nonlinearities. In their analysis, the mass properties of the structural components were lumped at the joints and the material

was assumed to be elastic-perfectly plastic, with inelastic deformations taking place at member ends only. Likewise, Toridis et al (24,25) presented an incremental finite element procedure for the dynamic analysis of framed structures with both geometric and material nonlinearities. Their solution was based on the concept of initial strain and the use of the geometric stiffness matrix for a beam element. Strain hardening and hysteretic effects were also taken into account.

More recently, McNamara and Marcal (26) developed a numerical procedure aimed at the use of the finite element method to analyze large elastic-plastic deformations of structures under a variety of dynamic loadings. In their procedure, the basic equations for nonlinear finite element analysis were linearized based on an incremental process and the addition of two error terms to account for discretization errors. It was shown that the corrected incremental equations, in the form used in their analysis give stable and accurate solutions even with relative large time increments.

1.2 Object and Scope

The objective of the present investigation has been the development of a procedure for determining the large dynamic response of structural systems consisting of beam and rectangular plate elements. The analysis takes into account both geometrical and material nonlinearities. The general approach to the problem is based on the finite element method and the incremental plasticity theory coupled with the use of the geometric stiffness matrices of the elements to account for significant changes in the geometry of

the structure. From the practical viewpoint, one of the additional objectives of this study has been the development of a general purpose computer program for the analysis of the type of structures under consideration. The computer program is designed with sufficient flexibility for possible use with various classes of structural elements. Presently, the classes of elements that have been incorporated into the program consist of two types of beam elements corresponding to plane or three-dimensional action, and five types of thin rectangular plate elements corresponding to membrane and/or bending and twisting action. The beam and plate elements may be used alone or in combination (beam-plate assemblage) to perform a static, elastic dynamic or free vibration analysis of a structural system. Likewise, a plastic dynamic analysis may be performed, but the type of plate elements that can be used for this purpose is presently restricted to rectangular elements with membrane (in-plane) action only.

II. BRIEF REVIEW OF BASIC CONCEPTS

The use of the finite element method in solving structural problems is well known. For comprehensiveness, related topics such as Castigliano's theorem, the strain energy expression, and the stress-strain relationship for the problem under consideration are briefly discussed. The concept of the direct stiffness method is next outlined and is followed by the formulation of the dynamical expressions governing the behavior of the system. Temperature is assumed to be constant throughout all the derivations.

2.1 Brief Review of Basic Concepts

2.1.1 Strains and Displacements

The structure under study is first partitioned into a set of idealized elements. For each idealized element, the interior displacements [u] are assumed to be expressible in terms of the nodal displacements [U] by the matrix equation

$$[u] = [a]\ [U] \tag{1}$$

where [a] = [a(x,y,z)] is a rectangular matrix and a function of the position coordinates. The matrix [a] is usually determined by assuming the form of the displacement distribution. This displacement distribution must be continuous and should preferably satisfy compatibility of deflections and slopes on the boundaries of the elements. The satisfaction of the stress-equilibrium equations is also desirable. It is thus clear that in general,

only approximate expressions for the matrix [a] are expected since the latter depends on the complete displacement distribution of the entire structure.

Since the total strains [ε] are functions of the displacements [u], which in turn are functions of [U], the following matrix equation is valid:

$$[\varepsilon] = [b]\ [U] \tag{2}$$

where [b] is again a rectangular matrix.

2.1.2 Castigliano's Theorem, Strain Energy Expression Stress-Strain Relationship

The well-known Castigliano's Theorem (27) states that if a structure is subjected to a system of external forces $S_1, S_2, \ldots, S_n$ and if only one virtual displacement δu_γ is applied in the direction of the load S_γ, and if V represents the strain energy of the system, then

$$S_\gamma = \frac{\partial V}{\partial u_\gamma}. \tag{3}$$

If u_γ is identified as a nodal displacement and if the index is varied from $\gamma = 1$ to $\gamma = n$, then the following matrix equation may be obtained from this set of n equations

$$[S] = \frac{\partial V}{\partial [U]}. \tag{4}$$

The strain energy, V, shown in Eq. (4), may be expressed in matrix notation as (dv represents an infinitesimal volume element)

$$V = \frac{1}{2} \int_V [\varepsilon]^T [\sigma]\ dv. \tag{5}$$

The stresses $[\sigma]$ and strains $[\varepsilon]$ shown in Eq. (5) are related by the following equation:

$$[\sigma] = [D]\,[\varepsilon] \tag{6}$$

where [D] is a rectangular matrix, referred to as the "elasticity matrix."

2.2 Stiffness and Inertial Properties of Elements

The concept underlying the direct stiffness method is the determination of the displacements of an idealized structure under some specified external loading by investigating the stiffness properties of individual structural elements which can be used to represent the idealized structure. The displacements will be considered as the unknowns throughout the analysis. The stiffness properties of an individual element may be obtained by substituting Eqs. (2), (6) into Eq. (5), so that

$$V = \frac{1}{2}\int_V [\varepsilon]^T [\sigma]\, dv = \frac{1}{2}\int_V [U]^T ([b]^T [D][b])[U]dv. \tag{7}$$

Differentiating the above equation with respect to the ith nodal displacement and substituting the result into Eq. (4), the following equation is obtained

$$[S] = \frac{\partial V}{\partial [U]} = \left(\int_V ([b]^T[D][b]dv\right)[U]. \tag{8}$$

Defining

$$[K] = \int_V ([b]^T[D][b]dv \tag{9}$$

where [K] represents the elastic stiffness matrix of the element, Eq. (8) now becomes

$$[S] = [K][U] \tag{9a}$$

which is the force-deformation relationship of the element under consideration. It can be observed from Eqs. (8)-(9a) that the stiffness matrix components may be represented as

$$K_{jk} = \frac{\partial^2 V}{\partial U_j \partial U_k} \tag{10}$$

It should also be observed that in view of Eqs. (7) and (9), the strain energy expression V may be represented as

$$V = \frac{1}{2} [U]^T [K] [U] \tag{11}$$

If only one element is used to idealize the structure, Eq. (9a) is the representative equation. However, in the general case of a structure consisting of several elements, the force-deformation relation of all the elements, as given in Eq. (9a), may be appropriately assembled to form the representative equation of the entire system.

In considering the dynamic response of a structure, the inertial properties of the system must first be determined. As shown in Refs. (25) and (27), the mass matrices of the individual elements of the structure may be computed through a process similar to the generation of the stiffness matrices. Again, an integration over the volume of the element is needed, so that, letting [M] represent the element mass matrix

$$[M] = \int_V \rho [a]^T [a] dv \tag{12}$$

where, ρ, represents the mass density of the material.

As in the case of the stiffness matrices, the mass matrices of the individual elements may be assembled appropriately to form the generalized mass matrix for the entire structure.

2.3 Effect of Geometric and Material Nonlinearities

As will be shown later in this report, the effect of significant changes in the geometry of the structure can be accounted for by the inclusion of higher order nonlinear terms in the strain-displacement relations. This, in turn, introduces an additional stiffness matrix K_G, referred to as the "geometric stiffness matrix." In such a case, it has already been demonstrated in Ref. (25) that for a framed structure consisting of beam elements, the strain energy expression given by Eq. (12) takes the form of

$$V = \frac{1}{2} [U]^T ([K] + [K_G]) [U] \tag{13}$$

where, as before, [K] represents the elastic (first order) stiffness matrix of the element defined by Eq. (9), and $[K_G]$ refers to the geometric stiffness matrix.

When inelastic deformations take place, it is assumed (24) that the total strain vector [ε] may be divided into an elastic part $[\varepsilon^e]$ and a plastic part $[\varepsilon^p]$. In turn, the plastic strain vector may be treated as an initial strain vector $[\varepsilon^\circ]$, so that

$$[\varepsilon^e] = [\varepsilon] - [\varepsilon^\circ] \tag{14}$$

In a similar manner, it is assumed that the nodal displacements of the element may be separated into an elastic part $[U^e]$ and plastic or initial part $[U^\circ]$. Furthermore, it is assumed that the interpolation or shape functions chosen to represent the elastic displacement distributions within the elements may also be used to represent the plastic displacement distribution in the elements. Following this approach, it is shown in Refs. (24) and (25) that the effect of the plastic actions occurring in the elements may be represented as equivalent forces acting at the nodal points of the elements. In this manner, the modified equilibrium equations can be easily formulated.

2.4 Transformation Matrices

So far, the discussion has centered on the generation of the stiffness and mass properties of an individual element referred to the local coordinate system of the element. In order to determine the corresponding properties of the entire structure, a global coordinate system must be established. The displacements and corresponding forces of the elements are then transformed to the global coordinate system, prior to the application of the direct stiffness method.

Let $[U]$ and $[S]$ be the element displacements and forces with respect to the local coordinate system, and $[\overline{U}]$ and $[\overline{S}]$ be the same element displacements and forces with respect to the global coordinate system, respectively. Let $[\lambda]$ be the transformation matrix between these two coordinate systems. Then,

$$[U] = [\lambda]\,[\overline{U}]. \tag{15}$$

Additionally, by using the principle of virtual work, the following expression may be written

$$[S] = [\lambda][\bar{S}]. \tag{16}$$

Substitution of these two equations into Eq. (10) yields

$$[\bar{S}] = [\bar{K}][\bar{U}] \tag{17}$$

where

$$[\bar{K}] = [\lambda]^T[K][\lambda] \tag{18}$$

Eq. (17) is analogous to Eq. (10) except that the stiffness matrix of anyone element is now expressed with reference to the global coordinate system.

The element mass matrices may be transformed in a similar manner. Letting $[\bar{M}]$ represent the element mass matrix with respect to the global coordinate system

$$[\bar{M}] = [\lambda]^T[M][\lambda] \tag{19}$$

2.5 The Basic Dynamical Equation

The dynamical equation of the system is derived based on Hamilton's Principle and the calculus of variations. The Hamiltonian function is formed by considering the total kinetic and potential energies of the system. The variation of the integral of the Hamiltonian function between two discrete times t_1 and t_2 is then set equal to zero in accordance with Hamilton's Principle. The basic dynamical equation for the structure under

consideration is then derived by following through some rather tedious mathematical operations, as reported in Refs. (24) and (25). Since details of the various steps involved in this derivation are given in the above references, they will not be repeated here. The resulting expression is in the form given below:

$$[m][\ddot{q}] + ([k] + [k_G])[q] = [F] + [F^\circ] \qquad (20)$$

where

$[m]$ = assembled (generalized) mass matrix.

$[q],[\ddot{q}]$ = generalized displacement and acceleration vectors, respectively.

$[k]$ = assembled (generalized) elastic stiffness matrix.

$[k_G]$ = assembled (generalized) geometric stiffness matrix.

$[F]$ = generalized nodal force vector.

$[F^\circ] = ([k] + [k_G])[q^\circ]$ = equivalent generalized nodal force vector due to plastic strains.

Eq. (20) represents the basic equation governing the dynamic behavior of the entire structure. In considering the effect of significant changes in the geometry of the structure due to large deformations (second order analysis), both the stiffness and mass matrices have to be recomputed at various time intervals, based on the current deformed configuration of the structure. On the other hand, eliminating the matrix $[k_G]$ from Eq. (20) leads to the basic equation for the small deformation (first order) analysis of the structure. Thus, it is clear that the particular expressions

corresponding to the first and second order static, elastic dynamic and plastic dynamic analysis of the structure under consideration may be obtained easily from Eq. (20) by considering only those terms in the equation that are appropriate in each case.

III. THE BEAM ELEMENT

The fundamental relations outlined in the previous chapter form the basis of the present study aimed at analyzing the behavior of a structural system consisting of straight beam and rectangular thin plate elements. In forming these expressions, the properties of the individual elements of the structure must first be derived. In this chapter the force-deformation and inertial properties of a three-dimensional beam member are discussed and the stiffness and mass matrices are presented. The behavior of a rectangular thin plate element is studied in the next chapter.

3.1 Strain Energy Expression for a Beam Element

Consider a typical beam element with an arbitrary orientation in space, as shown in Fig. 1. A set of axes X, Y, Z are chosen to represent a global coordinate system of reference. The element local coordinate axes are x, y, z with the x-axis extending along the axis of the element, and the y, z-axes pointing in the principal directions of the cross section. The set of element nodal (end) displacements and forces are designated by

$$[U] = [U_1, U_2, \ldots, U_{12}] \quad \text{and} \quad [S] = [S_1, S_2, \ldots, S_{12}],$$

respectively.

In order to define the element displacements and forces with respect to the global system of axes, both during the initial and

deformed configurations of the elements, a transformation matrix $[\lambda]$ is utilized (see Eq. (15)). Letting x,y,z represent the current coordinates of an element nodal point (the original coordinates of the nodal point plus the current translational displacements of the point), the transformation relation is expressed as

$$\begin{bmatrix} x \\ y \\ z \end{bmatrix} = [\lambda] \begin{bmatrix} X \\ Y \\ Z \end{bmatrix} \tag{21}$$

in which $[\lambda]$ is represented as a diagonal matrix, so that in partitioned form

$$[\lambda] = \text{diag}\,([T_1],[T_2],[T_3],[T_4]) \tag{22}$$

where

$$[T_1] = [T_2] = [T_3] = [T_4] = \begin{bmatrix} \ell_1 & \ell_2 & \ell_3 \\ m_1 & m_2 & m_3 \\ n_1 & n_2 & n_3 \end{bmatrix} \tag{23}$$

In the above ℓ_i, m_i and n_i are the instantaneous direction cosines of the ith local coordinate axis with reference to the X, Y and Z global axes, respectively.

Let [u] represent the vector of element displacements at any point in the interior of the element with components u_x, u_y and u_z along the x, y and z-directions, respectively. Making use of simple beam theory, [u] can be expressed in terms of the nodal displacement vector [U] as

$$[u] = \begin{bmatrix} u_x \\ u_y \\ u_z \end{bmatrix} = [a]\,[U] \tag{24}$$

where, the transpose of the matrix [a], containing the interpolation (shape) functions, has the form of

$$[a]^T = \begin{bmatrix}
1 - \frac{x}{\ell} & 0 & 0 \\
6\left(\frac{x}{\ell} - \frac{x^2}{\ell^2}\right)\frac{y}{\ell} & 1 - \frac{3x^2}{\ell^2} + \frac{2x^3}{\ell^3} & 0 \\
6\left(\frac{x}{\ell} - \frac{x^2}{\ell^2}\right)\frac{z}{\ell} & 0 & 1 - \frac{3x^2}{\ell^2} + \frac{2x^3}{\ell^3} \\
0 & -\left(1 - \frac{x}{\ell}\right)z & -\left(1 - \frac{x}{\ell}\right)y \\
\left(1 - \frac{4x}{\ell} + \frac{3x^2}{\ell^2}\right)z & 0 & -x + \frac{2x^2}{\ell} - \frac{x^3}{\ell^2} \\
\left(-1 + \frac{4x}{\ell} - \frac{3x^2}{\ell^2}\right)y & x - \frac{2x^2}{\ell} + \frac{x^3}{\ell^2} & 0 \\
\frac{x}{\ell} & 0 & 0 \\
6\left(-\frac{x}{\ell} + \frac{x^2}{\ell^2}\right)\frac{y}{\ell} & \frac{3x^2}{\ell^2} - \frac{2x^3}{\ell^3} & 0 \\
6\left(-\frac{x}{\ell} + \frac{x^2}{\ell^2}\right)\frac{z}{\ell} & 0 & \frac{3x^2}{\ell^2} - \frac{2x^3}{\ell^3} \\
0 & -\frac{xz}{\ell} & -\frac{xy}{\ell} \\
\left(-\frac{2x}{\ell} + \frac{3x^2}{\ell^2}\right)z & 0 & \frac{x^2}{\ell} - \frac{x^3}{\ell^2} \\
\left(\frac{2x}{\ell} - \frac{3x^2}{\ell^2}\right)y & -\frac{x^2}{\ell} + \frac{x^3}{\ell^2} & 0
\end{bmatrix} \tag{25}$$

When large deformations take place, the normal strain component ε_{xx} in the local x-direction contains certain non-linear terms which cannot be neglected. In terms of the element displacements, ε_{xx} may be represented as

$$\varepsilon_{xx} = \frac{\partial u_x}{\partial x} - y\frac{\partial^2 u_y}{\partial x^2} + \frac{1}{2}\left(\frac{\partial u_y}{\partial x}\right)^2 - z\frac{\partial^2 u_z}{\partial x^2} + \frac{1}{2}\left(\frac{\partial u_z}{\partial x}\right)^2 \qquad (26)$$

In this expression the first, second and fourth terms represent the contributions of the axial and bending forces in the usual small deflection theory. The third and fifth terms are approximations to the contributions due to rotations resulting from bending around the z and y-axes, respectively.

In order to obtain initial estimates of the displacements within each increment of loading, the elastic relations based on Hooke's Law may be utilized at the beginning of each time step. The strain energy in a beam element may then be expressed as

$$V = \frac{E}{2}\int_v \varepsilon_{xx}^2\, dv + \frac{G}{2}\int_v \varepsilon_{yz}^2\, dv \qquad (27)$$

where E is the modulus of elasticity. Combining Eqs. (26) and (27)

$$V = \frac{E}{2}\int_v \left[\frac{\partial u_x}{\partial x} - y\frac{\partial^2 u_y}{u_x^2} + \frac{1}{2}\left(\frac{\partial u_y}{\partial x}\right)^2 - z\frac{\partial^2 u_z}{\partial x^2} + \frac{1}{2}\left(\frac{\partial u_z}{\partial x}\right)^2\right]^2 dv$$

$$+ \frac{G}{2}\int_v \left[\left(\frac{\partial u_y}{\partial z} + \frac{\partial u_z}{\partial y}\right)\right]^2 dv \qquad (28)$$

Each individual term in the above brackets can be evaluated based on Eqs. (24) and (25). Substituting the resulting relations into the expression for V, neglecting higher order terms (such as,

$\frac{1}{4}\left(\frac{\partial u_y}{\partial x}\right)^4$, $\frac{1}{4}\left(\frac{\partial u_z}{\partial x}\right)^4$) and performing the indicated integration, Eq. (28) can then be rewritten in the form given previously as Eq. (13).

3.2 Stiffness and Mass Matrices for a Beam Element

Referring to Eq. (13), for a beam element, the elastic matrix [K] and geometric stiffness matrix $[K_G]$ have been derived in Refs. (25) and (27), and are in the form given below.

$$[K] = \begin{bmatrix}
\frac{EA}{\ell} & & & & & & & & & & & \\
0 & \frac{12EI_z}{\ell^3} & & & & & & & & & & \\
0 & 0 & \frac{12EI_y}{\ell^3} & & & & & & & & & \\
0 & 0 & 0 & \frac{GI_x}{\ell} & & & & & & & & \\
0 & 0 & -\frac{6EI_y}{\ell^2} & 0 & \frac{4EI_y}{\ell} & & & & & & & \\
0 & \frac{6EI_z}{\ell^2} & 0 & 0 & 0 & \frac{4EI_z}{\ell} & & & & & & \\
-\frac{EA}{\ell} & 0 & 0 & 0 & 0 & 0 & \frac{AE}{\ell} & & & & & \\
0 & -\frac{12EI_z}{\ell^3} & 0 & 0 & 0 & -\frac{6EI_z}{\ell^2} & 0 & \frac{12EI_z}{\ell^3} & & & & \\
0 & 0 & -\frac{12EI_y}{\ell^3} & 0 & \frac{6EI_y}{\ell^2} & 0 & 0 & 0 & \frac{12EI_y}{\ell^3} & & & \\
0 & 0 & 0 & -\frac{GI_x}{\ell} & 0 & 0 & 0 & 0 & 0 & \frac{GI_x}{\ell} & & \\
0 & 0 & -\frac{6EI_y}{\ell^2} & 0 & \frac{2EI_y}{\ell} & 0 & 0 & 0 & \frac{6EI_y}{\ell^2} & 0 & \frac{4EI_y}{\ell} & \\
0 & \frac{6EI_z}{\ell^2} & 0 & 0 & 0 & \frac{2EI_z}{\ell} & 0 & -\frac{6EI_z}{\ell^2} & 0 & 0 & 0 & \frac{4EI_z}{\ell}
\end{bmatrix} \quad \text{SYMMETRIC} \qquad (29)$$

$$[K]_G = N \begin{bmatrix}
0 & & & & & & & & & & & \\
0 & \frac{6}{5\ell} & & & & & & & & & & \\
0 & 0 & \frac{6}{5\ell} & & & & & & & & & \\
0 & 0 & 0 & \frac{I_x}{A\ell} & & & & & & & & \\
0 & 0 & -\frac{1}{10} & 0 & \frac{2\ell}{15} & & & & & & & \\
0 & -\frac{1}{10} & 0 & 0 & 0 & \frac{2\ell}{15} & & & & & & \\
0 & 0 & 0 & 0 & 0 & 0 & 0 & & & & & \\
0 & -\frac{6}{5\ell} & 0 & 0 & 0 & -\frac{1}{10} & 0 & \frac{6}{5\ell} & & & & \\
0 & 0 & -\frac{6}{5\ell} & 0 & \frac{1}{10} & 0 & 0 & 0 & \frac{6}{5\ell} & & & \\
0 & 0 & 0 & -\frac{I_x}{A\ell} & 0 & 0 & 0 & 0 & 0 & \frac{I_x}{A\ell} & & \\
0 & 0 & \frac{1}{10} & 0 & -\frac{\ell}{30} & 0 & 0 & 0 & \frac{1}{10} & 0 & \frac{2\ell}{15} & \\
0 & \frac{1}{10} & 0 & 0 & 0 & -\frac{\ell}{30} & 0 & -\frac{1}{10} & 0 & 0 & 0 & \frac{2\ell}{15}
\end{bmatrix} \quad \text{SYMMETRIC} \tag{30}$$

where, in Eqs. (29) and (30), GI_x is the torsional stiffness of the beam cross section and I_y and I_z refer to the moments of inertia around the y and z axes, respectively. A denotes the cross sectional area of the beam element, ℓ is its length and G represents the shear modulus. The axial force N is defined as

$$N \overset{\sim}{=} \text{constant} = \frac{EA}{\ell} (U_7 - U_1)$$

in which, according to the previous definition, U_1 and U_7 refer to the nodal displacements in the axial direction, corresponding to the left (first) and right (second) end of the beam element, respectively.

Based on Eq. (24) the velocity and acceleration distribution within the element may be approximated as

$$[\dot{u}] = [a]\,[\dot{U}] \tag{31}$$

$$[\ddot{u}] = [a]\,[\ddot{U}] \tag{32}$$

With the assumed velocity distribution within the element, the "consistent mass matrix", [M], of the element can be obtained easily (25). This matrix as defined by Eq. (12) is

$$[M] = \rho A \begin{bmatrix}
\frac{\ell}{3} & & & & & & & & & & & \\
0 & \frac{13\ell}{35}+\frac{6I_z}{5A\ell} & & & & & & & & & & \\
0 & 0 & \frac{13\ell}{35}+\frac{6I_y}{5A\ell} & & & & & & & & & \\
0 & 0 & 0 & \frac{I_x\ell}{3A} & & & & & & & & \\
0 & 0 & -\frac{11\ell^2}{210}-\frac{I_y}{10A} & 0 & \frac{\ell^3}{105}+\frac{2I_y\ell}{15A} & & & & & & & \\
0 & \frac{11\ell^2}{210}+\frac{I_z}{10A} & 0 & 0 & 0 & \frac{\ell^3}{105}+\frac{2I_z\ell}{15A} & & & & & & \\
\frac{\ell}{6} & 0 & 0 & 0 & 0 & 0 & \frac{\ell}{3} & & & & & \\
0 & \frac{9\ell}{70}-\frac{6I_z}{5A\ell} & 0 & 0 & 0 & \frac{13\ell^2}{420}-\frac{I_z}{10A} & 0 & \frac{13\ell}{35}+\frac{6I_z}{5A\ell} & & & & \\
0 & 0 & \frac{9\ell}{70}-\frac{6I_y}{5A\ell} & 0 & -\frac{13\ell^2}{420}+\frac{I_y}{10A} & 0 & 0 & 0 & \frac{13\ell}{35}+\frac{6I_y}{5A\ell} & & & \\
0 & 0 & 0 & \frac{I_x\ell}{6A} & 0 & 0 & 0 & 0 & 0 & \frac{I_x\ell}{3A} & & \\
0 & 0 & \frac{13\ell^2}{420}-\frac{I_y}{10A} & 0 & -\frac{\ell^3}{140}-\frac{I_y\ell}{30A} & 0 & 0 & 0 & \frac{11\ell^2}{210}+\frac{I_y}{10A} & 00 & \frac{\ell^3}{105}+\frac{2I_y\ell}{15A} & \\
0 & -\frac{13\ell^2}{420}+\frac{I_z}{10A} & 0 & 0 & 0 & -\frac{\ell^3}{140}-\frac{I_z\ell}{30A} & 0 & -\frac{11\ell^2}{210}-\frac{I_z}{10A} & 0 & 0 & 0 & \frac{\ell^3}{105}+\frac{2I_z\ell}{15A}
\end{bmatrix} \tag{33}$$

SYMMETRIC

where, the various symbols appearing in the above matrix have been defined previously in presenting the stiffness matrices of the element.

The element stiffness and mass matrices as given above (with respect to the element local coordinate system) can now be transformed to the global coordinate system by utilizing the transformation matrix represented by Eqs. (22) and (23). The matrix operations involved in such a transformation are given by Eqs. (18) and (19).

IV. THE RECTANGULAR PLATE ELEMENT

In this chapter the general strain energy expression for a thin rectangular plate subject to in-plane and bending effects is first derived. In the derivation, the interaction between the two effects is also taken into account. The stiffness and mass matrices for a rectangular plate under in-plane action and later under bending action are derived independently by assuming some suitable displacement functions. Following that, the derivation of the geometric stiffness matrix is given. The complete form of the stiffness and mass matrices with respect to both local and global coordinate systems are then given.

4.1 The General Strain Energy Expression

In order to derive the stiffness properties of a rectangular plate in which coupling between in-plane forces and bending is considered due to large deformations, it is convenient to obtain first the strain energy expression.

The middle plane of a plate before deformation is to be considered as the x-z plane, and y is to represent the axis perpendicular to this plane. The notation used in subsequent discussions is similar to the one used by Timoshenko (8).

The initial stresses and strains in a rectangular element of the plate are denoted by σ_x^0, σ_z^0, τ_{xz}^0 and ε_x^0, ε_z^0, γ_{xz}^0, respectively. It is assumed that stresses, σ_x^0, σ_z^0 τ_{xz}^0, have no influence on subsequent displacements of the element within the initial plane. They do, however, have a significant effect on displacements of the element out of its initial plane.

Starting from the initial position, subsequent deformation of the element is assumed to take place such that

$$\begin{aligned} \varepsilon_x &= \varepsilon_x^0 + \varepsilon_x^a \\ \varepsilon_z &= \varepsilon_z^0 + \varepsilon_z^a \\ \gamma_{xz} &= \gamma_{xz}^0 + \gamma_{xz}^a \end{aligned} \tag{34}$$

in which ε_x^a, ε_z^a, γ_{xz}^a are given by the following equations (8):

$$\begin{aligned} \varepsilon_x^a &= \frac{\partial u_x}{\partial x} + \frac{1}{2}\left(\frac{\partial u_y}{\partial x}\right)^2 - y\left(\frac{\partial^2 u_y}{\partial x^2}\right) \\ \varepsilon_z^a &= \frac{\partial u_z}{\partial z} + \frac{1}{2}\left(\frac{\partial u_y}{\partial z}\right)^2 - y\left(\frac{\partial^2 u_y}{\partial z^2}\right) \\ \gamma_{xz}^a &= \left(\frac{\partial u_x}{\partial z} + \frac{\partial u_z}{\partial x}\right) + \left(\frac{\partial u_y}{\partial x}\right)\left(\frac{\partial u_y}{\partial z}\right) - 2y\left(\frac{\partial^2 u_y}{\partial x \partial z}\right). \end{aligned} \tag{35}$$

In the above equations u_x, u_y and u_z represent the displacements of the middle surface in the x, y and z directions, respectively.

The strain energy expression for a thin rectangular plate may be found in various references, such as Timoshenko (8), and is in the form of:

$$V = \frac{1}{2}\iiint (\sigma_x \varepsilon_x + \sigma_z \varepsilon_z + \tau_{xz}\,\gamma_{xz})\,dx\,dz\,dy \tag{36}$$

If the generalized Hooke's Law for an isotropic material is used, then

$$\begin{bmatrix} \sigma_x \\ \sigma_z \\ \tau_{xz} \end{bmatrix} = \frac{E}{1-\nu^2} \begin{bmatrix} 1 & \nu & 0 \\ \nu & 1 & 0 \\ 0 & 0 & \lambda \end{bmatrix} \begin{bmatrix} \varepsilon_x \\ \varepsilon_z \\ \gamma_{xz} \end{bmatrix} \tag{37}$$

Here, E is Young's modulus; ν, Poisson's ratio and $\lambda = (1-\nu)/2$. Substitution of Eqs. (34), (37) into Eq. (36), leads to the following equation

$$V = V_0 + V_1 + V_2 \tag{38}$$

where

$$V_0 = \frac{E}{2(1-\nu^2)} \iiint [(\varepsilon_x^0)^2 + (\varepsilon_z^0)^2 + 2\nu(\varepsilon_x^0)(\varepsilon_z^0) + \lambda(\gamma_{xz}^0)^2] \, dxdzdy \tag{39}$$

$$V_1 = \frac{E}{2(1-\nu^2)} \iiint [(\varepsilon_x^a)^2 + (\varepsilon_z^a)^2 + 2\nu(\varepsilon_x^a)(\varepsilon_z^a) + \lambda(\gamma_{xz}^a)^2] \, dxdzdy \tag{40}$$

$$V_2 = \frac{E}{(1-\nu^2)} \iiint [\varepsilon_x^0 \varepsilon_x^a + \nu(\varepsilon_x^a \varepsilon_z^0 + \varepsilon_x^0 \varepsilon_z^a) + \varepsilon_z^0 \varepsilon_z^a + \lambda\gamma_{xz}^0 \gamma_{xz}^a] \, dxdzdy \tag{41}$$

Note that V_0 is a constant, and since its second order partial derivatives are zero (see Eq. (11), it does not contribute to the stiffness matrix. It can therefore, be ignored in subsequent discussions.

Suppose the following assumptions are made:

$$\begin{aligned} (1) \quad u_x &= u_x(x,z) \\ u_z &= u_z(x,z) \\ u_y &= u_y(x,z) \end{aligned} \tag{42}$$

(2) The cubic and higher order displacement terms are ignored.

The first assumption is a general assumption for solving the plate problem. This assumption allows the elimination of terms containing odd powers of y during the integration process. The second assumption limits the stiffness matrix to that of a constant matrix (2). Substitution of Eqs. (35) into Eq. (40) and utilizing these two assumptions, leads to the following:

$$V_1 = V_{1,P} + V_{1,B} \tag{43}$$

where

$$V_{1,P} = \frac{Eh}{2(1-\nu^2)} \iint \left[\left(\frac{\partial u_x}{\partial x}\right)^2 + \left(\frac{\partial u_z}{\partial z}\right)^2 + \lambda\left(\left(\frac{\partial u_x}{\partial z}\right) + \left(\frac{\partial u_z}{\partial x}\right)\right)^2 + 2\nu\left(\frac{\partial u_x}{\partial x}\right)\left(\frac{\partial u_z}{\partial z}\right)\right] dxdz \tag{44}$$

$$V_{1,B} = \frac{D}{2} \iint \left[\left(\frac{\partial^2 u_y}{\partial x^2} + \frac{\partial^2 u_y}{\partial z^2}\right)^2 - 2(1-\nu)\left(\frac{\partial^2 u_y}{\partial x^2}\frac{\partial^2 u_y}{\partial z^2} - \left(\frac{\partial^2 u_y}{\partial x \partial z}\right)^2\right)\right] dxdz \tag{45}$$

In Eqs. (44) and (45) the constant, h, is the thickness of the plate and $D = (Eh^3)/(12(1-\nu^2))$ is the flexural rigidity of the plate. It should be noted that the two terms represented by Eqs. (44) and (45) correspond to the strain energy due to in-plane forces and bending effects respectively.

Similarly, substitution of Eqs. (35) into Eq. (41) and using the same assumptions as in the derivation of Eq. (41), the following expression is obtained.

$$V_2 = V_{2,G} + V_{2,1} + V_{2,2} \tag{46}$$

where

$$V_{2,G} = \frac{1}{2} \iiint [\sigma_x^0 (\frac{\partial u_y}{\partial x})^2 + \sigma_z^0 (\frac{\partial u_y}{\partial z})^2 + 2\tau_{xz}^0 (\frac{\partial u_y}{\partial z} + \frac{\partial u_y}{\partial x})] dxdzdy \tag{47}$$

$$V_{2,1} = \iiint [\sigma_x^0 (\frac{\partial u_x}{\partial x}) + \sigma_z^0 (\frac{\partial u_z}{\partial z}) + \tau_{xz}^0 (\frac{\partial u_x}{\partial z} + \frac{\partial u_z}{\partial x})] dxdzdy \tag{48}$$

$$V_{2,2} = - \iiint y[\frac{\partial^2 u_y}{\partial x^2} + \frac{\partial^2 u_y}{\partial z^2} + 2 \frac{\partial^2 u_y}{\partial x \partial z}] dxdzdy \tag{49}$$

Note that $V_{2,1}$ contains only terms with first order displacement functions and hence does not contribute to the stiffness matrix. The integrand of $V_{2,2}$ is an odd function of y and hence the value of the integral is zero.

Combining results from Eqs. (38) to (49) the following equation is obtained

$$\begin{aligned} V = {} & \frac{Eh}{2(1-\nu^2)} \iint [(\frac{\partial u_x}{\partial x})^2 + (\frac{\partial u_z}{\partial z})^2 + \lambda(\frac{\partial u_x}{\partial z} + \frac{\partial u_z}{\partial x})^2 \\ & + 2\nu(\frac{\partial u_x}{\partial x})(\frac{\partial u_z}{\partial z})] dxdz \\ & + \frac{D}{2} \iint [(\frac{\partial^2 u_y}{\partial x^2} + \frac{\partial^2 u_y}{\partial z^2})^2 - 2(1-\nu)((\frac{\partial^2 u_y}{\partial x^2}\frac{\partial^2 u_y}{\partial z^2}) \\ & - (\frac{\partial^2 u_y}{\partial x \partial z})^2)] dxdz \\ & + \frac{h}{2} \iint [\sigma_x^0 (\frac{\partial u_y}{\partial x})^2 + \sigma_z^0 (\frac{\partial u_y}{\partial z})^2 + 2\tau_{xz}^0 (\frac{\partial u_y}{\partial x})(\frac{\partial u_y}{\partial z})] dxdz. \end{aligned} \tag{50}$$

This is the strain energy expression due to the coupling of in-plane and bending actions, including the effect of large deformations. The first term on the right-hand side of the above equation is the contribution of in-plane action; the second term represents the contribution of bending action; and the last term is the contribution due to large deformations.

Timoshenko (8) has indicated that the expression represented by Eq. (50) may be obtained by considering the strain energy expression separately for each of the effects due to in-plane, bending, and large deformations. These results are then added together to form the complete strain energy expression. The authors believe that the present derivation gives a better insight into the problem.

4.2 Coordinate Systems and Degrees-of-Freedom

A Cartesian coordinate system is used in the following derivation. As before, let the global coordinate system be defined as x,y,z (see Fig. 2). In general, a rectangular plate element may be oriented in any arbitrary direction in space, therefore, coordinate transformation relations have to be established as explained previously. However, for simplicity in this discussion let its middle plane be considered to be parallel to the X-Z plane. Let the origin of the local coordinate system x,y,z be placed at one of the corners of the plate such that the x-z plane coincides with the middle plane of the plate. In a general case, at each corner of the plate, there may be six possible degrees-of-freedom. For convenience, odd numbers are used to designate those pertaining to in-plane action, and even

numbers to designate those pertaining to bending action. Fig. 2 depicts a typical plate element and the associated element coordinates corresponding to both in-plane and bending actions. It may be observed that, in a general case, the plate element may possess a total of 24 degrees-of-freedoms corresponding to both in-plane and bending actions. Figs. 3 and 4 illustrate the element coordinates corresponding to membrane (in-plane) and bending actions, respectively.

In what follows, stiffness matrices for the plate elements are derived by considering in-plane and bending actions independently of each other on the basis of the expressions given in the previous section. The combination of these two matrices together with the so-called geometrical stiffness matrix gives the complete stiffness matrix of the structure. However, the complete mass matrix contains matrices contributed by in-plane action and bending action only.

4.3 Stiffness Matrix for In-Plane Action

This section considers the stiffness matrix contributed by in-plane action. Fig. 5 shows the plate element displacements corresponding to membrane action. The corner node points are labelled in a clockwise manner as i,j,k,ℓ, so that node i coincides with the origin of the element coordinate system. The x-dimension of the rectangular plate (distance from node i to node j, or ℓ to k) is designated as "a" and the z-dimension (distance from node j to node k, or i to ℓ) is designated as "b".

Let the nondimensional variables ξ and η be introduced, so that

$$\xi = \frac{x}{a}$$

$$\eta = \frac{y}{b}$$

A displacement vector U is defined containing the membrane displacements at the corner nodes of the element, so that (referring to Fig. 5)

$$U = (U_1, U_3, U_5, U_7, U_9, \ldots, U_{21})^T$$

The displacements in the x and z directions of any interior point of the plate are referred to, as before, by u_x and u_z, respectively. One of the critical steps in the analysis is to find suitable representations for u_x and u_z in terms of the nodal displacement. In this study, the following displacement shape functions given by Weaver et al (15) are used, on the basis that they represent shape functions that are compatible with those previously employed for beam elements.

$$u_x(\xi,\eta,U) = \begin{bmatrix} (1-\xi)(2\eta^3 - 3\eta^2 + 1) \\ 0 \\ b(1-\xi)(\eta^3 - 2\eta^2 + \eta) \\ \xi(2\eta^3 - 3\eta^2 + 1) \\ 0 \\ b\xi(\eta^3 - 2\eta^2 + \eta) \\ -\xi(2\eta^3 - 3\eta^2) \\ 0 \\ b\xi(\eta^3 - \eta^2) \\ -(1-\xi)(2\eta^3 - 3\eta^2) \\ 0 \\ b(1-\xi)(\eta^3 - \eta^2) \end{bmatrix}^T \begin{bmatrix} U_1 \\ U_3 \\ U_5 \\ U_7 \\ U_9 \\ U_{11} \\ U_{13} \\ U_{15} \\ U_{17} \\ U_{19} \\ U_{21} \\ U_{23} \end{bmatrix} \qquad (51)$$

$$u_z(\xi,\eta,U) = \begin{bmatrix} 0 \\ (1-\eta)(1-3\xi^2+2\xi^3) \\ -a(1-\eta)(\xi^3-2\xi^2+\xi) \\ 0 \\ -(1-\eta)(2\xi^3-3\xi^2) \\ -a(1-\eta)(\xi^3-\xi^2) \\ 0 \\ -\eta(2\xi^3-3\xi^2) \\ -a\eta(\xi^3-\xi^2) \\ 0 \\ \eta(2\xi^3-3\xi^2+1) \\ -a\eta(\xi^3-2\xi^2+\xi) \end{bmatrix}^T \begin{bmatrix} U_1 \\ U_3 \\ U_5 \\ U_7 \\ U_9 \\ U_{11} \\ U_{13} \\ U_{15} \\ U_{17} \\ U_{19} \\ U_{21} \\ U_{23} \end{bmatrix} \qquad (52)$$

These two displacement functions have the following properties:

(1) For an arbitrary set of nodal displacements, the edges of a series of elements describe continuous curves.

(2) For an arbitrary set of nodal displacements, the shear strain at each corner of an element is zero.

(3) They are compatible with displacement functions of beam elements described by Akkoush et al (25).

Although the stiffness matrix [K] of the plate element may be obtained by partial differentiation of the strain energy expression given by Eq. (50), it is more convenient (15) to evaluate its components by using the following equation, based on the principle of virtual work:

$$K_{ij} = h \iint [\sigma_i]^T [\varepsilon_j] \, dxdz \tag{53}$$

where the index j represents the corresponding strain due to a unit displacement in the jth direction and $[\sigma_i]$ represents the stress component corresponding to the strain component $[\varepsilon_i]$.

Appendix A contains the various strain and stress components corresponding to the displacement functions represented by Eqs. (51), and (52). Thus, the stiffness matrix $[K_I]$ contributed by the in-plane action with displacement functions given by Eqs. (51) and (52) can be obtained by the substitution into Eq. (51) of the stress and strain components given in Appendix A. The resulting matrix is shown below:

$$[K_I] = \frac{Eh}{(1-\nu^2)} \begin{bmatrix}
\rho_1 & & & & & & & & & & & \\
\rho_2 & \beta_2 & & & & & & & & & & \\
-\rho_3 & -\beta_3 & \gamma_3 & & & & & & & & & \\
\rho_4 & -\rho_5 & -\rho_6 & \rho_1 & & & & & & & & \\
\rho_5 & \beta_5 & \beta_6 & -\rho_2 & \beta_2 & & & & & & & \\
-\rho_6 & -\beta_6 & \gamma_6 & -\rho_3 & \beta_3 & \gamma_3 & & & & & & \\
\rho_{10} & -\rho_2 & \rho_{12} & \rho_7 & -\rho_5 & \rho_9 & \rho_1 & & & & & \\
-\rho_2 & \beta_{11} & \beta_{12} & \rho_5 & \beta_8 & \beta_9 & \rho_2 & \beta_2 & & & & \\
-\rho_{12} & -\beta_{12} & \gamma_{12} & -\rho_9 & \beta_9 & \gamma_9 & \rho_3 & \beta_3 & \gamma_3 & & & \\
\rho_7 & \rho_5 & \rho_9 & \rho_{10} & \rho_2 & \rho_{12} & \rho_4 & -\rho_5 & \rho_6 & \rho_1 & & \\
-\rho_5 & \beta_8 & -\beta_9 & \rho_2 & \beta_{11} & -\beta_{12} & \rho_5 & \beta_5 & -\beta_6 & -\rho_2 & \beta_2 & \\
-\rho_9 & -\beta_9 & \gamma_9 & -\rho_{12} & \beta_{12} & \gamma_{12} & \rho_6 & \beta_6 & \gamma_6 & \rho_3 & -\beta_3 & \gamma_3
\end{bmatrix} \tag{54}$$

Symmetric

where, the various symbols appearing in the above equation are defined in Table 1, given below (a and b, as before, pertain to the dimensions of the rectangular plate element and $\lambda = (1-\nu)/2$, where ν is Poisson's ratio):

TABLE 1 - Definition of Symbols Appearing in Equation (54)

i	ρ_i	β_i	γ_i
1	$\frac{13b}{35a} + \frac{2\lambda a}{5b}$	.....	.....
2	$\frac{(\lambda+\nu)}{4}$	$\frac{13a}{35b} + \frac{2\lambda b}{5a}$	.....
3	$\frac{-11b^2}{210a} + \frac{\nu a}{24} - \frac{3\lambda a}{40}$	$\frac{11a^2}{210b} - \frac{\nu b}{24} + \frac{3\lambda b}{40}$	$\frac{b^3}{105a} + \frac{a^3}{105b} - \frac{\nu ab}{72} + \frac{3\lambda ab}{40}$
4	$\frac{-13b}{35a} + \frac{\lambda a}{5b}$	.....	.....
5	$\frac{(\nu-\lambda)}{4}$	$\frac{9a}{70b} - \frac{2\lambda b}{5a}$	.....
6	$\frac{11b^2}{210a} - \frac{\nu a}{24} + \frac{\lambda a}{40}$	$\frac{-13a^2}{420b} + \frac{\nu b}{24} + \frac{3\lambda b}{40}$	$\frac{-b^3}{105a} - \frac{a^3}{140b} + \frac{\nu ab}{72} + \frac{\lambda ab}{40}$
7	$\frac{9b}{70a} - \frac{2\lambda a}{5b}$	.....	.....
8	.....	$\frac{-13a}{35b} + \frac{\lambda b}{5a}$	.....
9	$\frac{13b^2}{420a} - \frac{2\nu a}{24} - \frac{3\lambda a}{40}$	$\frac{-11a^2}{210b} + \frac{\nu b}{24} - \frac{\lambda b}{40}$	$\frac{-b^3}{140a} - \frac{a^3}{105b} + \frac{\nu ab}{72} + \frac{\lambda ab}{40}$
10	$\frac{-9b}{70a} - \frac{\lambda a}{5b}$	.....	.....
11	.....	$\frac{-9a}{70b} - \frac{\lambda b}{5a}$	.....
12	$\frac{-13b^2}{420a} + \frac{\nu a}{24} + \frac{\lambda a}{40}$	$\frac{13a^2}{420b} - \frac{\nu b}{24} - \frac{\lambda b}{40}$	$\frac{b^3}{140a} + \frac{a^3}{140b} - \frac{\nu ab}{72} - \frac{\lambda ab}{40}$

4.4 Mass Matrix for In-Plane Action

If the same displacement functions are used as represented by Eqs. (51) and (52) for a rectangular plate under in-plane action, then the corresponding mass matrix $[M_I]$ can be obtained based on Eq. (12). However, for the plate element under consideration, the matrix [a] in Eq. (12) is a 2 x 12 matrix in which the first and second rows are represented by the first matrices on the right-hand side of Eq. (51) and Eq. (52), respectively. Since the procedure involved is straight forward (although laborious), only the final result is presented below:

$$
[M_I] = \rho ab h \begin{bmatrix}
24\alpha & & & & & & & & & & & \\
0 & 24\alpha & & & & & & & & & & \\
2\beta b & -2\beta a & \gamma(a^2+b^2) & & & & & & & & & \\
12\alpha & 0 & \beta b & 24\alpha & & & & & & & & \\
0 & 2\rho & -2\alpha a & 0 & 24\alpha & & & & & & & \\
\beta b & 2\alpha a & \delta(-3a^2+2b^2) & 2\beta b & 2\beta a & \gamma(a^2+b^2) & & & & & & \\
\rho & 0 & \alpha b & 2\rho & 0 & 2\alpha b & 24\alpha & & & & & \\
0 & \rho & -\alpha a & 0 & 12\alpha & \beta a & 0 & 24\alpha & & & & \\
-\alpha b & \alpha a & -\lambda(a^2+b^2) & -2\alpha b & \beta a & \delta(2a^2-3b^2) & -2\beta b & 2\beta a & \gamma(a^2+b^2) & & & \\
2\rho & 0 & 2\alpha b & \rho & 0 & \alpha b & 12\alpha & 0 & -\beta b & 24\alpha & & \\
0 & 12\alpha & -\beta a & 0 & \rho & \alpha a & 0 & 2\rho & 2\alpha a & 0 & 24\alpha & \\
-2\alpha b & -\beta a & \delta(2a^2-3b^2) & -\alpha b & -\alpha a & -\lambda(a^2+b^2) & -\beta b & -2\alpha a & \delta(-3a^2+2b^2) & -2\beta b & -2\beta a & \gamma(a^2+b^2)
\end{bmatrix}
\qquad \text{(55)}
$$

Symmetric

where, $\alpha = 13/2520$, $\beta = 11/1260$, $\gamma = 1/315$, $\delta = 1/1260$, $\rho = 3/140$, and $\lambda = 1/840$.

4.5 Stiffness Matrix for Bending Action

Many displacement functions for a rectangular plate in bending have been proposed. Among these, the one which satisfies the deflection and slope compatibility has been chosen in this study because it satisfies not only compatibility between adjacent plate elements but also between beam and plate elements. Such a displacement function representing the transverse displacement u_y of the plate has been derived and verified by Bogner et al (28) and Przemieniecki (27,29). Fig. 6 illustrates the element displacements corresponding to bending action.

In terms of the geometry given by Fig. 6 and the non-dimensional variables $\xi = \frac{x}{a}$, $\eta = \frac{z}{b}$, this displacement function has the following form:

$$u_y(\xi,\eta,U) = \begin{bmatrix} (1+2\xi)(1-\xi)^2(1+2\eta)(1-\eta)^2 \\ -(1+2\xi)(1-\xi)^2\,\eta(1-\eta)^2 b \\ \xi(1-\xi)^2(1+2\eta)(1-\eta)^2 a \\ (3-2\xi)\xi^2(1+2\eta)(1-\eta)^2 \\ -(3-2\xi)\xi^2\eta(1-\eta)^2 b \\ -(1-\xi)\xi^2(1+2\eta)(1-\eta)^2 a \\ (3-2\xi)\xi^2(3-2\eta)\eta^2 \\ (3-2\xi)\xi^2(1-\eta)\eta^2 b \\ -(1-\xi)\xi^2(3-2\eta)\eta^2 a \\ (1+2\xi)(1-\xi)^2(3-2\eta)\eta^2 \\ (1+2\xi)(1-\xi)^2(1-\eta)\eta^2 b \\ \xi(1-\xi)^2(3-2\eta)\eta^2 a \end{bmatrix}^T \begin{bmatrix} U_2 \\ U_4 \\ U_6 \\ U_8 \\ U_{10} \\ U_{12} \\ U_{14} \\ U_{16} \\ U_{18} \\ U_{20} \\ U_{22} \\ U_{24} \end{bmatrix} \qquad (56)$$

For a plate in bending, the strain components have the following form:

$$\begin{bmatrix} \varepsilon_x \\ \varepsilon_z \\ \gamma_{xz} \end{bmatrix} = -y \begin{bmatrix} \dfrac{\partial^2 u_y}{\partial x^2} \\ \dfrac{\partial^2 u_y}{\partial z^2} \\ 2\dfrac{\partial^2 u_y}{\partial x \partial z} \end{bmatrix} \tag{57}$$

The matrix [b] given in Eq. (2) may be obtained by substitution of Eq. (56) into Eq. (57). In turn, substitution of matrix [b] into Eq. (9) allows evaluation of the stiffness matrix $[K_B]$, corresponding to bending action.

The matrix $[K_B]$ in partitioned form is represented as

$$[K_B] = \begin{bmatrix} [K_{B1}] & \text{Symmetric} \\ [K_{B2}] & [K_{B3}] \end{bmatrix} \tag{58}$$

The submatrices $[K_{B1}]$, $[K_{B2}]$, and $[K_{B3}]$ are presented below as Eqs. (60) - (62). In all three equations, the scalar multiplier κ is defined as

$$\kappa = \frac{Eh^3}{12(1-\nu^2)ab} \tag{59}$$

The other symbols appearing in the submatrices are defined and compiled in Table 2.

$$[K_{B1}] = K \begin{bmatrix} \sigma_4(\alpha+\omega)+\lambda_5 & & & & & & \\ -(\theta_2\alpha+\sigma_3\omega+\lambda_3\delta)b & (\gamma_1\alpha+\gamma_2\omega+\lambda_4)b^2 & & & \text{Symmetric} & & \\ (\sigma_3\alpha+\theta_2\omega+\lambda_3\delta)a & -(\theta_1(\alpha+\omega)+\lambda_1\varepsilon)ab & (\gamma_2\alpha+\gamma_1\omega+\lambda_4)a^2 & & & & \\ -\sigma_4\alpha+\rho_3\omega-\lambda_5 & (\theta_2\alpha-\rho_2\omega+\lambda_3\delta)b & (-\sigma_3\alpha+\sigma_2\omega-\lambda_3)a & \sigma_4(\alpha+\omega)+\lambda_5 & & & \\ (\theta_2\alpha-\rho_2\omega+\lambda_3\delta)b & (-\gamma_1\alpha+\rho_4\omega-\lambda_4)b^2 & (\theta_1\alpha-\sigma_1\omega+\lambda_1\delta)ab & (-\theta_2\alpha-\sigma_3\omega-\lambda_3\delta)b & (\gamma_1\alpha+\gamma_2\omega+\lambda_4)b^2 & & \\ (\sigma_3\alpha-\sigma_2\omega+\lambda_3)a & (-\theta_1\alpha+\sigma_1\omega-\lambda_1\delta)ab & (\gamma_3\alpha-\rho_1\omega-\lambda_2)a^2 & (-\sigma_3\alpha-\theta_2\omega-\lambda_3\delta)a & (\theta_1(\alpha+\omega)+\lambda_1\varepsilon)ab & (\gamma_2\alpha+\gamma_1\omega+\lambda_4)a^2 & \end{bmatrix} \quad (60)$$

$$[K_{B2}] = K \begin{bmatrix} -\rho_3(\alpha+\omega)+\lambda_5 & (\sigma_2\alpha+\rho_2\omega-\lambda_3)b & (-\rho_2\alpha-\sigma_2\omega+\lambda_3)a & \rho_3\alpha-\sigma_4\omega-\lambda_5 & (-\sigma_2\alpha+\sigma_3\omega+\lambda_3)b & (-\rho_2\alpha+\theta_2\omega+\lambda_3\delta)a \\ (-\sigma_2\alpha-\rho_2\omega+\lambda_3)b & (\rho_1\alpha+\rho_5\omega+\lambda_2)b^2 & (-\sigma_1(\alpha+\omega)+\lambda_1)ab & (\sigma_2\alpha-\sigma_3\omega-\lambda_3)b & (-\rho_1\alpha+\gamma_3\omega-\lambda_2)b^2 & (-\sigma_1\alpha+\theta_1\omega+\lambda_1\delta)ab \\ (\rho_2\alpha+\sigma_2\omega-\lambda_3)a & (-\sigma_1(\alpha+\omega)+\lambda_1)ab & (\rho_5\alpha+\rho_1\omega+\lambda_2)a^2 & (-\rho_2\alpha+\theta_2\omega+\lambda_3\delta)a & (\sigma_1\alpha-\theta_1\omega-\lambda_1\delta)ab & (\rho_4\alpha-\gamma_1\omega-\lambda_4)a^2 \\ \rho_3\alpha-\sigma_4\omega-\lambda_5 & (-\sigma_2\alpha+\sigma_3\omega+\lambda_3)b & (\rho_2\alpha-\theta_2\omega-\lambda_3\delta)a & -\rho_3(\alpha+\omega)+\lambda_5 & (\sigma_2\alpha+\rho_2\omega-\lambda_3)b & (\rho_2\alpha+\sigma_2\omega-\lambda_3)a \\ (\sigma_2\alpha-\sigma_3\omega-\lambda_3)b & (-\rho_1\alpha+\gamma_3\omega-\lambda_2)b^2 & (\sigma_1\alpha-\theta_1\omega-\lambda_1\delta)ab & (-\sigma_2\alpha-\rho_2\omega+\lambda_3)b & (\rho_1\alpha+\rho_5\omega+\lambda_2)b^2 & (\sigma_1(\alpha+\omega)-\lambda_1)ab \\ (\rho_2\alpha-\theta_2\omega-\lambda_3\delta)a & (-\sigma_1\alpha+\theta_1\omega+\lambda_1\delta)ab & (\rho_4\alpha-\gamma_1\omega-\lambda_4)a^2 & (-\rho_2\alpha-\sigma_2\omega+\lambda_3)a & (\sigma_1(\alpha+\omega)-\lambda_1)ab & (\rho_5\alpha+\rho_1\omega+\lambda_2)a^2 \end{bmatrix} \quad (61)$$

$$[K_{B3}] = K \begin{bmatrix} \sigma_4(\alpha+\omega)+\lambda_5 & & & & & & \\ (\theta_2\alpha+\sigma_3\omega+\lambda_3\delta)b & (\gamma_1\alpha+\gamma_2\omega+\lambda_4)b^2 & & & \text{Symmetric} & & \\ -(\sigma_3\alpha+\theta_2\omega+\lambda_3\delta)a & -(\theta_1(\alpha+\omega)+\lambda_1\varepsilon)ab & (\gamma_2\alpha+\gamma_1\omega+\lambda_4)a^2 & & & & \\ -\sigma_4\alpha+\rho_3\omega-\lambda_5 & (-\theta_2\alpha+\rho_2\omega-\lambda_3\delta)b & (\sigma_3\alpha-\sigma_2\omega+\lambda_3)a & \sigma_4(\alpha+\omega)+\lambda_5 & & & \\ (-\theta_2\alpha+\rho_2\omega-\lambda_3\delta)b & (-\gamma_1\alpha+\rho_4\omega-\lambda_4)b^2 & (\theta_1\alpha-\sigma_1\omega+\lambda_1\delta)ab & (\theta_2\alpha+\sigma_3\omega+\lambda_3\delta)b & (\gamma_1\alpha+\gamma_2\omega+\lambda_4)b^2 & & \\ (-\sigma_3\alpha+\sigma_2\omega-\lambda_3)a & (-\theta_1\alpha+\sigma_1\omega-\lambda_1\delta)ab & (\gamma_3\alpha-\rho_1\omega-\lambda_2)a^2 & (\sigma_3\alpha+\theta_2\omega+\lambda_3\delta)a & (\theta_1(\alpha+\omega)+\lambda_1\varepsilon)ab & (\gamma_2\alpha+\gamma_1\omega+\lambda_4)a^2 & \end{bmatrix} \quad (62)$$

TABLE 2 - Definition of Symbols Appearing in Equations (60)-(62)

	i = 1	i = 2	i = 3	i = 4	i = 5
$\alpha = (b/a)^2$					
$\omega = (a/b)^2$					
$\delta = 1+5\nu$					
$\varepsilon = 1+60\nu$					
$\rho_i =$	3/35	27/35	54/35	18/35	9/35
$\gamma_i =$	4/35	52/35	26/35		
$\theta_i =$	11/35	22/35			
$\sigma_i =$	13/70	13/35	78/35	156/35	
$\lambda_i =$	1/50	2/25	6/25	8/25	72/25

4.6 Mass Matrix for Bending Action

In generating the mass matrix for the plate element in bending, if the same displacement function given by Eq. (56) for a rectangular plate in bending is used, then the corresponding mass matrix $[M_B]$ can be obtained by using Eq. (12). The matrix [a] in Eq. (12) is a 1 x 12 matrix represented by the first matrix on the right-hand side of Eq. (56). The resulting matrix $[M_B]$ is shown below.

$$[M_B] = abh\rho$$

$$\begin{array}{cccccccccccc}
\alpha^2 & & & & & & & & & & & \\
-\alpha\gamma b & \alpha\varepsilon b^2 & & & & & & & & & & \\
\gamma\alpha a & -\gamma^2 ab & \varepsilon\alpha a^2 & & & & & & & & & \\
\beta\alpha & -\beta\gamma b & \delta\alpha a & \alpha^2 & & & & & & & & \\
-\beta\gamma b & \beta\varepsilon b^2 & -\delta\gamma ab & -\alpha\gamma b & \alpha\varepsilon b^2 & & & & & & & \\
-\delta\alpha a & \delta\gamma ab & -\lambda\alpha a^2 & -\gamma\alpha a & \gamma^2 ab & \varepsilon\alpha a^2 & & & & & & \\
\beta^2 & -\beta\delta b & \delta\beta a & \alpha\beta & -\alpha\delta b & -\gamma\beta a & \alpha^2 & & & & & \\
\beta\delta b & -\beta\lambda b^2 & \delta^2 ab & \alpha\delta b & -\alpha\lambda b^2 & -\gamma\delta ab & \alpha\gamma b & \alpha\varepsilon b^2 & & & & \\
-\delta\beta a & \delta^2 ab & -\lambda\beta a^2 & -\gamma\beta a & \gamma\delta ab & \varepsilon\beta a^2 & -\gamma\alpha a & -\gamma^2 ab & \varepsilon\alpha a^2 & & & \\
\alpha\beta & -\alpha\delta b & \gamma\beta a & \beta^2 & -\beta\delta b & -\delta\beta a & \beta\alpha & \beta\gamma b & -\delta\alpha a & \alpha^2 & & \\
\alpha\delta b & -\alpha\lambda b^2 & \gamma\delta ab & \beta\delta b & -\beta\lambda b^2 & -\delta^2 ab & \beta\gamma b & \beta\varepsilon b^2 & -\delta\gamma ab & \alpha\gamma b & \alpha\varepsilon b^2 & \\
\gamma\beta a & -\gamma\delta ab & \varepsilon\beta a^2 & \delta\beta a & -\delta^2 ab & -\lambda\beta a^2 & \delta\alpha a & \delta\gamma ab & -\lambda\alpha a^2 & \gamma\alpha a & \gamma^2 ab & \varepsilon\alpha a^2
\end{array}$$

Symmetric

(63)

where the various symbols appearing in Eq. (63) are defined as

$$\alpha = \frac{13}{35}$$

$$\beta = \frac{9}{70}$$

$$\gamma = \frac{11}{210}$$

$$\delta = \frac{13}{420}$$

$$\varepsilon = \frac{1}{105}$$

$$\lambda = \frac{1}{140}$$

and, as before, a and b refer to the edge dimensions and h to the thickness of the plate, and ρ represents the mass density of the material.

4.7 The Complete Form of Stiffness and Mass Matrices

The results obtained in Sections 4.3 and 4.5 may now be incorporated for the complete form of the local stiffness matrix of a rectangular plate with coupling between in-plane and bending effects. Let $[K_I]$ and $[K_B]$ be the stiffness matrices corresponding to in-plane and bending actions, respectively, then, the force-displacement relationship for the combined effects has the following form:

$$[S] = [K][U] \tag{64}$$

where

$$[S] = \begin{bmatrix} [S_I] \\ \\ [S_B] \end{bmatrix} \tag{65}$$

and $[S_I]$, $[S_B]$ are the nodal forces corresponding to in-plane and bending actions, respectively. They are represented by the following equations:

$$[S_I] = [S_1\ S_3\ S_5\ S_7\ S_9\ S_{11}\ S_{13}\ S_{15}\ S_{17}\ S_{19}\ S_{21}\ S_{23}]^T \tag{66}$$

$$[S_B] = [S_2\ S_4\ S_6\ S_8\ S_{10}\ S_{12}\ S_{14}\ S_{16}\ S_{18}\ S_{20}\ S_{22}\ S_{24}]^T. \tag{67}$$

Similarly,

$$[U] = \begin{bmatrix} [U_I] \\ \\ [U_B] \end{bmatrix} \tag{68}$$

and $[U_I]$, $[U_B]$ are the nodal displacements corresponding to in-plane and bending actions, respectively. They have the following forms:

$$[U_I] = U_1\ U_3\ U_5\ U_7\ U_9\ U_{11}\ U_{13}\ U_{15}\ U_{17}\ U_{19}\ U_{21}\ U_{23}]^T \tag{69}$$

$$[U_B] = U_2\ U_4\ U_6\ U_8\ U_{10}\ U_{12}\ U_{14}\ U_{16}\ U_{18}\ U_{20}\ U_{22}\ U_{24}]^T. \tag{70}$$

Finally, the matrix [K] may be represented as follows:

$$[K] = \begin{bmatrix} [K_I] & [0] \\ [0] & [K_B] \end{bmatrix} \tag{71}$$

The linear orthogonal transformation [T] is introduced for the purpose of rearranging the forces and displacements according to the numbering scheme used in Fig. 2, so that:

$$[T] = [\ [T_1]\ [T_2]\ ] \tag{72}$$

where $[T_1]$, $[T_2]$, in partitioned form, are diagonal matrices defined as:

$$[T_1] = \text{diag}\ ([\lambda_1],[\lambda_1],[\lambda_1],[\lambda_1]) \tag{73}$$

$$[T_2] = \text{diag}\ ([\lambda_2],[\lambda_2],[\lambda_2],[\lambda_2]) \tag{74}$$

and

$$[\lambda_1] = \begin{bmatrix} 1 & 0 & 0 \\ 0 & 0 & 0 \\ 0 & 1 & 0 \\ 0 & 0 & 0 \\ 0 & 0 & 1 \\ 0 & 0 & 0 \end{bmatrix} \tag{75}$$

$$[\lambda_2] = \begin{bmatrix} 0 & 0 & 0 \\ 1 & 0 & 0 \\ 0 & 0 & 0 \\ 0 & 1 & 0 \\ 0 & 0 & 0 \\ 0 & 0 & 1 \end{bmatrix} \tag{76}$$

It is clear from the definition of [T] that

$$[T]^T [T] = [T][T]^T = [I]$$

in which $[T]^T$ represents the transpose of [T], and [I], the identity matrix.

Therefore, if

$$[S] = [K][U] \tag{77}$$

then

$$[T][S] = [T][K][U] = [T][K]([T]^T[T])[U]$$

$$= ([T][K][T]^T)\ [T][U].$$

Setting

$$[S'] = [T][S], \tag{78}$$

$$[U'] = [T][U], \tag{79}$$

and

$$[K'] = [T][K][T]^T. \tag{80}$$

Equation (77) is thus transformed to

$$[S'] = [K'][U'] \tag{81}$$

which is the complete force-displacement relationship for a rectangular plate with coupling between in-plane and bending effects in accordance with the numbering scheme indicated in Fig. 2.

The complete mass matrix for a rectangular plate with coupling between in-plane and bending effects again according to the numbering scheme used in Fig. 2 may be obtained in a similar way. It has the form of:

$$[M'] = [T][M][T]^T \tag{82}$$

where

$$[M] = \begin{bmatrix} [M_I] & [0] \\ [0] & [M_B] \end{bmatrix} \tag{83}$$

The matrices $[M_I]$ and $[M_B]$ are the mass matrices corresponding to in-plane and bending actions, as given by Eqs. (55) and (63), respectively.

4.8 Geometrical Stiffness Matrix

It has been indicated above that the stiffness property of a rectangular plate is contributed by three terms that appear in the strain energy expression for the plate. Thus far, first and second term contributions have been dealt with in the derivations. The remaining term, i.e., the third term, is the one which leads to the geometrical stiffness matrix. Since this term involves only one displacement function u_y, it is necessary

to assume only this function. The derivation of this geometrical stiffness matrix is very tedious, consequently, many investigators have tended to use other simpler displacement functions, (e.g., see Gallagher et al. (30)) coupled with finer partitioning to compensate for this effect. For the sake of being consistent, the same displacement function as shown in Eq. (56) is used here.

The strain energy contributed by large deformations which corresponds to the third term on the right of Eq. (50) may be rewritten as follows (see also Eq. (47))

$$V_{2,G} = \frac{h}{2} \int\int [\sigma_x^0 (\frac{\partial u_y}{\partial x})^2 + \sigma_z^0 (\frac{\partial u_y}{\partial z})^2 + 2\tau_{xz}^0 (\frac{\partial u_y}{\partial x})(\frac{\partial u_y}{\partial z})] dxdz. \quad (84)$$

The derivation of the geometrical stiffness matrix may be carried out in three parts, each of which corresponds to a term in Eq. (84). Accordingly then

$$[K_G] = \sigma_x^0 [K_{G_x}] + \sigma_z^0 [K_{G_z}] + \tau_{xz}^0 [K_{G_{xz}}] \quad (85)$$

where $[K_{G_x}]$, $[K_{G_z}]$, and $[K_{G_{xz}}]$ are the parts contributed by the first, second, and third terms, respectively, on the right of Eq. (84). Utilizing Eqs. (56), (11) and the chain rules of differentiation, the matrices $[K_{G_x}]$, $[K_{G_z}]$, and $[K_{G_{xz}}]$ may be obtained. They are presented below as Eqs. (86) - (88).

$$[K_{G_x}] = h\,\frac{b}{a}$$

$$\begin{bmatrix}
\frac{78}{175} & & & & & & & & & & & & \\
-\frac{11}{175}b & \frac{2}{175} & & & & & & & & & & & \\
\frac{13}{350}a & -\frac{11}{2100}ab & \frac{26}{525}a^2 & & & & & & & & & & \\
-\frac{78}{175} & \frac{11}{175}b & -\frac{13}{350}a & \frac{78}{175} & & & & & & & & & \\
\frac{11}{175}b & -\frac{2}{175}b^2 & \frac{11}{2100}ab & -\frac{11}{175}b & \frac{2}{175}b^2 & & & & & & & & \\
\frac{13}{350}a & -\frac{11}{2100}ab & -\frac{13}{1050}a^2 & -\frac{13}{350}a & \frac{11}{2100}ab & \frac{26}{525}a^2 & & & & & & & \\
-\frac{27}{175} & \frac{13}{350}b & -\frac{9}{700}a & \frac{27}{175} & -\frac{13}{350}b & -\frac{9}{700}a & \frac{78}{175} & & & & & & \\
-\frac{13}{350}b & \frac{3}{350}b^2 & -\frac{13}{4200}ab & \frac{13}{350}b & -\frac{3}{350}b^2 & -\frac{13}{4200}ab & \frac{11}{175}b & \frac{2}{175}b^2 & & & & & \\
\frac{9}{700}a & -\frac{13}{4200}ab & -\frac{3}{700}a^2 & -\frac{9}{700}a & \frac{13}{4200}ab & \frac{3}{175}a^2 & -\frac{13}{350}a & -\frac{11}{2100}ab & \frac{26}{525}a^2 & & & & \\
\frac{27}{175} & -\frac{13}{350}b & \frac{9}{700}a & -\frac{27}{175} & \frac{13}{350}b & \frac{9}{700}a & -\frac{78}{175} & -\frac{11}{175}b & \frac{13}{350}a & \frac{78}{175} & & & \\
\frac{13}{350}b & -\frac{3}{350}b^2 & \frac{13}{4200}ab & -\frac{13}{350}b & \frac{3}{350}b^2 & \frac{13}{4200}ab & -\frac{11}{175}b & -\frac{2}{175}b^2 & \frac{11}{2100}ab & \frac{11}{175}b & \frac{2}{175}b^2 & & \\
\frac{9}{700}a & -\frac{13}{4200}ab & \frac{3}{175}a^2 & -\frac{9}{700}a & \frac{13}{4200}ab & -\frac{3}{700}a^2 & -\frac{13}{350}a & -\frac{11}{2100}ab & -\frac{13}{1050}a^2 & \frac{13}{350}a & \frac{11}{2100}ab & \frac{26}{525}a^2
\end{bmatrix}$$

Symmetric

(86)

$$[K_{G_z}] = h\,\frac{a}{b}\begin{bmatrix}
\frac{78}{175} & & & & & & & & & & & \\
-\frac{13}{350}b & \frac{26}{525}b^2 & & & & & & & & & & \\
\frac{11}{175}a & -\frac{11}{2100}ab & \frac{2}{175}a^2 & & & & & & & & & \\
\frac{27}{175} & -\frac{9}{700}b & \frac{13}{350}a & \frac{78}{175} & & & & & & & & \\
-\frac{9}{700}b & \frac{3}{175}b^2 & -\frac{13}{4200}ab & -\frac{13}{350}b & \frac{26}{525}b^2 & & & & & & & \\
-\frac{13}{350}a & \frac{13}{4200}ab & -\frac{3}{350}a^2 & -\frac{11}{175}a & \frac{11}{2100}ab & \frac{2}{175}a^2 & & & & & & \\
-\frac{27}{175} & \frac{9}{700}b & -\frac{13}{350}a & -\frac{78}{175} & \frac{13}{350}b & \frac{11}{175}a & \frac{78}{175} & & & & & \\
-\frac{9}{700}b & -\frac{3}{700}b^2 & -\frac{13}{4200}ab & -\frac{13}{350}b & -\frac{13}{1050}b^2 & \frac{11}{2100}ab & \frac{13}{350}b & \frac{26}{525}b^2 & & & & \\
\frac{13}{350}a & -\frac{13}{4200}ab & \frac{3}{350}a^2 & \frac{11}{175}a & -\frac{11}{2100}ab & -\frac{2}{175}a^2 & -\frac{11}{175}a & -\frac{11}{2100}ab & \frac{2}{175}a^2 & & & \\
-\frac{78}{175} & \frac{13}{350}b & -\frac{11}{175}a & -\frac{27}{175} & \frac{9}{700}b & \frac{13}{350}a & \frac{27}{175} & \frac{9}{700}b & -\frac{13}{350}a & \frac{78}{175} & & \\
-\frac{13}{350}b & -\frac{13}{1050}b^2 & -\frac{11}{2100}ab & -\frac{9}{700}b & -\frac{3}{700}b^2 & \frac{13}{4200}ab & \frac{9}{700}b & \frac{3}{175}b^2 & -\frac{13}{4200}ab & \frac{13}{350}b & \frac{26}{525}b^2 & \\
-\frac{11}{175}a & \frac{11}{2100}ab & -\frac{2}{175}a^2 & -\frac{13}{350}a & \frac{13}{4200}ab & \frac{3}{350}a^2 & \frac{13}{350}a & \frac{13}{4200}ab & -\frac{3}{350}a^2 & \frac{11}{175}a & \frac{11}{2100}ab & \frac{2}{175}a^2
\end{bmatrix} \qquad (87)$$

Symmetric

$$[K_{G_{xz}}] = h \begin{bmatrix}
\frac{1}{2} & & & & & & & & & & \\
0 & 0 & & & & & & & & & \\
0 & -\frac{1}{50}ab & 0 & & & & & & & & \\
0 & -\frac{1}{10}b & 0 & \frac{1}{2} & & & & & & & \\
\frac{1}{10}b & 0 & \frac{1}{50}ab & 0 & 0 & & & & & & \\
0 & \frac{1}{50}ab & 0 & 0 & -\frac{1}{50}ab & 0 & & & & & \\
-\frac{1}{2} & \frac{1}{10}b & -\frac{1}{10}a & 0 & 0 & \frac{1}{10}a & \frac{1}{2} & & & & \\
-\frac{1}{10}b & \frac{1}{60}b^2 & -\frac{1}{50}ab & 0 & 0 & \frac{1}{50}ab & 0 & 0 & & & \\
\frac{1}{10}a & -\frac{1}{50}ab & \frac{1}{60}a^2 & -\frac{1}{10}a & \frac{1}{50}ab & 0 & 0 & -\frac{1}{50}ab & 0 & & \\
0 & 0 & \frac{1}{10}a & \frac{1}{2} & -\frac{1}{10}b & -\frac{1}{10}a & 0 & \frac{1}{10}b & 0 & -\frac{1}{2} & \\
0 & 0 & \frac{1}{50}ab & \frac{1}{10}b & -\frac{1}{60}b^2 & -\frac{1}{50}ab & -\frac{1}{10}b & 0 & \frac{1}{50}ab & 0 & 0 \\
-\frac{1}{10}a & \frac{1}{50}ab & 0 & \frac{1}{10}a & -\frac{1}{50}ab & -\frac{1}{60}a^2 & 0 & \frac{1}{50}ab & 0 & 0 & -\frac{1}{50}ab & 0
\end{bmatrix} \quad \text{Symmetric} \qquad (88)$$

The complete geometrical stiffness matrix may now be obtained by substitution of the values $[K_{G_x}]$, $[K_{G_z}]$, and $[K_{G_{xz}}]$ into Eq. (85). This is the stiffness property contributed by the large deformation. Note that σ_x^0, σ_z^0, and τ_{xz}^0 are treated as constants during the derivation since these quantities are assumed to be known during the current state of deformation of the structure.

Since the geometrical stiffness matrix has contributions only due to bending action, it can be rearranged easily to correspond to the numbering scheme indicated in Fig. 2.

4.9 Transformation to the Global Coordinate System

In order to assemble individual elements to form a complete structure, the local properties must be represented with respect to the global coordinate system. It is seen from Eq. (18) that the $[\lambda]$ transformation matrix between the local and global coordinates has to be determined first. The stiffness matrix with respect to the global coordinate system may then be obtained by evaluating the quantity $[\lambda]^T[K][\lambda]$. For the present case, let i,j,k,ℓ represent the four corners of the plate, then

$$[\lambda] = \text{diag}\,([T_i],[T_i],[T_j],[T_j],[T_k],[T_k],[T_\ell],[T_\ell]) \qquad (89)$$

where

$$[T_i] = \begin{bmatrix} \frac{x_j-x_i}{L_{ij}} & \frac{y_j-y_i}{L_{ij}} & \frac{z_j-z_i}{L_{ij}} \\ \frac{(y_\ell-y_i)(z_j-z_i)}{L_{ij}L_{i\ell}} & \frac{(x_j-x_i)(z_\ell-z_i)}{L_{ij}L_{i\ell}} & \frac{(x_\ell-x_i)(y_j-y_i)}{L_{ij}L_{i\ell}} \\ -\frac{(y_j-y_i)(z_\ell-z_i)}{L_{ij}L_{i\ell}} & -\frac{(x_\ell-x_i)(z_j-z_i)}{L_{ij}L_{i\ell}} & -\frac{(x_j-x_i)(y_\ell-y_i)}{L_{ij}L_{i\ell}} \\ \frac{x_\ell-x_i}{L_{i\ell}} & \frac{y_\ell-y_i}{L_{i\ell}} & \frac{z_\ell-z_i}{L_{i\ell}} \end{bmatrix} \quad (90)$$

is the transformation matrix between the global coordinate system and the local coordinate system at vertex "i". This transformation $[T_i]$ is actually determined by the direction cosines of the two edges ij and iℓ (see Figs. 5,6). In Eq. (90), x_i, y_i, z_i denote the respective coordinates of vertex "i" from the origin and L_{ij}, $L_{i\ell}$ represent the distance between vertices "i" and "j" and vertices "i" and "ℓ", respectively. Moreover, the matrices $[T_j]$, $[T_k]$, $[T_\ell]$ have the same form as $[T_i]$ except that they are determined by the direction cosines of the edges ij and jk, jk and ℓk and iℓ and ℓk, respectively, rather than ij and iℓ.

The transformations of mass and geometrical stiffness matrices may be achieved by a similar procedure.

V. PROCEDURE OF NUMERICAL ANALYSIS AND THE SOFTWARE PACKAGE

In this chapter, first the general procedure is outlined for the plastic dynamic analysis of a structure undergoing large deformations. This is followed by some general information pertaining to the software package that has been developed for the analysis of the class of structures under consideration.

5.1 General Procedure of Numerical Analysis

The general procedure for the numerical analysis of the problem is based on an incremental approach which allows the computation of the response of the structure at discrete time instances. Within each interval of time the structure is assumed to deform as a linear system in order to obtain initial estimates of the incremental deformations. Nonlinear effects due to changes in the geometry of the structure and plastic deformations are then taken into account before considering a new increment of time.

It is assumed that the response of the structure at time $t = t_1$ has already been determined. Considering a sufficiently small increment of time, Δt, the various steps for computing the response of the structure at $t_2 = t_1 + \Delta t$ are outlined below:

1. Using the known accelerations at t_1, the displacements at t_2 can be determined based on a numerical integration algorithm such as the following

$$[q]_{t_2} = [q]_{t_1} + \Delta t[\dot{q}]_{t_1} + 0.5(\Delta t)^2 [\ddot{q}]_{t_1} \qquad (91)$$

in which $[q]$, $[\dot{q}]$ and $[\ddot{q}]$ represent the generalized displacement, velocity and acceleration vectors, respectively. The displacement increment vector $[\Delta q]$ is then defined as follows

$$[\Delta q] = [q]_{t_2} - [q]_{t_1} \tag{92}$$

2. The incremental element displacement vector, $[\Delta U_g]$, with respect to the global (generalized) coordinate system, is determined from $[\Delta q]$ by considering the compatibility between generalized and element displacements. Then, the incremental displacement vector, $[\Delta U]$, with respect to the local (element) coordinate system, is found based on the transformation relations between the global and local coordinate systems, so that

$$[\Delta U] = [\lambda]_{t_1} [\Delta U_g] \tag{93}$$

where $[\lambda]_{t_1}$ refers to the transformation matrix determined on the basis of the deformed configuration of the structure at t_1.

3. Using the incremental element displacement components, the corresponding incremental forces can be found easily by employing the force-deformation properties of the elements. However, it is not necessary at this time to compute all components of the incremental force vectors. Thus, in the case of a beam element, only the

force increment in the axial direction is needed in order to compute the geometric stiffness matrix of the element. In the case of a plate element (see Fig. 2) the components S_1, S_7, S_{13}, S_{19} pertaining to the forces in the x-direction and S_3, S_9, S_{15}, S_{21} in the z-direction, $S_4, S_{10}, S_{16}, S_{22}$ pertaining to the moment around the x-axis and $S_6, S_{12}, S_{18}, S_{24}$ around the z-axis are needed to compute the scalar multiplicative factors operating on the elements of the geometric stiffness matrices. Corresponding approximate stress components σ_x^0, σ_z^0, τ_{xz}^0 may be obtained by dividing the forces S_x^0, S_z^0 and S_{xz}^0 by the thickness of the plate. These forces are computed based on an averaging process of the absolute values of the force components, as follows:

$$S_x^0 = \pm \frac{1}{2L_z} \left(\frac{|S_7+S_{13}|}{2} + \frac{|S_1+S_{19}|}{2} \right) \tag{94}$$

$$S_z^0 = \pm \frac{1}{2L_x} \left(\frac{|S_{21}+S_{15}|}{2} + \frac{|S_3+S_9|}{2} \right) \tag{95}$$

$$S_{xz}^0 = \frac{1}{L_x L_z} \left(\frac{(S_4+S_{10}+S_{16}+S_{22})}{4} + \frac{(S_6+S_{12}+S_{18}+S_{24})}{4} \right) \tag{96}$$

in which L_x, L_z are the dimensions of the plate in the x and z directions, respectively. The sign on the right hand side of the above equations is taken as positive for extension, and negative for compression.

Obviously, this procedure of obtaining the stress components σ_x^0, σ_z^0, and σ_{xz}^0 is only an approximation; nevertheless, it has been utilized by other investigators (for example, see Ref. (30)) and has been indicated that no serious error will occur if sufficiently large numbers of idealized elements are used to assemble the structure.

In the case of a beam element the geometric stiffness matrix is computed based on Eq. (30). The cumulative geometric stiffness matrix (see Eq. (85)) for a plate element is found by adding together the three matrices computed from Eqs. (86) - (88). The geometric stiffness matrix, $[K_G]_{t_2}$, computed in this manner for a beam or plate element reflects the current deformed configuration of the structure at time t_2.

4. The total element stiffness matrix, $[K_{tot}]_{t_2}$, at t_2 is then formed by adding the elastic and geometric stiffness matrices for the element under consideration. Thus,

$$[K_{tot}]_{t_2} = [K]_{t_2} + [K_G]_{t_2} \tag{97}$$

It should be noted that although the elastic stiffness matrix [K] is computed based on the element coordinate system and the small deformation (first order) theory, the effect of the large deformation of the structure enters into the analysis through

the transformation relations pertaining to the deformed and undeformed configurations. Thus, the total element stiffness matrix is transformed to the global coordinate system through a matrix operation represented by Eq. (18), i.e.,

$$[K_{tg}]_{t_2} = [\lambda]^T_{t_2} [K_{tot}]_{t_2} [\lambda]_{t_2} \tag{98}$$

where, $[K_{tg}]$ represents the total element stiffness matrix with respect to the global coordinate system and $[\lambda]_{t_2}$ is the current transformation matrix corresponding to the deformed configuration of the structure at t_2.

Now, considering the entire structure, the generalized stiffness matrix $[k_{tot}]$ for the entire system is obtained in the usual manner, through the application of the stiffness method (27). The basic process involved is that of considering the equilibrium at each nodal point of the forces transmitted by all elements which are incident to that particular node.

5. Although some parts of the structure may undergo plastic deformations, in order to obtain estimates of the element forces, initially the deformations are assumed to be entirely elastic. On this basis, the increments of the stress resultants acting at the nodal points of the element can be found to be

$$[\Delta S] = [K_{tot}]_{t_2} [\Delta U] \tag{99}$$

The total internal forces at time $t = t_2$ are then obtained from

$$[S]_t = [S]_{t_1} + [\Delta S] \tag{100}$$

6. The internal stresses computed above may be used in connection with the Mises-Hencky yield criterion (22) to determine whether the element under consideration undergoes elastic or inelastic deformations. In terms of the stress resultants this criterion is expressed as

$$\Phi(\bar{S}_1, \bar{S}_2, \ldots, \bar{S}_j, \ldots) = Y \tag{101}$$

where $\bar{S}_1, \bar{S}_2, \ldots$, represent the normalized form of the element forces $S_1, S_2, \ldots$, and Y denotes the "yield value" which may change through straining (for simplicity, the subscript t_2 is omitted here and in subsequent discussions, except where necessary).

7. If the yield function Φ is less than Y the element under consideration is deforming elastically. However, if the yield function is greater than Y or equal to Y and its rate of change is positive, then plastic deformations are taking place. If the material of the element is assumed to have isotropic strain hardening properties, subsequent yielding of the element will occur whenever Φ attains a value equal to or greater than the "current" value of Y. However, the consideration of kinematic hardening properties is physically more realistic and accounts for the Bauschinger effect.

If all elements are found to behave elastically within the current time increment, then the accelerations can be found using Eq. (20), but omitting the term [F°]. Then returning to Step 1, the above process can be repeated for the next increment of time.

8. The stress resultants used in forming Φ have been found using stress increments based on elastic considerations. In the case of plastic deformations, these stresses, being only crude approximations to the actual values, do not satisfy the plastic flow relations. Therefore, for a plastically deforming material the correct values of the stress resultants have to be approximated more closely by using the procedure explained below.

As discussed previously, it is assumed that any typical displacement increment ΔU_j may be expressed as the sum of an elastic and a plastic part, i.e.,

$$\Delta U_j = \Delta U_j^e + \Delta U_j^p \tag{102}$$

The increments of the elastic components $[\Delta U^e]$ of each element are related to the internal force increments through the inverse of the total element stiffness matrix

$$[\Delta U^e] = [K_{tot}]^{-1}_{t_2} [\Delta S] \tag{103}$$

9. The j-th plastic component of the displacement increment vector may be found using the generalized form of the Reuss-Mises plastic flow rule, so that

$$\Delta U_j^p = \lambda \frac{\partial \Phi}{\partial \bar{S}_j} \tag{104}$$

where λ is a constant of proportionality which usually changes through straining.

This approach is applicable to the general case of a stress-strain curve as shown in Fig. 7. However, in order to simplify the numerical computations a piecewise linear stress strain curve may be used. For example, the trilinear curve indicated in Fig. 8 is a frequently used approximation. Let H' represent the inelastic loading curve and S the slope of the unloading curve. The initial estimates of the force components may be computed as

$$(\Delta S_j)_{est} = H' \Delta U_j \tag{105}$$

10. The elastic and plastic components of the displacements are then found to be

$$\Delta U_j^e = \frac{(\Delta S_j)_{est}}{S} \tag{106}$$

$$\Delta U_j^p = \Delta U_j - \Delta U_j^e \tag{107}$$

11. Using the current element stiffness matrix (see Eq. (97)), the final values of the force components (stress resultants) may be found from

$$[\Delta S]_f = [K_{tot}][\Delta U^e] \tag{108}$$

12. The above procedure is repeated for all other elements deforming plastically. The vector $[\Delta U^\circ] = [\Delta U^p]$ is then formed and used to find the increments of the equivalent generalized nodal forces due to plastic deformations, i.e.,

$$[\Delta F^\circ] = [k_{tot}][q^\circ] = [\lambda]^T[K_{tot}][\Delta U^\circ] \tag{109}$$

Also,

$$[F^\circ]_{t_2} = [F^\circ]_{t_1} + [\Delta F^\circ] \tag{110}$$

13. The acceleration vector $[\ddot{q}]$ at $t = t_2$ can now be found based on the governing equation of motion for the entire system as given by Eq. (20). Also the velocity vector $[\dot{q}]_{t_2}$ is determined by numerical integration.

14. The entire procedure explained above may be repeated for a new time increment Δt, and in fact for any prescribed number of time increments. Thus, the history of internal forces and displacements of the structure for a given time interval can be determined.

5.2 General Remarks

It should be emphasized that the computation of the plastic displacement components as indicated in Steps 9-11 of the above procedure represents a somewhat simple and perhaps crude method of calculation of these components. The main intent has been to

minimize to the extent possible the size of a fairly complex problem in order to realize solutions that are economically feasible from the computational viewpoint. However, for comparison purposes a more sophisticated method of computation of plastic deformations has also been utilized. This alternative method is based on an iterative scheme aimed at examining the accuracy of estimated quantities at successive steps of iteration.

In the iterative scheme, initial estimates of the incremental element forces are utilized in order to compute the plastic and elastic components of the displacement increments from Eqs. (104) or (106) - (107). An initial value of the effective strain is then calculated by utilizing well known relations, as given for example, by Hill (22). New estimates of the incremental element forces are now found from Eq. (108) and are used to calculate a second set of plastic and elastic displacement components. A new value of the effective strain is then computed and compared with the previously determined value. If the difference between the two values is within a specified tolerance, then the iterative process is terminated. Otherwise, the new estimates of the incremental element forces are used towards a new iterative step.

Comparison of the two methods has been made in the case of a simple structure which was analyzed by means of the computer program discussed in Section 5.3 of this report. Results indicate that there is no significant difference in the two methods. However, before a final conclusion can be reached more extensive

numerical experimentation should be undertaken.

It should also be pointed out that the same general procedure outlined in Section 5.1 can be used in the case of relatively small deformations in the plastic range by neglecting the effect of the geometric stiffness matrix, i.e., not taking into account the matrix $[K_G]$. This is equivalent to formulating the equilibrium equations with respect to the original (undeformed) configuration of the structure. In this manner, the need of recomputing the total stiffness, mass, and transformation matrices at specified time steps is eliminated.

Simplified forms of the general procedure in Section 5.1 may be used to treat the case of the elastic deformations of the structure. Thus, the procedures involved in the elastic static and elastic dynamic analyses of a structure may be deduced easily from the general procedure by following through those steps that are appropriate to each particular type of analysis. It should be emphasized, however, that in the case of the static large deformation analysis, increments in the loading system rather than time have to be considered. For each increment in the load vector the corresponding increment in the displacement vector is computed and added to the previously accumulated displacements. The current total stiffness and transformation matrices are then determined prior to considering a new load increment. This process is continued until the loads attain their final values.

5.3 Plastic Behavior of In-Plane Stressed Plate Element

The implementation of the general procedure in Section 5.1 to the case of a plate element undergoing plastic deformations poses some practical difficulties. If the most general type of plate element with in-plane, bending and twisting action is used, then the element possesses 24 degrees-of-freedom (see Fig. 2), as indicated previously. Thus, if a plate subassembly of an actual structure is modelled by several plate elements of this type, the number of degrees-of-freedom for the structure under consideration would increase rapidly. This may not be as significant in the case of an elastic analysis of the structure, but tends to be critical when attempting a plastic dynamic analysis of the system, due to excessive computational times involved. In such a case, a method of reducing the size of the problem is highly desirable. In this study, a technique has been developed for treating a rectangular plate element with in-plane action as a single degree-of-freedom system only when plastic deformations take place.

Consider the plate element shown in Fig. 9, with 8 degrees-of-freedom at the nodal points corresponding to in-plane action with no rotational displacements at the corners. The degrees-of-freedom are labelled according to the numbering scheme indicated in Fig. 2, and the corresponding stress resultants (generalized stresses) are designated as S_1, S_3, S_7, S_9, S_{13}, S_{15}, S_{19} and S_{21}. Considering the stress resultants acting on each edge of the plate an average shear stress can be found as an approximation to the

stresses acting over the area of the edge. Thus, referring to Fig. 9

$$\tau_A = \frac{S_1+S_7}{2L_x h}$$

$$\tau_B = \frac{S_{13}+S_{19}}{2L_x h} \qquad (111)$$

$$\tau_C = \frac{S_9+S_{15}}{2L_z h}$$

$$\tau_D = \frac{S_3+S_{21}}{2L_z h}$$

An average shear stress for each pair of parallel edges is then found using the stresses computed from Eqs. (111) and utilizing the usual sign convention in the theory of elasticity. Denoting by τ_{AB} and τ_{CD} the average shear stresses acting on the edges parallel to the x and z axes, respectively

$$\tau_{AB} = \mp \frac{|\tau_A|+|\tau_B|}{2} \qquad (112)$$

$$\tau_{CD} = \pm \frac{|\tau_C|+|\tau_D|}{2} \qquad (113)$$

where, the minus sign in Eq. (112) is used when τ_A is positive, while the plus sign in Eq. (113) corresponds to the case of τ_C being positive.

Finally, an average shear stress for the entire plate element is computed as follows

$$\tau_{AV} = \pm \frac{|\tau_{AB}|+|\tau_{CD}|}{2} \qquad (114)$$

The sign in Eq. (114) is chosen to concide with the sign of either τ_{AB} or τ_{CD}. This is based on whether $|\tau_{AB}|>|\tau_{CD}|$, or $|\tau_{AB}|<|\tau_{CD}|$. In the former case, the sign of τ_{AV} is taken to be the same as that of τ_{AB}, and in the latter case it is chosen to be the same as that of τ_{CD}. In implementing the above procedure in a computational algorithm several intermediate checks are performed to verify that the plate is in equilibrium in both the x and z directions within specified tolerances.

The average shear stress found from Eq. (114) for each plate element is then used in connection with the procedure in Section 5.1 to determine whether plastic deformations are taking place in the element. Also, in the computer program, τ_{AV} is automatically checked against the ultimate stress of the material (see Fig. 8) to determine whether the element has failed due to excessive straining. If the ultimate stress is not exceeded but plastic deformations have been found to take place, then an initial estimate of the actual shear stress, τ_{est}, in the element is computed from

$$\tau_{est} = \tau_{t_1} \pm \left(\frac{|\tau_{AV}| - Y}{S}\right) H' \qquad (115)$$

where, τ_{t_1} refers to the known shear stress in the element at the end of time t_1, and as before, H' and S pertain to the slope of the inelastic loading and elastic unloading curve, respectively, and Y is the current yield value. The sign in front of the second term on the right hand side of Eq. (115) is chosen to agree with the sign of τ_{t_1}.

The equivalent element nodal force increment vector, $[\Delta S^{\circ}]$, due to plastic deformations can now be found based on the usual procedure in the application of the initial strain method (20), i.e., referring to the jth equivalent element force increment ΔS_j°

$$\Delta S_j^{\circ} = (S_j)_{t_2} \left(\frac{\tau_{AV} - \tau_{est}}{\tau_{AV}}\right) \tag{116}$$

where, the $(S_j)_{t_2}$'s are again calculated from Eqs. (99) and (100). The transformation of the equivalent element force increment vectors of all plate elements to the global coordinate system and consideration of the equilibrium conditions at each nodal point yields the vector $[\Delta F^{\circ}]$. The usual procedure outlined in Section 5.1 is then followed. As explained in the previous section, an iterative scheme can also be used in order to improve on the values of the estimated stresses.

5.4 The Software Package

A general purpose computer program has been developed for the analysis of frame and plate structures. This program represents an extension of a previously reported (31) computer program known as the GWU-FAP (George Washington University - Frame Analysis Program) which deals with the analysis of rigid frame structures. Extensions to GWU-FAP have been accomplished in order to incorporate a rectangular thin plate element and to develop the capability for second order (large deformation) analysis that accounts for geometric nonlinearities. In addition, the plastic dynamic analysis branch of the program has been augmented in order to

allow for the analysis of structures consisting of in-plane stressed rectangular plate elements (see Section 5.3). A simplified form of the flow chart for the modified GWU-FAP is presented in Appendix B.

The modified GWU-FAP is a general purpose program which enables the user to perform the following types of analysis for both frame and/or plate structures (with certain exceptions in the case of a plastic dynamic analysis as explained below):

(a) Elastic static small deformation (first order) analysis

(b) Elastic static large deformation (second order) analysis which considers the effect of geometric nonlinearities

(c) Free vibration analysis leading to the natural frequencies and modes of vibration, using the consistent mass matrix of the structure

(d) Elastic dynamic first order analysis

(e) Elastic dynamic second order analysis

(f) Plastic dynamic first order analysis of structures consisting of beam or in-plane stressed rectangular plate elements.

When performing any of the above types of analysis for a rigid (skeletal) frame, the structure is modelled as an assembly of plane or three-dimensional beam elements, depending on the loading and deformation states of the structure. When considering a structure which contains rectangular plate elements, different types of plate action may be distinguished. In the present study, five possible modes of plate action have been

considered and are classified according to the following scheme:

Class 1 - In-plane action without rotational displacement at the nodes.

This type of element possesses 8 degrees-of-freedom corresponding to element coordinate directions 1,3,7,9,13,15,19 and 21 indicated in Fig. 2 (see also Fig. 9).

Class 2 - In-plane action with rotational displacements at the nodes.

This type of element possesses 12 degrees-of-freedom corresponding to element coordinate directions 1,3,5,7,9,11,13,15,17,19,21 and 23 indicated in Fig. 2 (see also Fig. 3).

Class 3 - Bending action only.

This type of plate element also has 12 degrees-of-freedom represented by coordinate directions 2,4,6,8,10,12,14,16,18,20,22 and 24 in Fig. 2 (see also Fig. 4).

Class 4 - Bending and in-plane action without rotational displacements at the nodes.

This type of plate element possesses 20 degrees-of-freedom represented by element coordinate directions 1,2,3,4,6,7,8,9,10,12,13,14,15,16,18, 19,20,21,22 and 24 in Fig. 2.

Class 5 - Bending and in-plane action with rotational displacements at the nodes.

This type of plate element is the most general type used in the present study and possesses 24 degrees-of-freedom as indicated in Fig. 2.

Any of the above classes of rectangular plate elements may be used when performing an analysis of type (a) through (e) for a structure consisting of plate elements or a combination of beam and plate elements. On the other hand, in the case of a structure containing rectangular plate elements, a plastic dynamic analysis corresponding to type (f) can be performed only with Class 1 plate elements.

The computer program has been designed so as to minimize the amount of input needed for any of the above types of analysis. Most of the input information to be supplied by the user of the program pertains to the type of the structure, its geometry, its material, cross-sectional and inertial properties, the type and duration of loading and the type of analysis desired. The input format for some typical structures corresponding to different types of analysis is given in Appendix C.

The computer program is written in Fortran IV language for use on an IBM-OS/360 digital computer. It has been made operational on both the APL Model 91 and the George Washington University Model 50 Computer System.

VI. COMPUTER ANALYSIS OF TYPICAL STRUCTURES-SUMMARY OF NUMERICAL RESULTS

The software package discussed in the previous chapter is used here to obtain solutions to typical problems. For this purpose, different types of structures are analyzed and the results of the numerical solutions are summarized in this chapter. Several of the solutions presented in the initial part of the chapter pertain to simple structures and serve the purpose of checking the various branches of the computer program by comparing with known solutions.

6.1 First Order Static Analysis of a Plate

One of the simplest type of structures considered in this study for the purpose of testing the computer program consists of a simply supported plate with a concentrated load at the center. Both rectangular and square plates with dimensions (length x width x thickness) 40 x 20 x 0.50 in and 20 x 20 x 0.50 in, respectively, are used. The other constants are:

Young's Modulus: $E = 30 \times 10^6$ lb/in^2

Poisson's Ratio: $\nu = 0.3$

Concentrated load: $P = 10{,}000$ lb.

The type of plate element used corresponds to Class 3, described in Section 5.4. As mentioned previously, this type of plate element is subjected only to bending action, and possesses 3 degrees-of-freedom at each node (corner) point, or,

a total of 12 degrees-of-freedom. In order to compare the accuracy of the numerical results, solutions are obtained for the rectangular plate by subdividing it into 4, 16, and 32 plate elements; similarly, solutions are obtained for the square plate by subdividing it into 4 and 16 elements.

Table 3 shows the comparison of the center deflections of the plate obtained by the finite element method and the exact method as given in Timoshenko (8):

TABLE 3 - STATIC ANALYSIS OF SIMPLY SUPPORTED PLATE--COMPARISON OF CENTRAL DEFLECTION BETWEEN FINITE ELEMENT AND EXACT METHODS

Displacements (in)		
Square Plate a = 20 in		Rectangular Plate a = 20 in b = 40 in
4 Elements	.11767	.16920
16 Elements	.12564	.17706
32 Elements	--	.18332
Timoshenko (6) (exact)	.1351	.1923

It may be observed that in both cases the solutions appear to converge to the exact values as the number of elements is increased.

6.2 Free Vibration Analysis of a Simply Supported Plate

A free vibration solution is obtained for a simply supported square plate with the following physical input:

Young's Modulus: $E = 30 \times 10^6$ lb/in^2

Dimensions of plate: a x b x h = 20 x 20 x 0.50 in

Poisson's Ratio: $\nu = 0.3$

Density of plate: $\rho = 0.001$ lb-sec^2/in.

Again, a Class 3 plate element is used in modelling the structure which is subdivided into 4 and 16 elements.

The theoretical results used for comparison are obtained from Volterra (32). The eigenvalues, ω_{mn}, and the corresponding eigenvectors, $W_{mn}(x,y)$, for the problem under consideration are given as follows:

$$\omega_{mn} = \pi^2 \beta \left(\frac{m^2}{a^2} + \frac{n^2}{b^2}\right) \tag{117}$$

$$W_{mn}(x,y) = \sin\left(\frac{m\pi x}{a}\right) \sin\left(\frac{n\pi y}{b}\right) \tag{118}$$

where

$$\beta = Eh^2/(12\rho(1-\nu^2)),$$

is a numerical constant.

Table 4 shows the comparison of the fundamental frequencies between results obtained by the use of Eq. (117) and the finite element method as applied in this study.

TABLE 4 - FREE VIBRATION OF SIMPLY SUPPORTED SQUARE PLATE--
COMPARISON OF FUNDAMENTAL FREQUENCIES BETWEEN
FINITE ELEMENT AND EXACT METHODS

	4 elements	16 elements	Volterra(22)-(exact)
Fundamental Frequency	.217630E0cyc/sec	.212534E03cyc/sec	.205913E03cyc/sec
Corresponding Period	.459496E-02 sec.	.470513E-02 sec.	.485642E-02 sec.

It may be seen that even with the use of a small number of elements the finite element solutions are fairly close to the exact solution.

Table 5 shows the comparison of the fundamental normal mode shape between the finite element (16 elements) and the exact method.

TABLE 5 - FREE VIBRATION OF SIMPLY SUPPORTED SQUARE PLATE--COMPARISON OF FUNDAMENTAL NORMAL MODE SHAPES BETWEEN FINITE ELEMENT AND EXACT METHODS

Volterra (32) (exact)		16 Elements (39 degrees-of-freedom)	
-0.536411E-01	-0.478539E-04	-0.549793E-01	-0.665452E-07
-0.758360E-01	0.340921E 00	-0.777525E-01	0.340488E 00
-0.535734E-01	0.338058E-04	-0.549791E-01	0.110401E-06
0.536411E-01	-0.536749E-01	0.549792E-01	-0.549792E-01
0.241449E 00	-0.758359E-01	0.240762E 00	-0.777516E-01
-0.379180E-01	0.535734E-01	-0.388762E-01	0.549787E-01
0.379180E-01	0.241144E 00	0.388764E-01	0.240760E 00
0.341353E 00	0.379659E-01	0.340489E 00	0.388763E-01
-0.536072E-01	0.378701E-01	-0.549791E-01	0.388761E-01
-0.338485E-04	0.340921E 00	-0.503340E-07	0.340487E 00
0.241144E 00	0.536749E-01	0.240762E 00	0.549793E-01
-0.378701E-01	-0.338058E-04	-0.388761E-01	-0.116132E-06
-0.379659E-01	0.240840E 00	-0.388764E-01	0.240760E 00
-0.536410E-01	0.379179E-01	-0.549790E-01	0.388762E-01
0.758360E-01	-0.379179E-01	0.777519E-01	-0.388762E-01
0.341353E 00	-0.535733E-01	0.340488E 00	-0.549784E-01
0.338485E-04	0.536410E-01	0.144227E-07	0.549785E-01
0.536072E-01	0.758359E-01	0.549793E-01	0.777512E-01
0.482593E 00	0.535733E-01	0.481525E 00	0.549783E-01
0.478539E-04		0.443147E-07	

Comparison between the two methods indicates that in most cases the agreement is good, except when the amplitude of vibration is very small. This is attributed to rounding and truncation errors in the computational process.

A comparison of higher frequencies corresponding to the two methods is shown in Table 6.

TABLE 6 - FREE VIBRATION OF SIMPLY SUPPORTED SQUARE PLATE--COMPARISON OF HIGHER FREQUENCIES OF VIBRATION BETWEEN FINITE ELEMENT AND EXACT METHODS

4 Elements	16 Elements	(m,n)	Volterra (22) (exact)
.217630E03/sec.	.212534E03/sec.	(1,1)	.205913E03/sec.
.614070E03/sec.	.530795E03/sec.	(1,2)	.514782E03/sec.
.614070E03/sec.	.530796E03/sec.	(2,1)	.514782E03/sec.
.123725E04/sec.	.870523E03/sec.	(2,2)	.823651E03/sec.
	.106759E04/sec.	(1,3)	.102956E04/sec.
	.106759E04/sec.	(3,1)	.102956E04/sec.
.131904E04/sec.	.142567E04/sec.	(2,3)	.133843E04/sec.
	.142567E04/sec.	(3,2)	.133843E04/sec.

It is worth noting that, even with only 16 plate elements, the comparison of higher frequencies obtained in this study with the frequencies given in Volterra (32) is in general favorable even for the higher frequencies of vibration.

6.3 Second Order Static Analysis of a Square Plate

The second order static analysis of a square plate under a concentrated load at the center is studied in this section.

Two types of boundary conditions are used for this structure: (1) all four edges clamped and (2) all four edges simply supported. The plate dimensions are 30 x 30 x 0.25 in, Young's modulus and Poisson's ratio are taken as 30×10^6 lb/in^2 and 0.3, respectively.

For the purpose of comparison with the work of other investigators, the type of plate element chosen is of Class 4 (see Section 5.4). This type of plate element is subjected to bending and in-plane action without rotational degrees of freedom at the nodes. The ultimate load is 50,000 lb., and 16 elements are used to idealize the square plate. Numerical results corresponding to the clamped plate solution are compared with results obtained by Brebbia and Connor (12), and Adotte (33). Table 7 below, shows the similarities and differences among the three methods.

TABLE 7 - COMPARISON OF METHODS USED IN SOLVING THE NONLINEAR PROBLEM OF A SQUARE PLATE CLAMPED AT FOUR EDGES WITH A CONCENTRATED LOAD AT THE CENTER

	Adotte	Brebbia and Connor	Present Study
Method	Finite difference and experimental	Finite element	Finite element
Number of Elements	--	36	16
Degrees-of-freedom at each corner	--	5	5
In-plane displacement functions	--	simpler	more complex
Numerical procedure	--	used linearized equations for a limited number of load steps, then applied corrections based on a Newton-Raphson iterative method	100 piecewise linear incremental steps

Figure 10 shows the results obtained by the three different methods. It is seen that Adotte's curve is enveloped by the curve obtained in the present study and that of Brebbia and Connor, with the former below and the latter above it. All three results are, however, very close, and the characteristic of the second order analysis in which the structure becomes stiffer as the load increases is clearly evident.

Figure 11 shows the results of both the clamped plate and simply supported plate plotted on a different scale with the coordinate axes switched around. Both curves show the same characteristic of increasing stiffness of the structure with increasing load.

6.4 First and Second Order Static and Elastic Dynamic Analysis of a Beam-Plate Assemblage

In this section is presented the analysis of a beam-plate assemblage including the first and second order static, the free vibration, and the first and second order elastic dynamic analysis. The structure consists of a horizontal square plate elastically supported by four edge beams which, in turn, are supported in the vertical direction by four edge beams. The plate is subjected to a uniformly distributed load.

The following numerical values are used for the problem under consideration:

Plate dimensions: 30 x 30 x 0.25 in

Poisson's ratio: $\nu = 0.3$

$I_x = 0$

EI_z = aD, where a is the length of square plate and D the plate stiffness.

Both a total of 4 and 16 Class 3 plate elements are used to idealize the square plate in order to compare results with solutions given by other investigators, such as, Timoshenko (8) and Zienkiewicz (13). For this purpose, initially a uniformly distributed load q = 1 lb/in^2 is used. A comparison of the results is given in Table 8.

TABLE 8 - FIRST ORDER STATIC ANALYSIS OF A SQUARE PLATE WITH FOUR EDGE BEAMS--COMPARISON OF RESULTS WITH KNOWN SOLUTIONS

	Center Point Deflection	Deflection at mid-point of edge
4 Elements	0.1274	0.0626
16 Elements	0.1584	0.0713
ν = 0.30		
Timoskenko (exact)	0.1639	not available
ν = 0.25		
Zienkiewicz	0.1639	0.0697
36 Elements		
ν = 0.30		

It is seen from the above table that the 16 element solution obtained in this study agrees fairly closely with the solutions given by Timoshenko and Zienkiewicz.

6.4.1 Second Order Static Analysis - A uniform load of 10 lb/in^2 is now applied to the plate in order to study the effect of geometric nonlinearities. For this purpose a second order analysis

is performed using a total of 100 incremental steps. Fig. 12 shows the force-deformation curve for the center of the plate and for the mid-point of the edges. For comparison purposes, also the first order force-deformation curve is plotted. It may be observed again that the structure tends to become stiffer as the intensity of the load is increased.

6.4.2 Free Vibration Analysis - The free vibration analysis of the structure under consideration yields the following results:

Lowest Frequency = 0.766 cyc/sec.

Largest Period = 1.31 sec.

Highest Frequency = 410.6 cyc/sec.

Smallest Period = 0.0024 sec.

6.4.3 First and Second Order Elastic Dynamic Analysis - The frequencies and periods from the free vibration analysis may be used as a guideline for the numerical input to the elastic dynamic analysis. Thus, a time increment of 0.001 seconds and a final time of 2.7 seconds is used for the numerical integration process as applied to the first order analysis. In the case of the second order dynamic analysis, a smaller time increment has to be used since the structure becomes stiffer as the deformations increase, due to stretching of the middle surface of the plate. It has been found that a time increment of 0.0001 seconds satisfies the stability criterion for the numerical integration algorithm and yields satisfactory results.

For the first order dynamic analysis, uniformly distributed loads of intensity 1 and 10 lb/in^2 are used. In the case of the

second order analysis load intensities of 1,2,5 and 10 lb/in^2 are utilized in conjunction with an incremental procedure. For comparison purposes the time-history curves from both analyses are plotted on the same figure (Fig. 13).

Curves S_1 and S_{10} in Fig. 13 correspond to the first order dynamic analysis for load intensities of 1 and 10 lb/in^2, respectively. Within a time interval of 2.4 seconds, two nearly identical complete cycles are seen for each curve, each possessing a period of oscillations of about 1.2 seconds, but, of course, differing in amplitude by a factor of approximately 10. The corresponding static displacements can be found from Fig. 12 and although not plotted on Fig. 13, they represent horizontal equilibrium lines for the dynamic oscillations.

Curves L_1 and L_{10} in Fig. 13 represent results obtained based on a second order analysis for similar load intensities of 1 and 10 lb/in^2, respectively. Those two curves clearly demonstrate the difference between the first and second order analyses. Within the same time interval of 1.2 seconds, approximately four complete cycles appear for the 1 lb/in^2 loading and twelve complete cycles for the 10 lb/in^2. The maximum amplitudes are much smaller than those of the first order analysis. This is because the plate becomes stiffer due to the stretching of the middle surface. It is also seen that initially, the results for both first and second order analyses are quite close (as may be observed by comparing curve S_{10} with L_{10} and S_1 with L_1). However, after some time has elapsed (for a load intensity

of 10 lb/in^2, this corresponds to about 0.2 seconds, and in the case of 1 lb/in^2, to about 0.4 seconds), the solutions of the first and second order dynamic analyses become markedly different.

Figures 14 shows the comparison of second order dynamic analyses for uniformly distributed loads of different intensities. Curves L_1, L_2, L_5, and L_{10} represent the time history of the center deflection of the square plate under uniformly distributed loads of 1, 2, 5, and 10 lb/in^2, respectively.

These curves show the following characteristics:

(1) All curves are periodic, or at least tend to be periodic, after some initial time has elapsed, since no damping has been introduced into the analysis.

(2) The period of oscillations becomes shorter as the load increases. There are about five complete cycles in L_1 but about fifteen or more complete cycles in L_{10} for the same time interval. Again, this reveals the fact that the plate is much stiffer and vibrates much faster as the load increases.

(3) The amplitudes of oscillations increase but in a nonlinear manner due to the nonlinear stiffness properties of the structure.

6.5 Square Plate Subjected to a Lateral Load and In-Plane Compressive Forces

In this section is discussed both the elastic static and dynamic analyses of a simply supported square plate under a lateral concentrated load at center and uniform compressive forces in the x-direction.

Up to now, only one direction of loading has been considered. When a plate is under the effect of both a lateral load and a uniform compressive load acting in its middle plane, the work done by both the transverse load and the compressive forces has to be considered in formulating the solution to the problem. This problem may be solved by using the analytical expressions given in Chapter IV since the work done by the compressive forces is equivalent to the last term on the right hand side of Eq. (50). In order to compare results with Timoshenko (16), the case of a simply supported square plate under a concentrated load at center and uniformly compressed in the x-direction is considered. The deflection surface of a simply supported rectangular plate as given by Timoshenko is:

$$W(x,z) = \sum_{m=1}^{\infty} \sum_{n=1}^{\infty} A_{mn} \sin \frac{m\pi x}{a} \sin \frac{n\pi z}{b} \tag{119}$$

where

$$A_{mn} = 4P \sin \frac{m\pi\xi}{a} \sin \frac{n\pi\eta}{b} / abD\pi^4 \left[\left(\frac{m^2}{a^2} + \frac{n^2}{b^2}\right)^2 - \frac{m^2 N_x}{\pi^2 a^2 D}\right] \tag{120}$$

and, P represents the concentrated force at the point (ξ,η), N_x is the compressive force in the x-direction.

It is seen that when $N_x = 0$, the above equation reduces to the solution of a simply supported rectangular plate under a lateral concentrated load. In order to compare results, the concentrated load, P, is kept constant at 1000 lb., acting at

the center of the square plate, whereas N_x is varied. In the present solution by the finite element method, in most cases a total of 16 Class 4 (see Section 5.4) plate elements are used to idealize the square plate. The numerical constants used in the first order static analysis are:

Young's Modulus $E = 30 \times 10^6$ lb/in^2.

Poisson's ratio $\nu = 0.3$.

Dimensions of plate = 30 x 30 x 0.25 in.

Flexural rigidity, $D = 0.429258 \times 10^5$ lb-in.

As long as the denominator on the right hand side of Eq. (120) does not approach zero, the double series on the right hand side of Eq. (119) converges rapidly. Hence the solution obtained by the finite element method is compared only with the first term of the series using the coefficient A_{11}, and the results of the comparison are shown in Table 9.

TABLE 9 - FIRST ORDER STATIC ANALYSIS OF A SIMPLY SUPPORTED SQUARE PLATE UNDER A 1000 LB. LOAD AT CENTER AND UNIFORM COMPRESSIVE FORCES IN THE X-DIRECTION--COMPARISON OF CENTRAL DEFLECTION BETWEEN FINITE ELEMENT AND EXACT METHODS

Deflection - Inches			
N_x (lb/in)	F.E. Method		Timoshenko (24) (exact)
	4 Elements	16 Elements	
0	----	.22615	.21489
100.	----	.23694	.22694
200.	----	.24892	.24041
400.	----	.27727	.27280
600.	----	.31358	.31528
800.	----	.36180	.37342
1000.	.39909	.42901	.45787
1200.	----	.52926	.59166
1400.	----	.69523	.83592
1600.	----	1.02366	1.42366
1800.	----	1.98451	4.7953
1900.	----	----	∞

It may be observed that, in general, the comparison is fairly good for N_x less than 1200 lb/in. However, when N_x is greater than 1200 lb/in, A_{11} increases very rapidly due to the fact that its denominator tends to become very small. This is because the critical value of N_x is between 1800 to 1900 lb/in.

The same structure is now analyzed by performing a second order static analysis to determine the center deflection of the plate. The loads are increased to their final values by applying 10 equal increments. Table 10 shows a comparison of the accuracy between a 4 and 16 element idealization of the square plate, with P = 1000 lb., and N_x = 1000 lb/in.

TABLE 10 - SECOND ORDER STATIC ANALYSIS OF A SIMPLY SUPPORTED SQUARE PLATE WITH P = 1000 LB AT THE CENTER AND UNIFORM COMPRESSIVE FORCES N_x = 1000 LB/IN--COMPARISON OF CENTRAL DEFLECTION FOR 4 AND 16 ELEMENT IDEALIZATIONS

Deflection - Inches		
Step	16 Elements	4 Elements
1	.02369	.02221
2	.04807	.04503
3	.07188	.06729
4	.09397	.08793
5	.11372	.10642
6	.13107	.12272
7	.14624	.13704
8	.15957	.14968
9	.17134	.16089
10	.18182	.17091

The values in the last line of Table 10 represent the deflections at the center of the plate when the loads have attained their full values. It is seen that the difference between the two idealizations is about 6%.

The effect of geometric nonlinearities can best be studied by varying both the lateral load and in-plane compressive forces applied in the x-direction. For this purpose, values of P = 500, 1,000, 2,000, 10,000 lb. and N_x = 0, 1,000, 2,000, 3,000 and 4,000 lb/in. are used. The results of the investigation are summarized in Table 11.

TABLE 11 - SECOND ORDER STATIC ANALYSIS OF A SIMPLY SUPPORTED SQUARE PLATE WITH VARYING LATERAL AND COMPRESSIVE FORCES-- COMPARISON OF CENTRAL DEFLECTIONS

	Deflection - Inches				
P \ N_x	0	1000	2000	3000	4000
500	.0932	.1118	.1364	.1644	.1904
1000	.1542	.1709	.1891	.2079	.2264
2000	.2312	.2440	.25695	.2700	.28292
10000	.48755	.49481	.50235	.51026	.51865

It may be observed from the above table that for smaller lateral concentrated loads, the effect of varying N_x on the deflection of the plate is much more pronounced. For large values of P, large deformations of the plate are accompanied by stretching of the middle surface. This, in turn, nearly counteracts the compressive effect of the in-plane forces.

An elastic dynamic analysis has also been performed for the same structure. Initially, a free vibration solution is obtained which indicates that the largest period is about 0.7 seconds. Therefore, a time interval of 1.4 seconds is used for the numerical solution process in the forced vibration analysis. The time increment used is 0.001 seconds. In Fig. 15 are shown the time-history curves corresponding to the first order dynamic analysis. Curves D_{N_x}, S_{N_x} are the dynamic and static displacement curves for P = 2000, N_x = 1000; D_o, S_o are the dynamic and static displacement curves for P = 2000, N_x = 0. It is seen that D_{N_x} has a much greater amplitude and slightly longer period of oscillations than D_o. In fact, the fundamental period obtained from the free vibration analysis no longer matches the period of oscillations corresponding to response curve D_{N_x}, due to the existence of the in-plane compressive forces.

6.6 First Order Elastic and Plastic Dynamic Analysis of a Plate Structure

In several of the numerical solutions presented in this chapter, it has been assumed that the stresses and strains in every part of the structure remain elastic even when large deformations are taking place. In such cases it is more realistic to take into account plasticity effects which are brought about by the yielding of the material. To accomplish this the "Plastic Dynamic" branch of the computer program discussed in Section 5.4 is used to solve some typical problems.

One of the simple structures considered for this purpose consists of a square plate which is fixed along one of its edges and free along the others (see Fig. 16). The dimensions of the plate are 30 x 30 x 0.50 in. The structure is discretized using 4 plate elements corresponding to Class 1, as discussed in Section 5.4. This type of plate element can sustain only in-plane action without twist at the corner nodes. As shown in Fig. 16, three concentrated in-plane loads of magnitude F = 100 kips are applied in the x-direction at the nodes C, D and E on the free edge of the plate parallel to the fixed support. For comparison purposes, first a static analysis of the structure is performed. The results indicate that the maximum displacement due to the applied loads is 0.146 in. and occurs in the x-direction at the nodes C and E. The corresponding displacement at node D is 0.137 in. Likewise, in order to obtain an estimate of the time increment of integration to be used in the dynamic analysis of the structure, a free vibration analysis is first performed. The results of this analysis are

Lowest Frequency = 25.88 cyc/sec.

Largest Period = 0.0386 sec.

Highest Frequency = 233.7 cyc/sec

Smallest Period = 0.0043 sec.

Based on the above results, an elastic and plastic dynamic analysis of the structure is performed. The same concentrated loads used in the static analysis are now applied to the structure dynamically and are assumed to remain constant with time.

A time increment of 0.0002 sec. is used for the numerical integration process. In the case of the plastic dynamic analysis a trilinear stress-strain curve is used. Referring to Fig. 8, the values of the various parameters defining the curve are:

Param. 1: Stress σ_1 = 20,000 lb/in^2

Param. 2: Slope 2 = 11.50 x 10^6 lb/in^2

Param. 3: Stress σ_2 = 33,000 lb/in^2

Param. 4: Slope 3 = 2.50 x 10^6 lb/in^2

Param. 5: Ultimate Stress = 130,000 lb/in^2

Param. 6: Yield Point Stress = 33,000 lb/in^2

It should be pointed out that initially a more realistic value of 65,000 lb/in^2 was used for the ultimate stress of the material. However, it was found that the average stresses in some elements exceeded the ultimate stress. This, in turn, led to an automatic interruption of the computer analysis, as explained in Section 5.3.

The time-history curve of the x-displacement at node C for both the elastic and plastic dynamic analysis is plotted in Fig. 17. A comparison of the two curves indicates that in the case of plastic deformations there is an increase of about 5% in the maximum displacement and a slight increase in the period of oscillations. However, the main difference between the results of the two analyses is that plastic deformations are accompanied by an noticeable permanent set, as may be seen from Fig. 17.

6.7 Elastic and Plastic Dynamic Analysis of a Plane Frame

The structure considered in this case consists of a plane frame, as indicated in Fig. 18(a), that was previously analyzed

in Ref. (25). The frame is made up of standard 4 inch diameter steel pipe whose cross-sectional area A = 3.174 in^2 and the moment of inertia I = 7.233 in^4. Furthermore, the modulus of elasticity E is taken to be 29 x 10^6 lb/in^2, and a value of 46,000 lb/in^2 is used for the yield value of the material. For simplicity in the computation of plastic deformations a bilinear stress-strain curve is used, with the inelastic branch having a slope of 1/10 of that of the elastic branch. The loading consists of two dynamically applied forces, F_V = 20 kips and F_H = 5 kips having a rise time of 0.20 seconds, as shown in Fig. 18(b).

The time-history of deflection at the point of application of the vertical load is shown in Fig. 19. Also included in the figure is the corresponding deflection if the loads are applied statically and the structure is assumed to respond as a linear system. The three time history curves shown in the figure correspond to the elastic dynamic response with or without geometric nonlinearity effects, and the plastic dynamic response of the structure. As may be observed, the dynamic character of the load results in a dynamic load factor of approximately 2.0 for the case where the effects of geometric nonlinearities are neglected (first order analysis). However, when such effects are retained (second order analysis) the load factor increases to approximately 2.4 (20% increase). In the case of inelastic deformations, the dynamic load factor becomes much larger. This is due to the large magnitude of the applied loads which causes initiation of yielding at an early stage of the response (i.e., at approximately

0.16 sec.) and thus leads to considerable inelastic deformations.

6.8 Elastic and Plastic Dynamic Analysis of a Three-Dimensional Structure Consisting of In-Plane Stressed Plate Elements

The static, elastic and plastic dynamic analysis of the structure shown in Fig. 20 is studied in this section. The structure is composed of aluminum plates of uniform thickness. It consists of three vertical walls (parallel to the y - z plane) at 6 ft. apart and three horizontal floor decks at 2 ft. apart. The plate thicknesses chosen are 1/8 in. for the vertical walls and upper deck and 1/16 in. for the lower two decks. The structure is supported rigidly along the bottom edges of the vertical walls and is restrained from movement in the x-direction.

A discrete model of the structure is obtained by inserting a node at each corner point corresponding to the interconnection between vertical and horizontal members. In this manner, each vertical wall is subdivided into three and each deck into two plate elements. These plate elements are of the type that can sustain only in-plane stresses (see Sections 5.3 and 5.4) with no twisting action. Thus, at each node point only a translational movement in the y and z-directions is allowed, and therefore the number of degrees of freedom for the entire structure is 36.

The structure is subjected to a concentrated load of $F = 900$ kips applied at node 16 and acting in the positive z-direction. Initially, the load is considered to act statically in order to determine the static displacement distribution of the structure. Numerical results indicate that, as expected, the

maximum displacement occurs in the direction of the applied load and is equal to $0.^{887}$ in. Also, a free vibration analysis of the structure has been performed leading to the following results:

Lowest Frequency = 236.2 cyc/sec.

Largest Period = 0.00423 sec.

Highest Frequency = 4540 cyc/sec.

Smallest Peroid = 0.00022 sec.

It may be observed that the three-dimensional character of the structure results in a fairly stiff system and corresponding high frequencies of vibration. Although not plotted here, a study of the fundamental mode of vibration indicates that the structure deforms in a manner analogous to a cantilever beam. Thus, as far as the z-direction is concerned, all nodal points move together in the same direction. However, the movement in the y-direction is such that while all points in the frontal plane (parallel to the x-y plane) move in one direction, all points in the rear plane (x-y) plane move in the opposite direction.

The same concentrated load used in the static analysis is now applied to the structure dynamically and is assumed to remain constant with time. The elastic dynamic response of the structure is first obtained by assuming the structure to act as a linear elastic system. The time-history curve of the displacement in the direction of the applied load is shown in Fig. 20. Some secondary oscillatory effects are observed in the plot due to the interaction between inertial effects in the two perpendicular directions and the superposition of higher modes of vibration.

For the plastic dynamic analysis a trilinear stress-strain curve is used as represented by Fig. 8. The following values of the parameters are used in this case:

Param. 1: Stress σ_1 = 6,530 lb/in^2

Param. 2: Slope 2 = 3.87 x 10^6 lb/in^2

Param. 3: Stress σ_2 = 20,800 lb/in^2

Param. 4: Slope 3 = 0.03 x 10^{6}lb/in^2

Param. 5: Ultimate Stress = 30,000 lb/in^2

Param. 6: Yield Point Stress = 20,800 lb/in^2

The same magnitude of the load, i.e., F = 900 kips, is used in the plastic dynamic analysis of the structure. The time-history curve of the displacement in the direction of the load is plotted also in Figure 21. The same oscillatory behavior is observed as the case of the elastic dynamic analysis, however, the displacements are larger. Also, plastic action is accompanied by relatively large permanent deformations, indicating possible damage to the structure.

VII. SUMMARY AND CONCLUSIONS

A procedure of analysis has been presented for determining the plastic dynamic response of structural systems consisting of beam and rectangular plate elements. The analysis takes into account both the geometric and material nonlinearities.

The general approach to the problem is based on the finite element method using displacement interpolation functions. The strain energy expressions for both the beam and plate elements are obtained and are used to generate the stiffness and mass matrices of the elements. Also, the geometric stiffness matrices are derived that account for the effect of geometric nonlinearities. Plastic deformations are taken into account by means of an incremental theory of plasticity coupled with the concept of initial strain. The governing dynamical equation of the system is written based on Hamilton's Principle.

A general purpose computer program has been constructed based on the analytical procedures developed in this study. Although the program is primarily intended for the solution of plastic dynamic problems, it can also be used to perform an elastic static or elastic dynamic analysis with or without geometric nonlinearities, as well as a free vibration analysis. The program is used in this study to solve several simple structures subjected to static or dynamic loads. It is found that even with the use of a relatively small number of elements of the type chosen in this study, the results agree fairly well

with solutions given by other investigators (whenever such solutions are available). Results also indicate that both material and geometric nonlinearities have a significant effect in the total deformation of structures which consist of beam and plate elements. In the case of plate structures subjected to large bending effects, it is found that tension in the middle surface of the plate causes a significant stiffening and an appreciable change in the vibrational characteristics of the structure.

In conclusion, the feasibility of the numerical procedure developed in this study has been demonstrated by the solution of some simple problems. The computer program generated as a result of this study should be a useful tool to structural analysts. However, further numerical experimentation may be needed before the full potential of the program is realized.

ACKNOWLEDGMENTS

Portions of this report pertaining to the properties of the rectangular plate element are based on the doctoral dissertation of H. K. Huang submitted to the George Washington University. This dissertation was prepared under the direction of and in close cooperation with T. G. Toridis, the author of this report. The author is also grateful to E. A. Akkoush and K. Khozeimeh, graduate research assistants at the School of Engineering and Applied Science of the George Washington University, for their assistance and cooperation in the development of the computer program GWU-FAP, used in this study.

The author is indebted to Dr. Shou-ling Wang of Code 1745, the immediate supervisor of this project, for his skillful guidance and cooperation. The project was under the general supervision and guidance of Mr. Edward Habib of Code 1745.

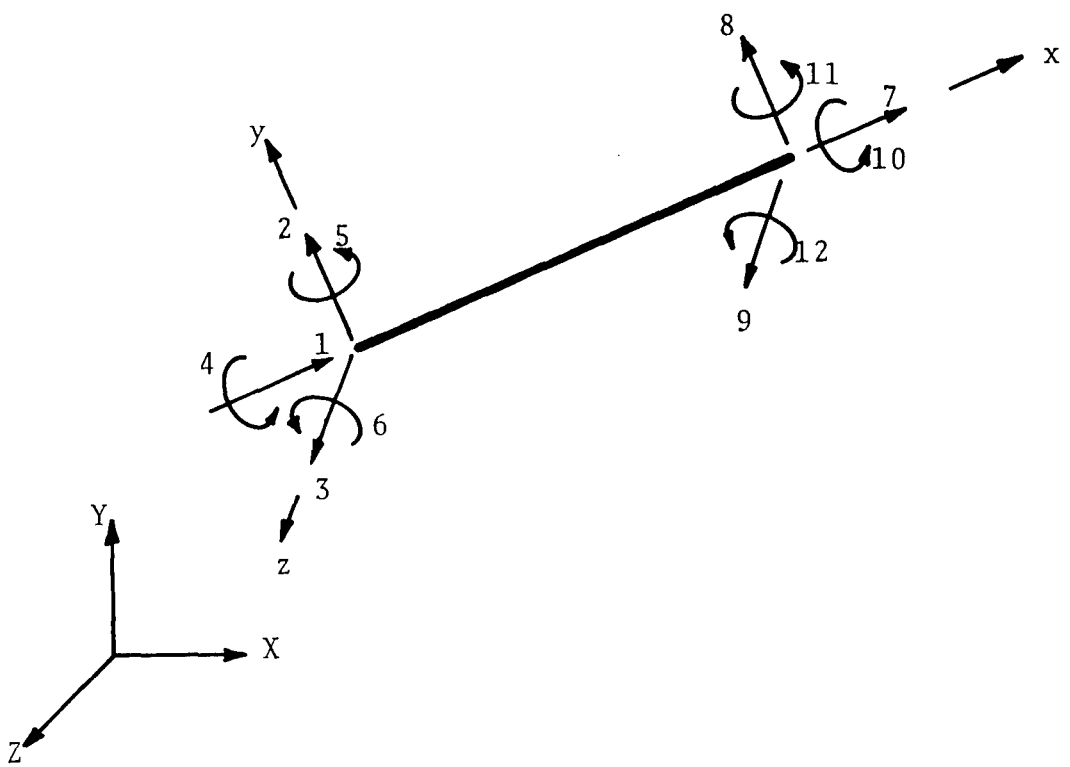

Figure 1 - Typical Beam Element

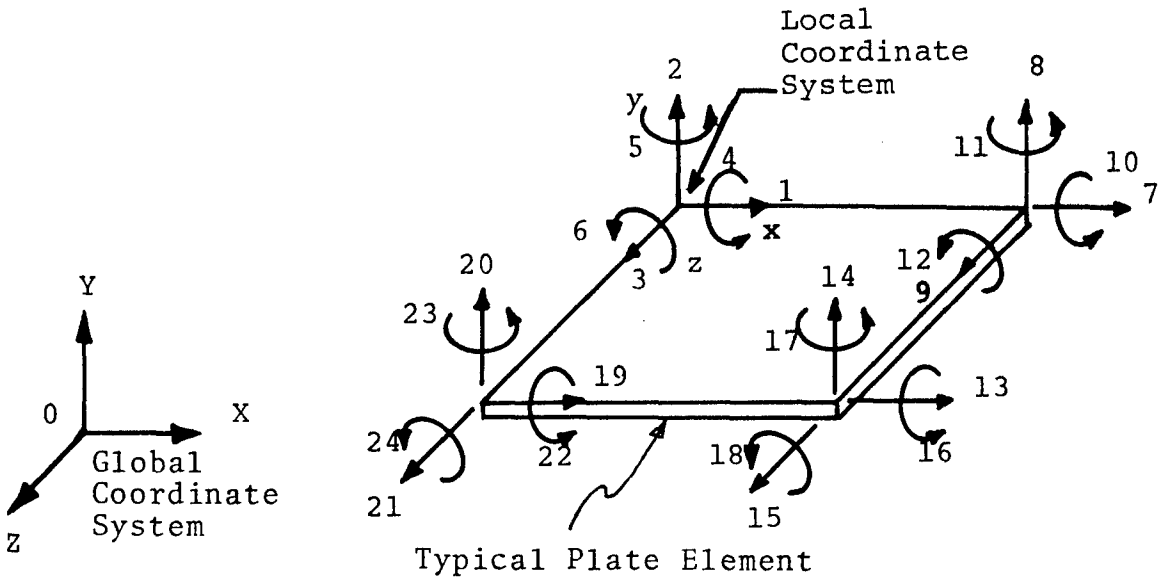

Figure 2 - Plate Element with In-Plane and Bending Actions

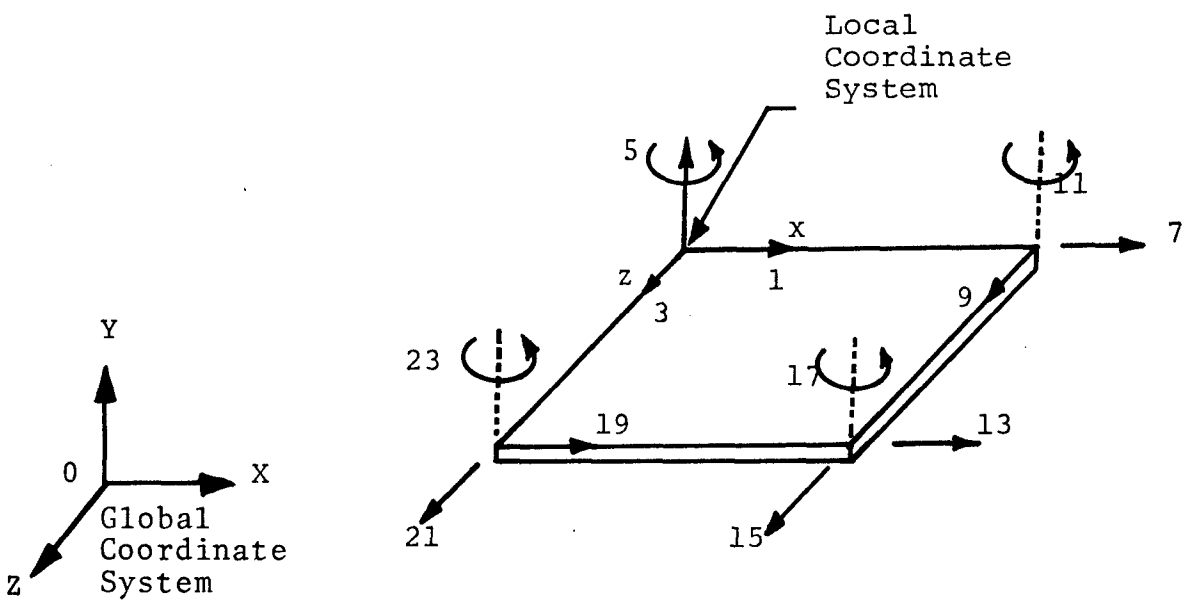

Figure 3 - Plate Element with In-Plane Action Only

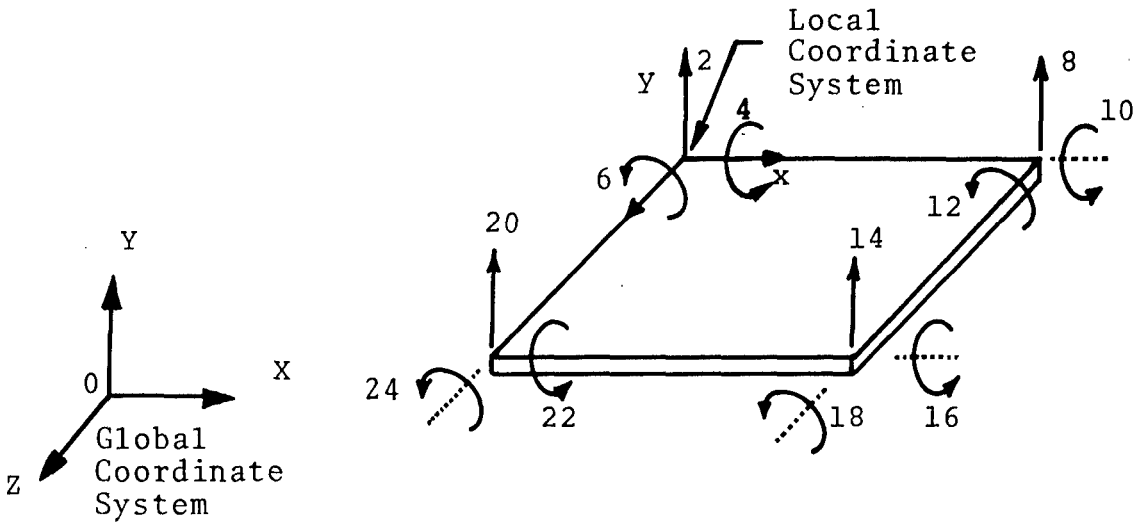

Figure 4 - Plate Element with Bending Action Only

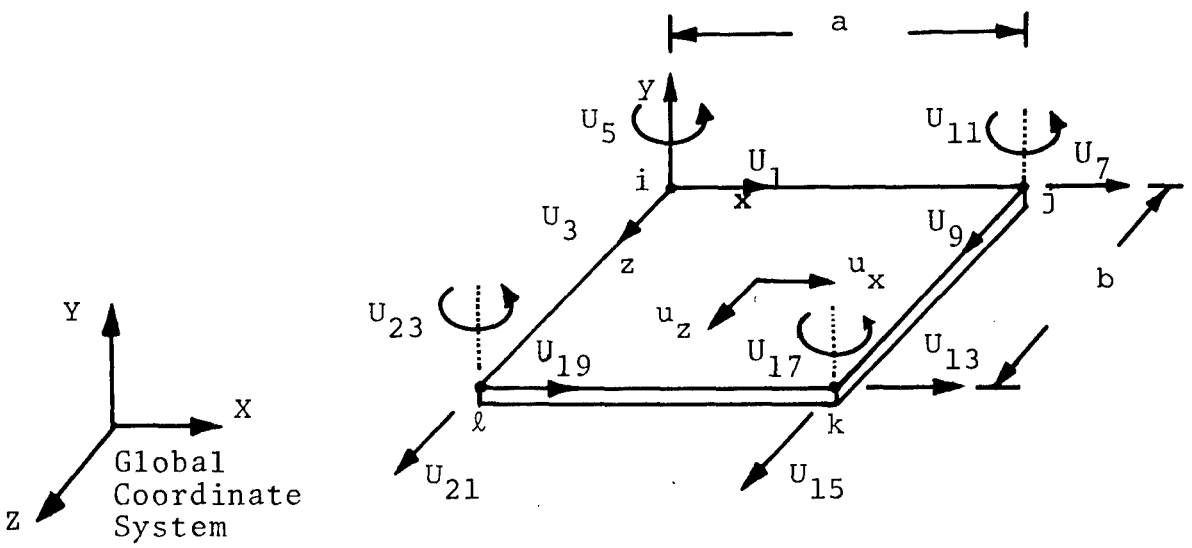

Figure 5 - Element Displacements Corresponding to In-Plane Action
(i, j, k, ℓ represent the four nodes of the plate)

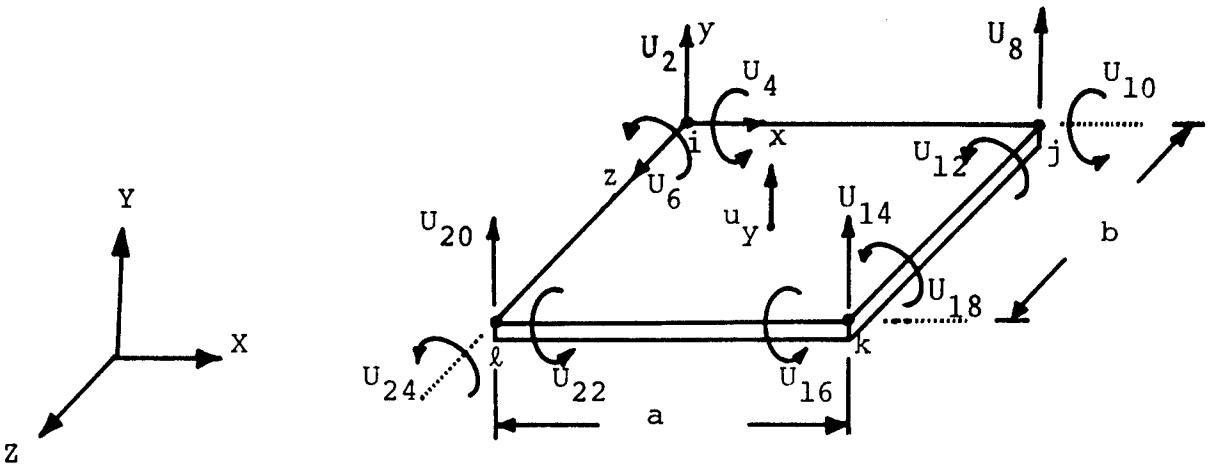

Figure 6 - Element Displacements Corresponding to Bending Action
(i, j, k, ℓ represent the four nodes of the plate)

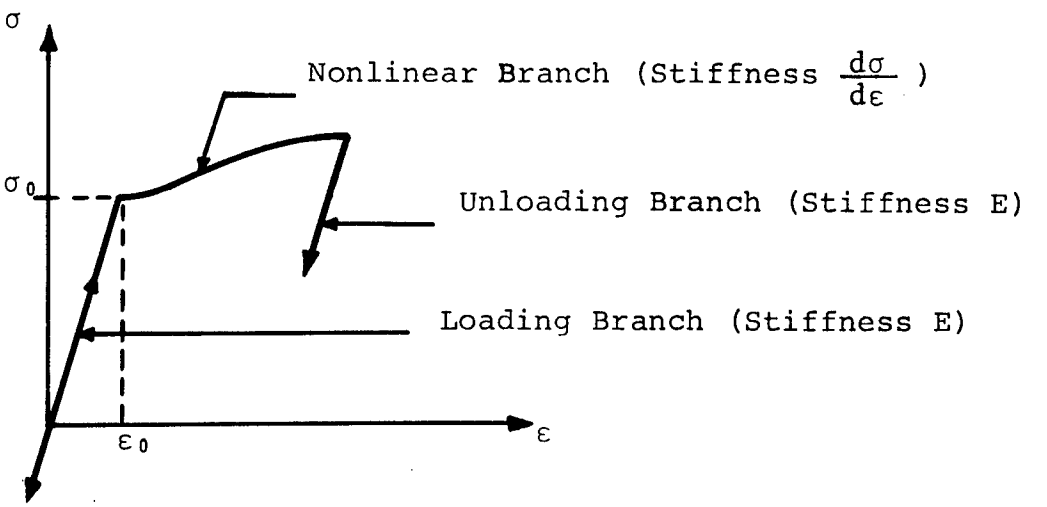

Figure 7 - General Stress-Strain Curve

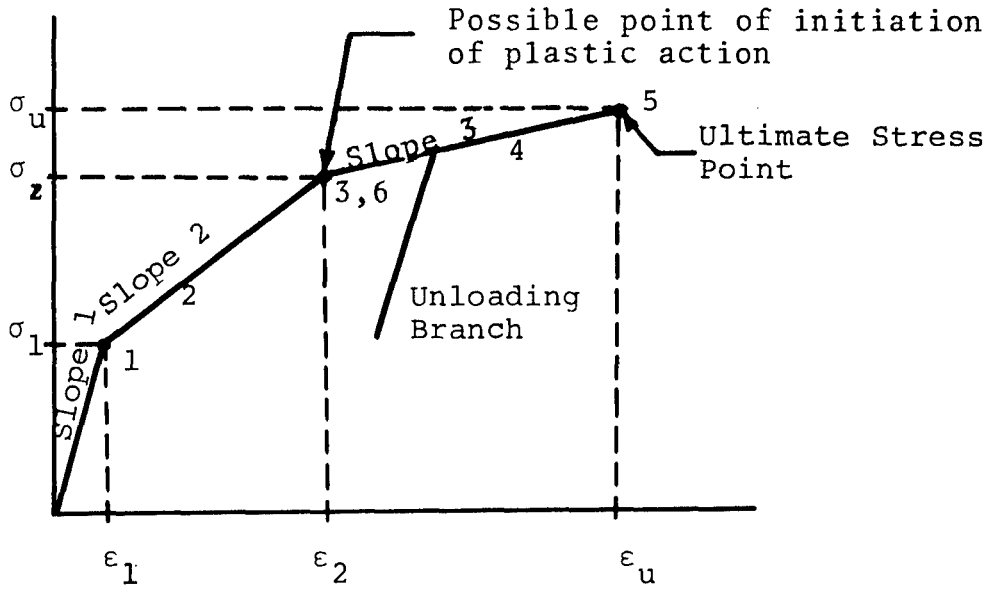

Figure 8 - Trilinear Stress-Strain Curve

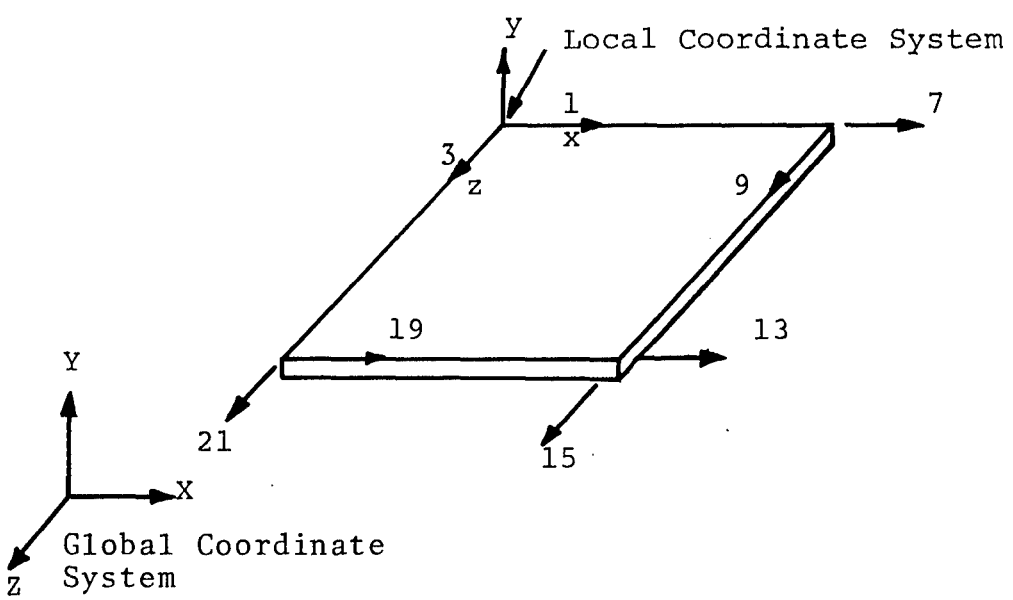

Figure 9 - In-Plane Stressed Plate Element with 8 D.O.F.

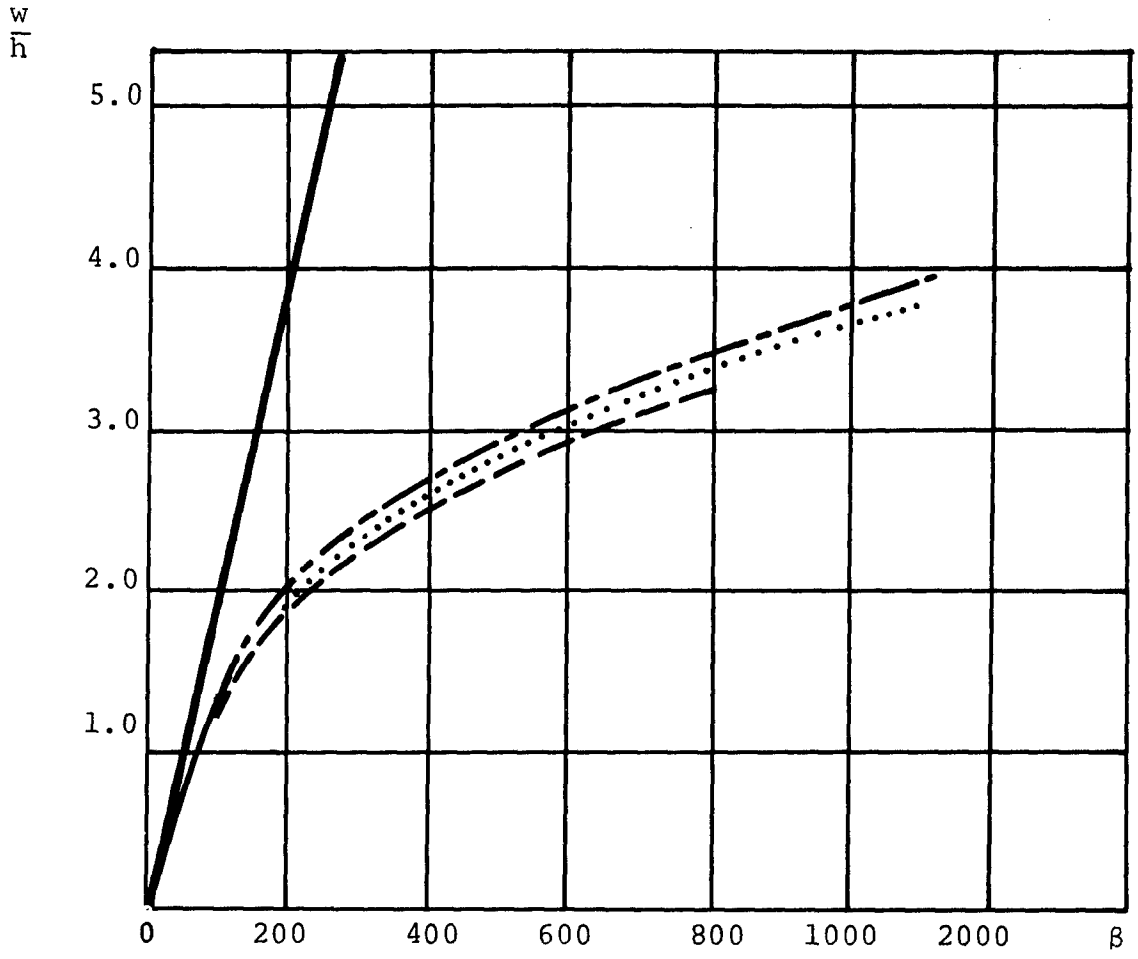

w = center deflection, h = thickness, $\beta = Pa^2/Dh$, $D = Eh^3/12(1-\nu^2)$, $\nu = 0.3$.

——— Linear

— - — Brebbia and Connor (12)

..... Adotte (33)

— — Present study

Figure 10 - Comparison of Central Deflections for a Clamped Square Plate with Concentrated Load P at Center

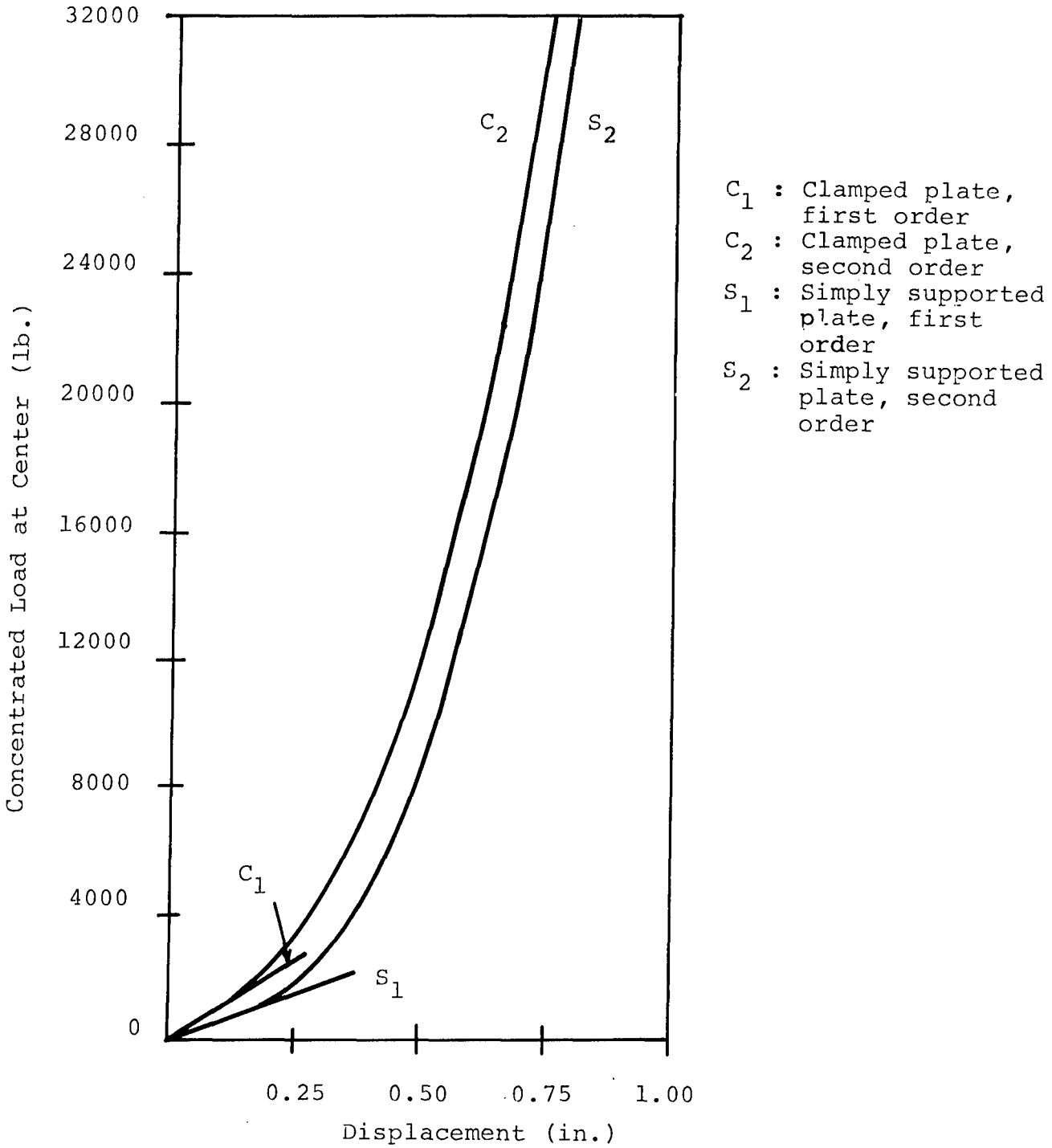

Figure 11 - Force-Deformation Relationships for Clamped and Simply Supported Square Plates

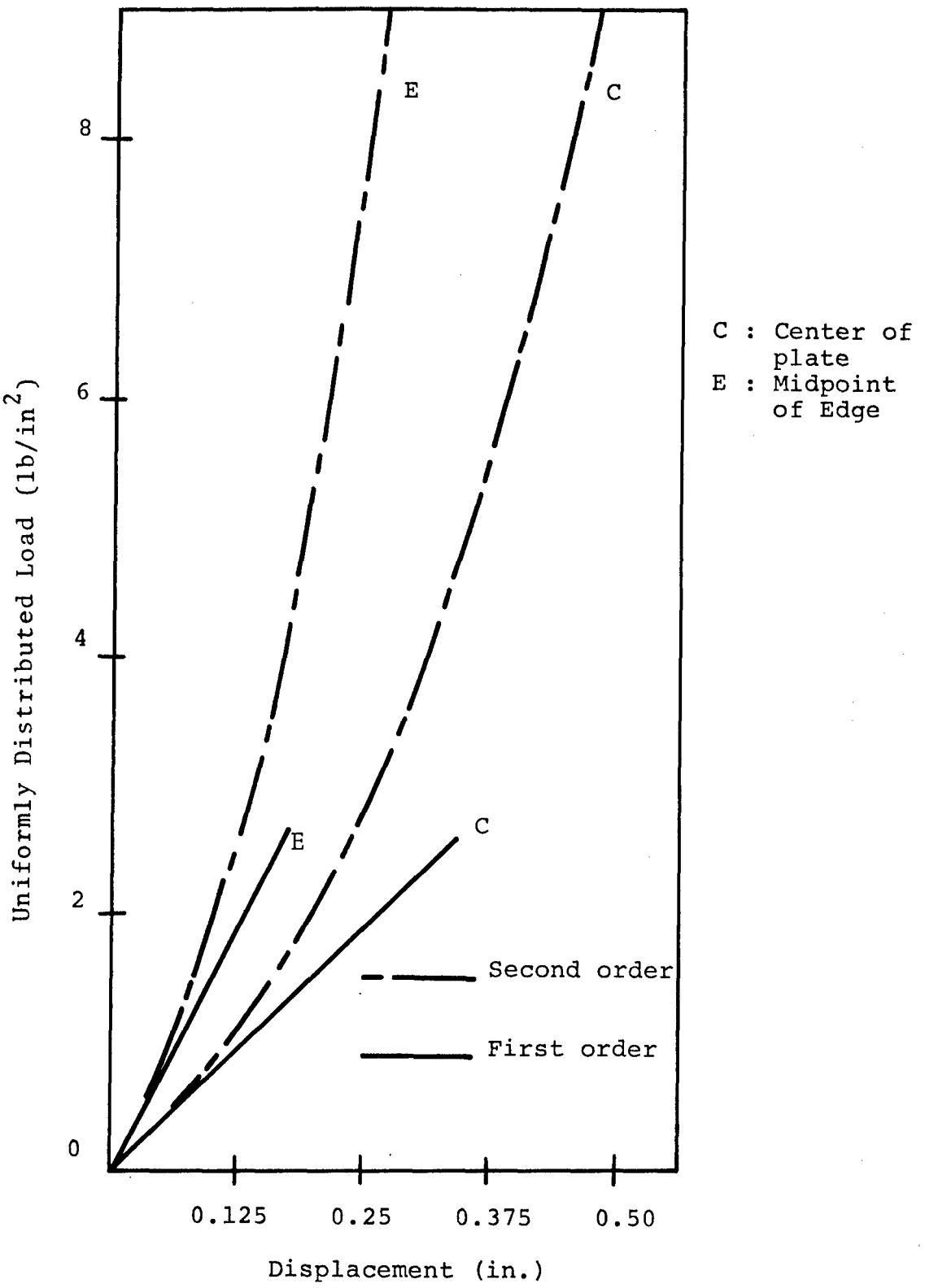

Figure 12 - Force-Deformation Curves for First and Second Order Static Analyses of a Plate Supported by Edge Beams

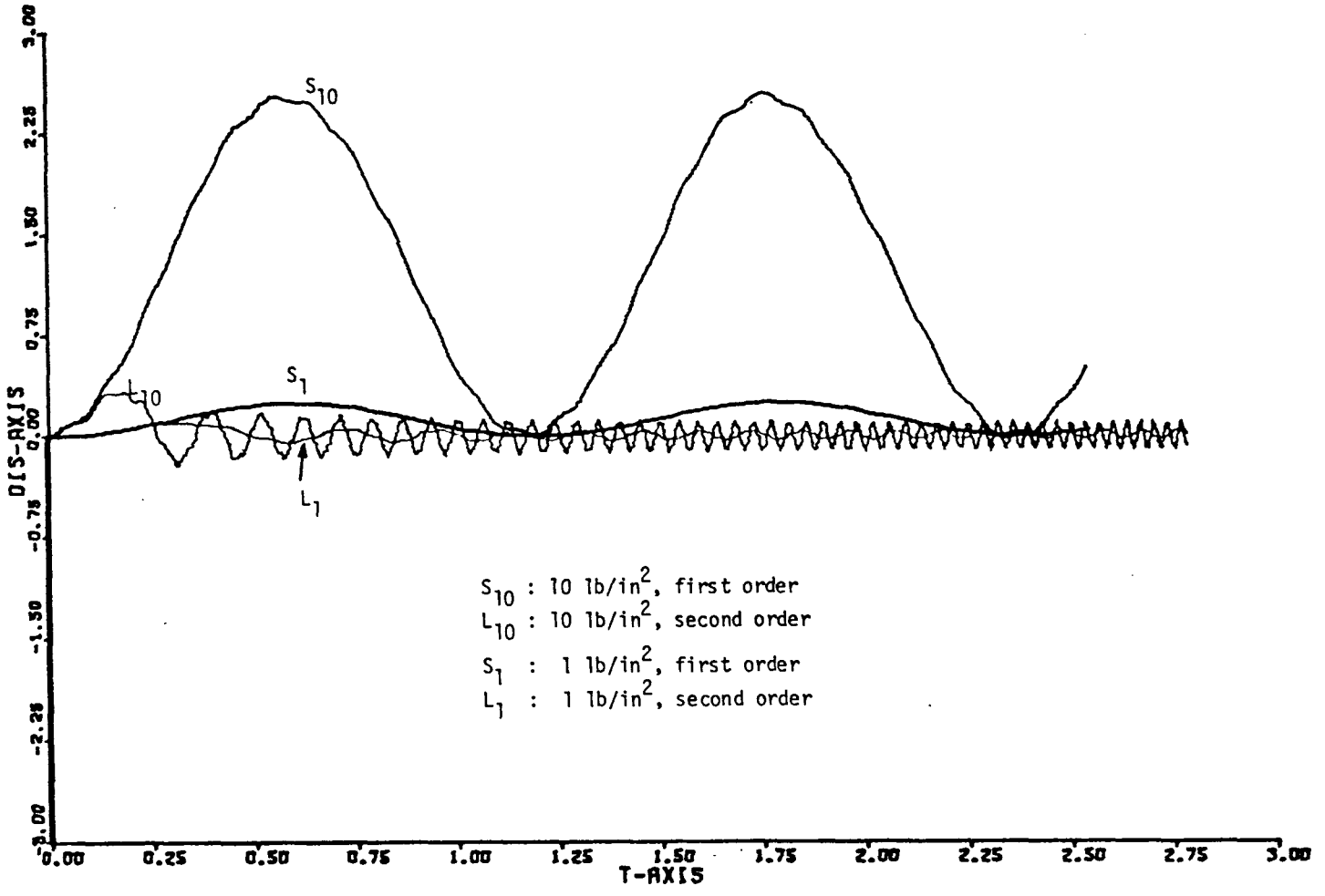

Figure 13 - First and Second Order Elastic Dynamic Analysis of a Plate Supported by Edge Beams--Time-History of Center Deflection for Load Intensities of 1 and 10 lb/in^2

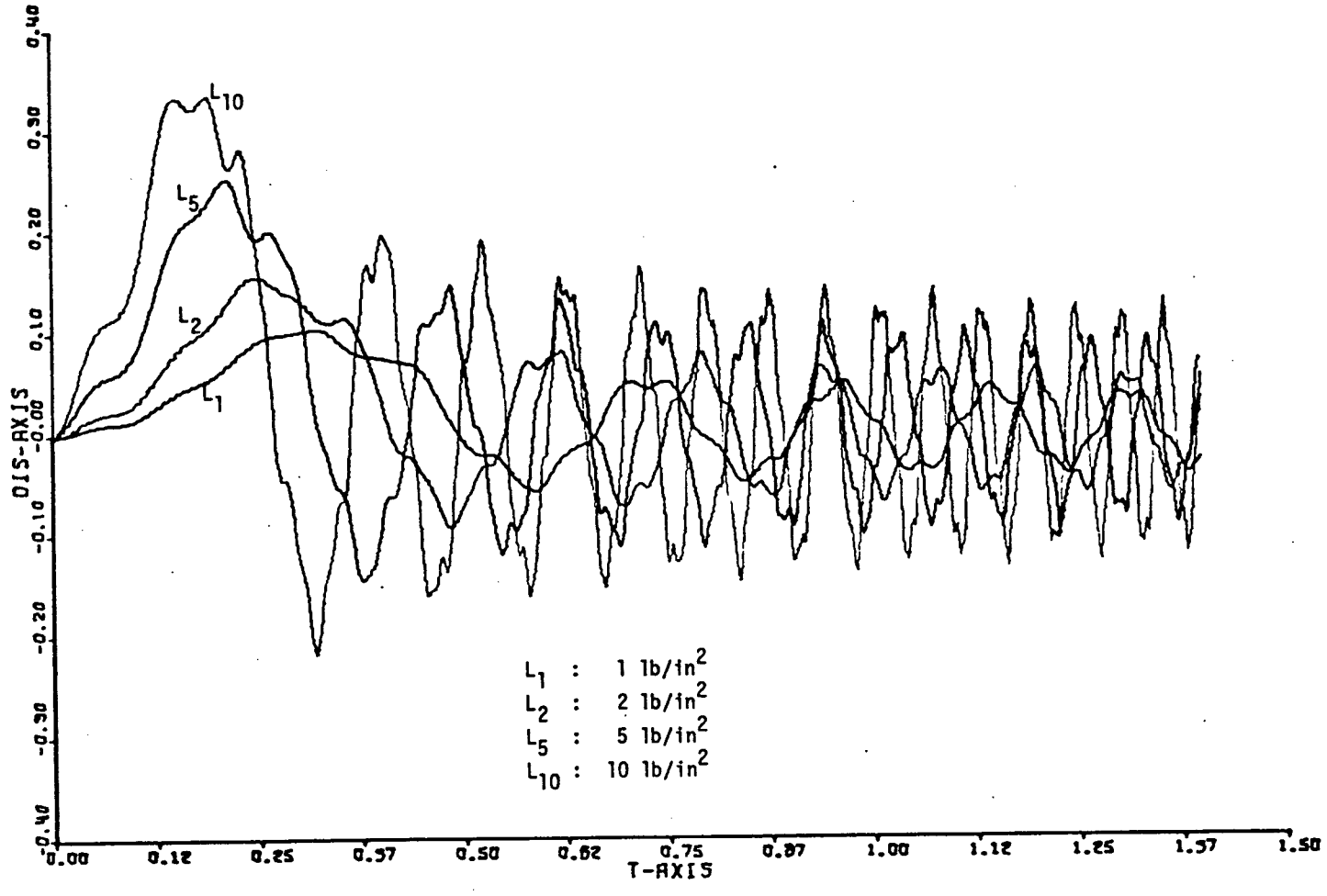

Figure 14 - Second Order Elastic Dynamic Analysis of a Plate Supported by Edge Beams--Time-History of Center Deflection for Load Intensities of 1, 2, 5 and 10 lb/in^2

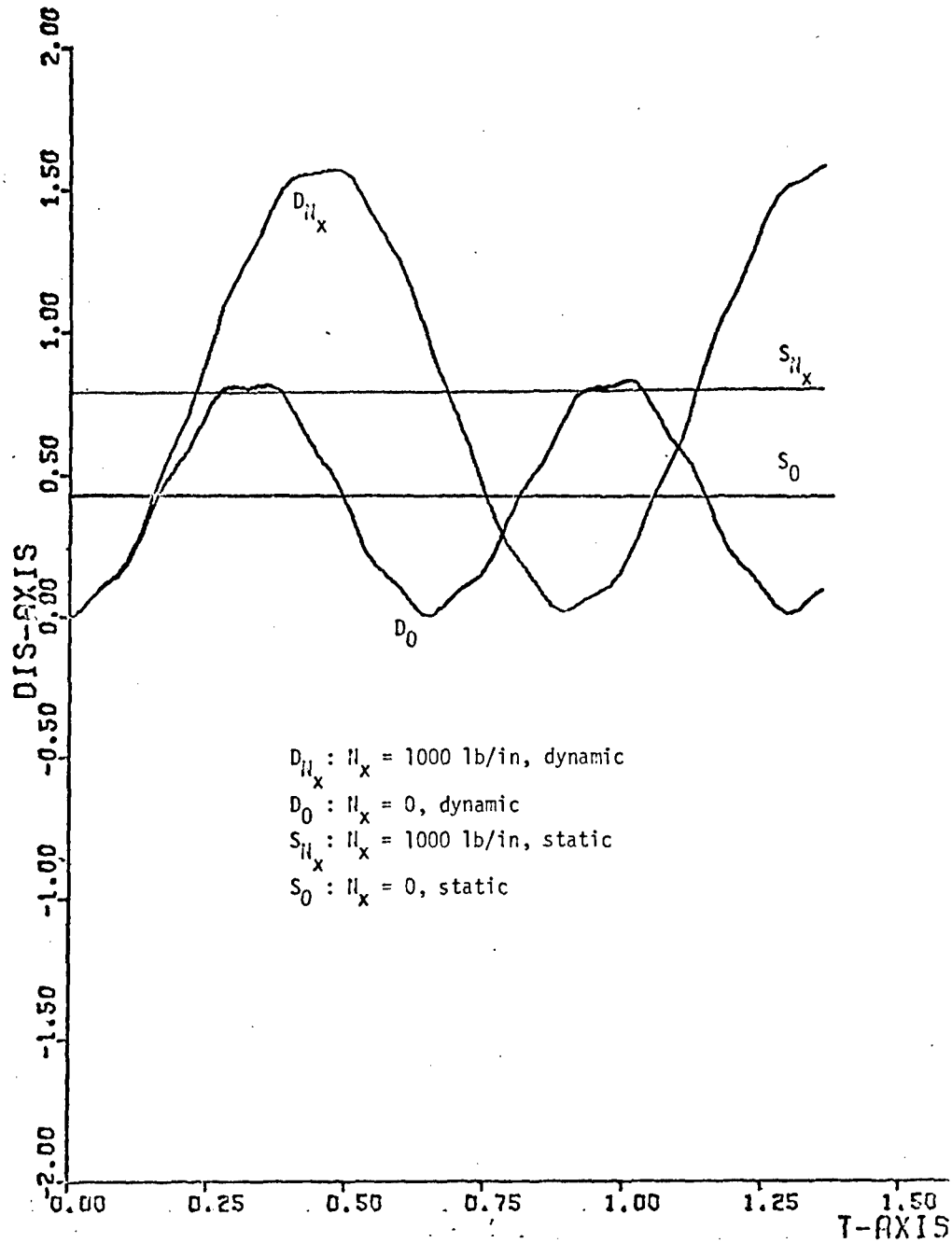

Figure 15 - First Order Elastic Dynamic Analysis of Simply Supported Square Plate with Lateral and In-Plane Compressive Forces--Time-History of Center Deflection

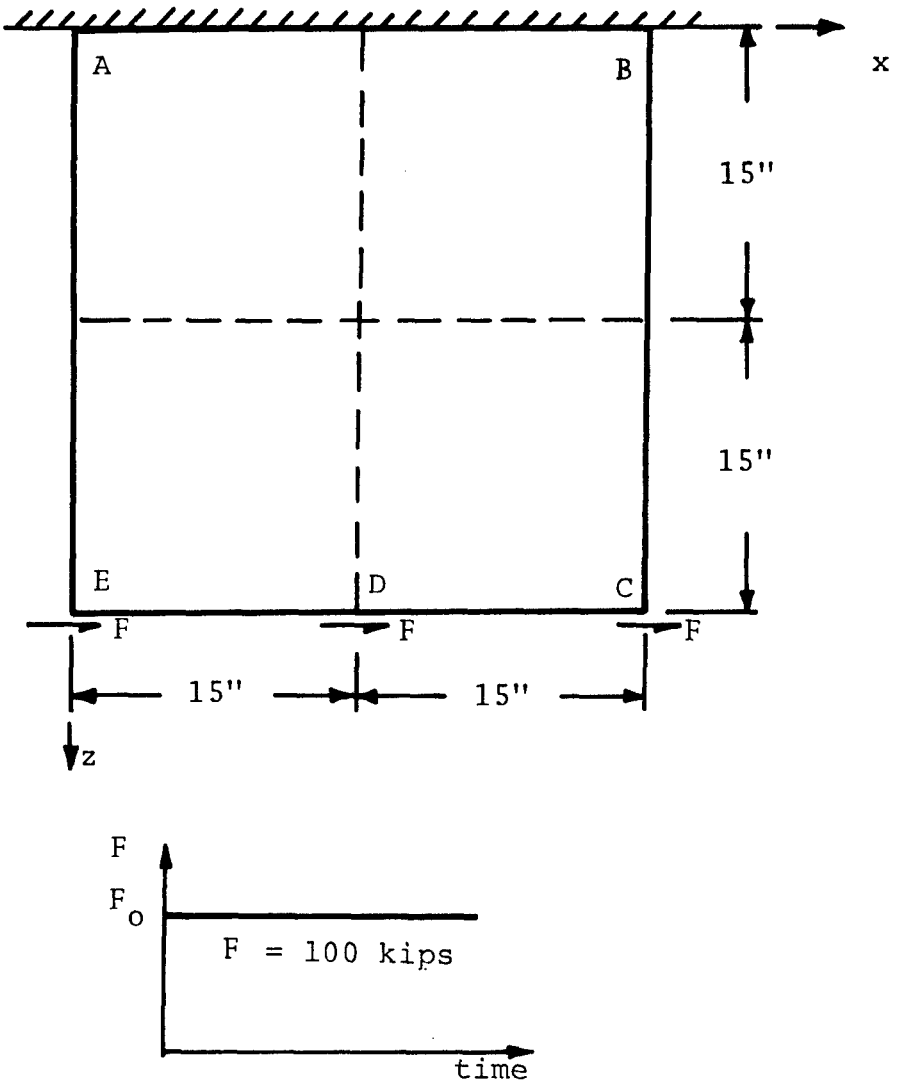

Figure 16 - Plate Structure Subject to In-Plane Action

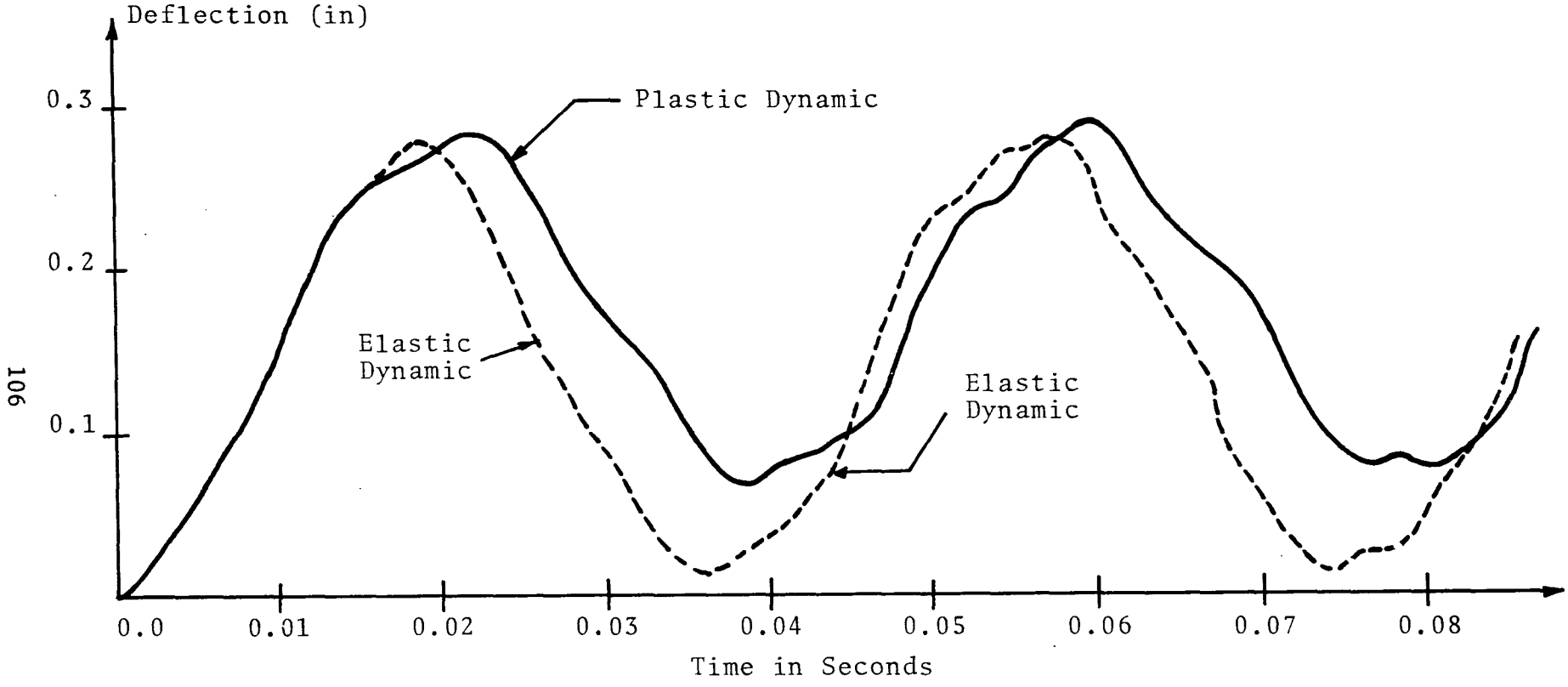

Figure 17 - Elastic and Plastic Dynamic Analysis of Plate Structure--
Time-History of Deflection at Node C

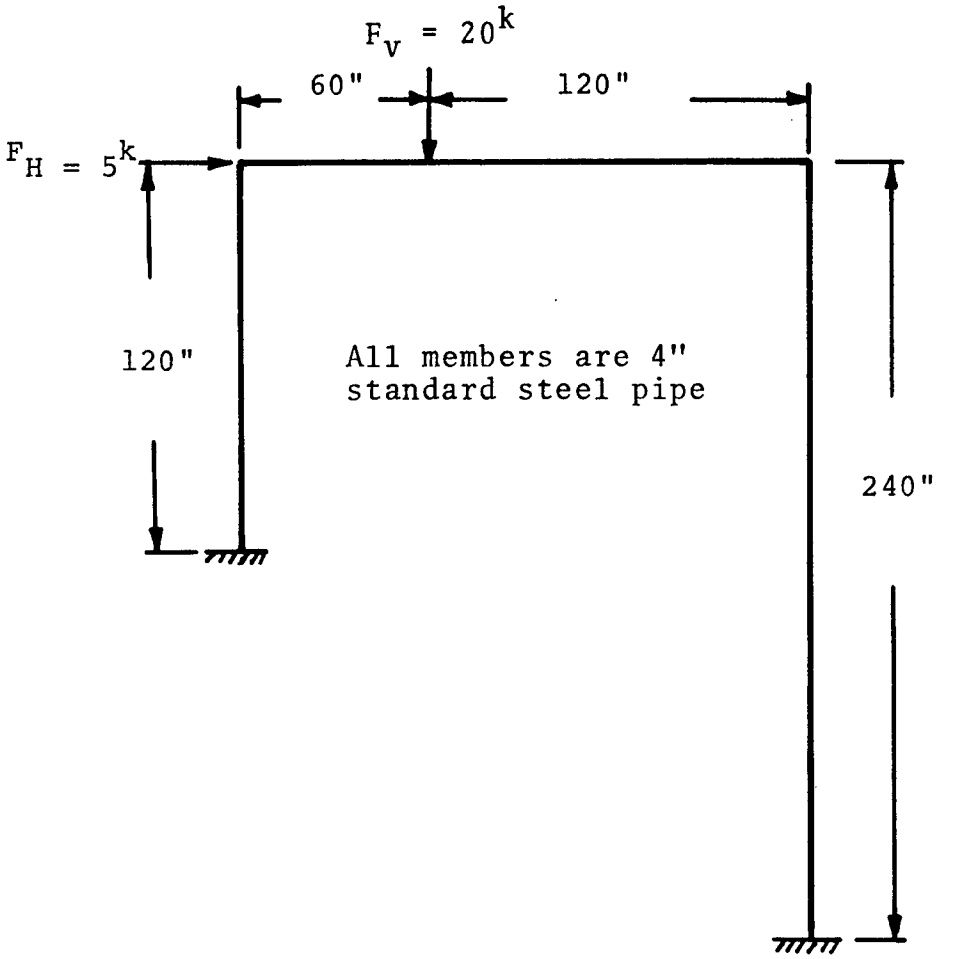

Figure 18a - Properties and Loading

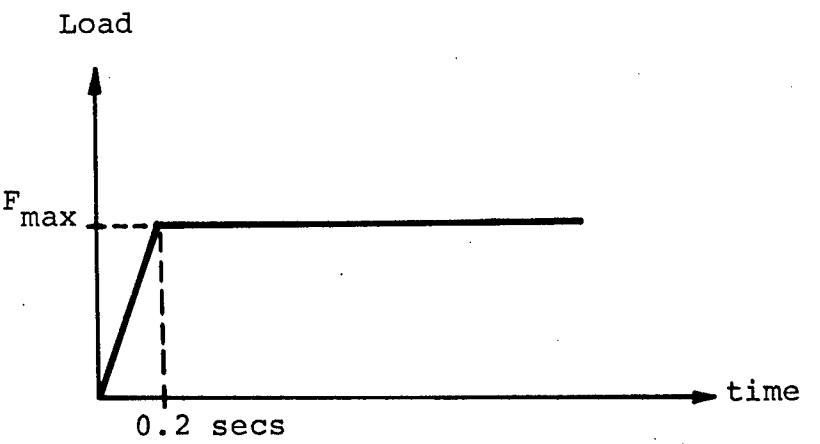

Figure 18b - Time Variation of the Applied Loading

Figure 18 - Plane Frame Subjected to Dynamic Loads

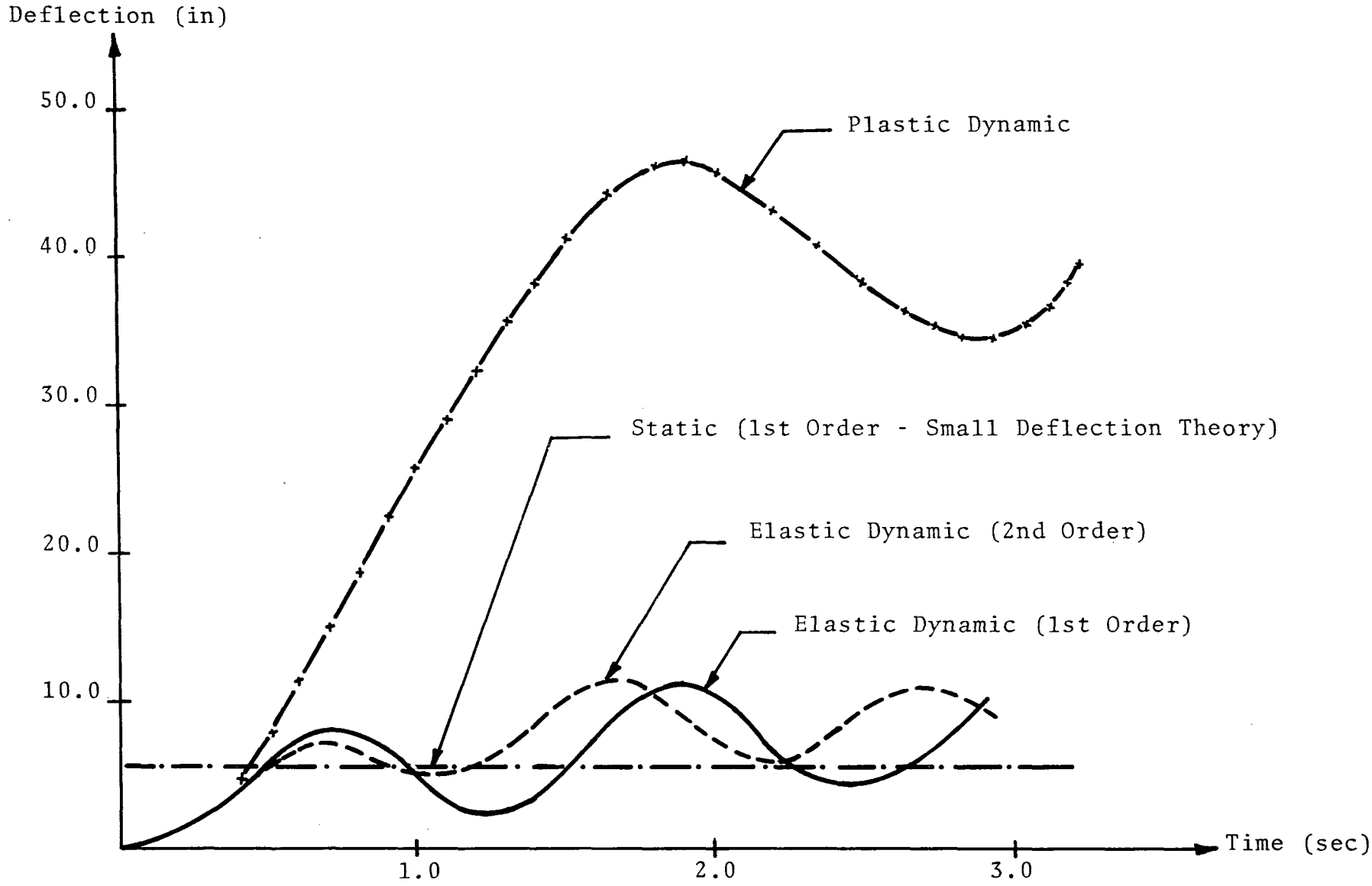

Figure 19 - Elastic and Plastic Dynamic Analysis of Plane Frame--
Time-History of Deflection in the Direction of F_v

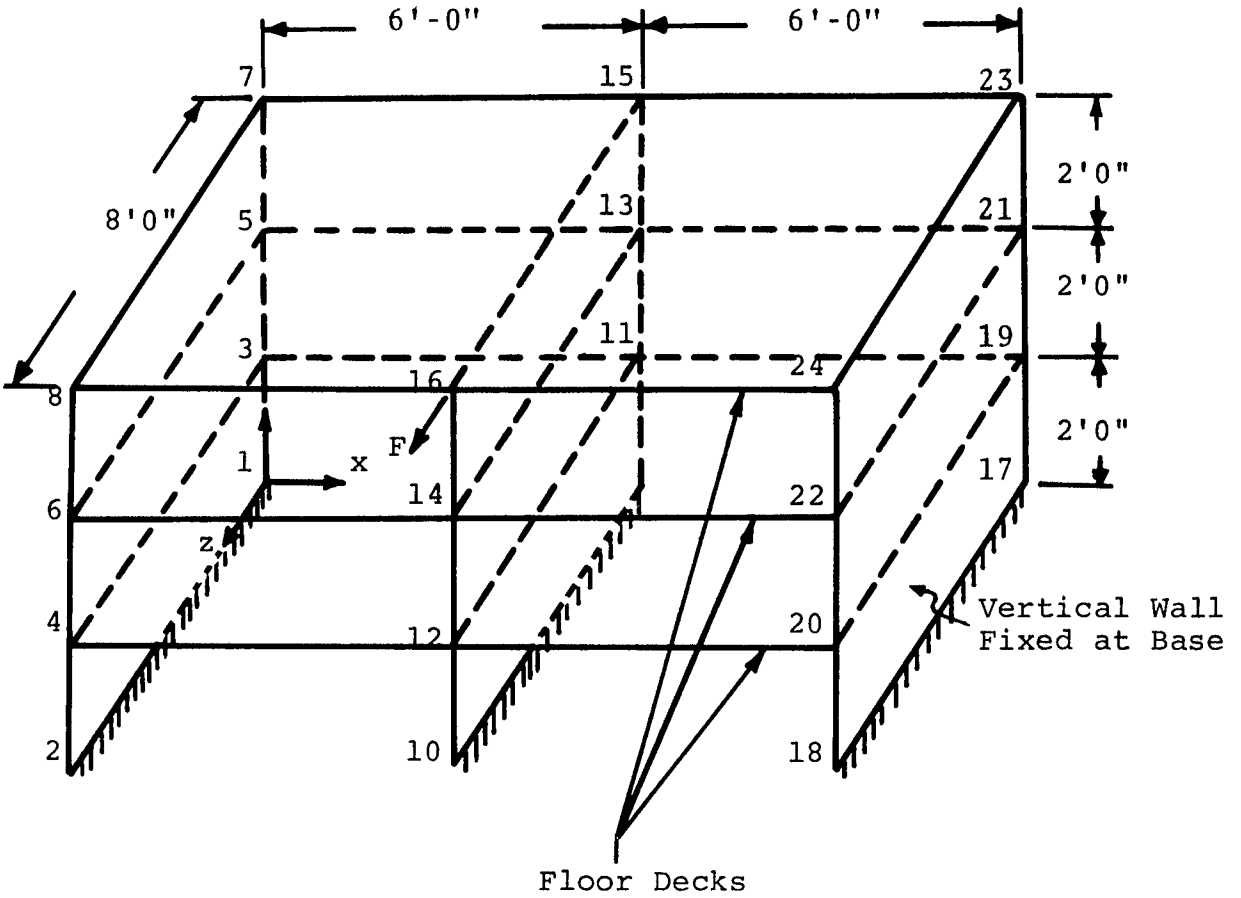

Figure 20 - Three-Dimensional Structure Consisting of In-Plane Stressed Plate Elements

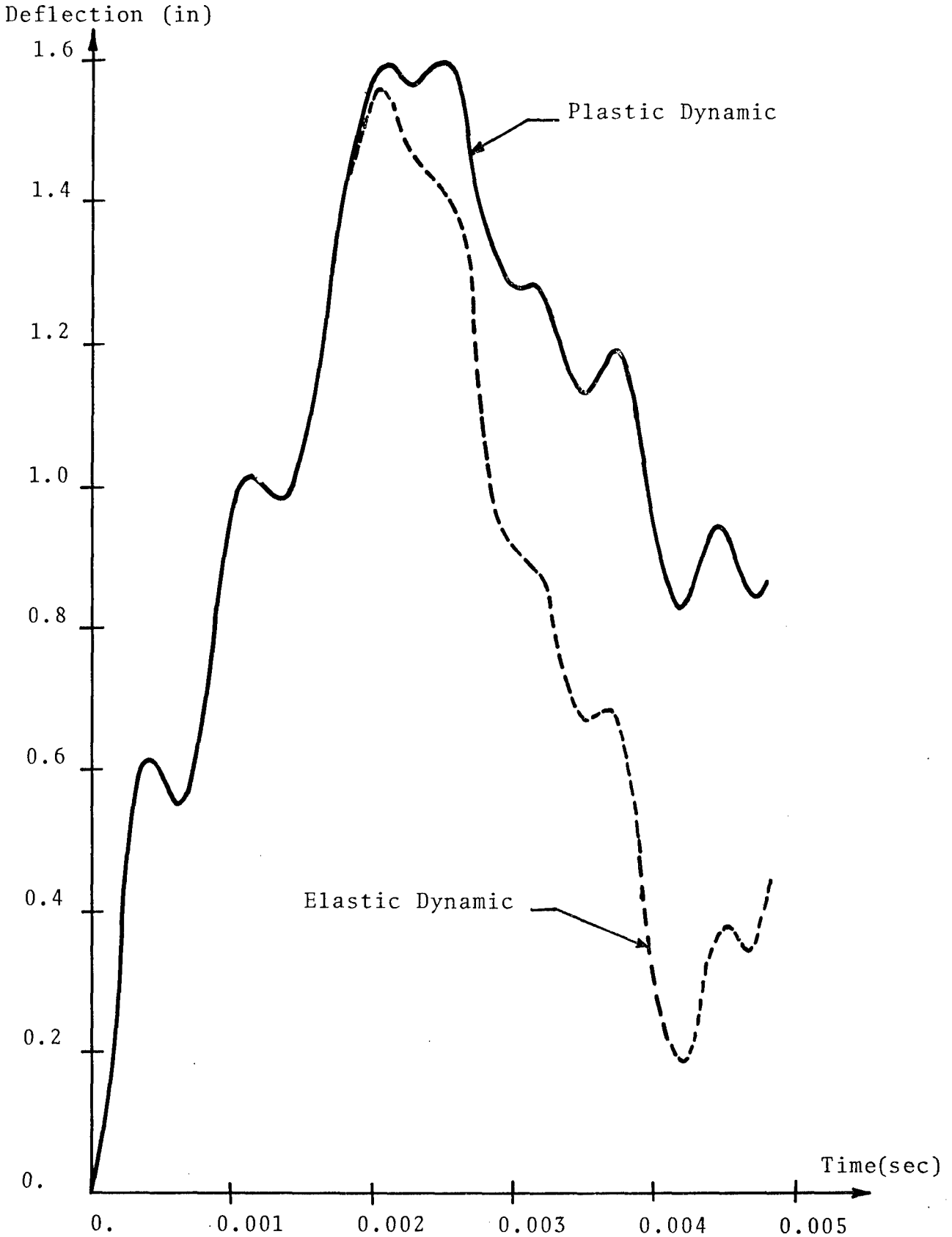

Figure 21 - Elastic and Plastic Dynamic Analysis of 3-D Structure Composed of In-Plane Stressed Plate Elements--Time-History of Deflection in the Direction of F

APPENDIX A

STRAIN AND STRESS COMPONENTS DUE TO IN-PLANE ACTION

Strain and stress components to be used in Eq. (53) corresponding to the displacement functions defined by Eqs. (51), and (52) are presented in this appendix.

A.1 Strain Components

The strain components corresponding to the in-plane action may be obtained by substitution of Eqs. (51), and (52) into the following equation

$$[\varepsilon_i] = \begin{bmatrix} \varepsilon_x \\ \varepsilon_z \\ \gamma_{xz} \end{bmatrix}_i = \begin{bmatrix} u_{x,x} \\ u_{z,z} \\ u_{x,z} + u_{z,x} \end{bmatrix}_i = \begin{bmatrix} \frac{1}{a} u_{x,\xi} \\ \frac{1}{b} u_{z,\eta} \\ \frac{1}{b} u_{x,\eta} + \frac{1}{a} u_{z,\xi} \end{bmatrix}_i$$

The results are as follows:

$$[\varepsilon_1] = \begin{bmatrix} -\frac{1}{a}(2\eta^3 - 3\eta^2 + 1) \\ 0 \\ \frac{1}{b}(1 - \xi)(6\eta^2 - 6\eta) \end{bmatrix}$$

$$[\varepsilon_3] = \begin{bmatrix} 0 \\ -\frac{1}{b}(2\xi^3 - 3\xi^2 + 1) \\ \frac{1}{a}(1 - \eta)(6\xi^2 - 6\xi) \end{bmatrix}$$

$$[\varepsilon_5] = -\begin{bmatrix} \frac{b}{a}(\eta^3 - 2\eta^2 + \eta) \\ -\frac{a}{b}(\xi^3 - 2\xi^2 + \xi) \\ -(1-\xi)(3\eta^2 - 4\eta + 1) + (1-\eta)(3\xi^2 - 4\xi + 1) \end{bmatrix}$$

$$[\varepsilon_7] = \begin{bmatrix} \frac{1}{a}(2\eta^3 - 3\eta^2 + 1) \\ 0 \\ \frac{1}{b}\xi(6\eta^2 - 6\eta) \end{bmatrix}$$

$$[\varepsilon_9] = \begin{bmatrix} 0 \\ \frac{1}{b}(2\xi^3 - 3\xi^2) \\ -\frac{1}{a}(1-\eta)(6\xi^2 - 6\xi) \end{bmatrix}$$

$$[\varepsilon_{11}] = -\begin{bmatrix} -\frac{b}{a}(\eta^3 - 2\eta^2 + \eta) \\ -\frac{a}{b}(\xi^3 - \xi^2) \\ -\xi(3\eta^2 - 4\eta + 1) + (1-\eta)(3\xi^2 - 2\xi) \end{bmatrix}$$

$$[\varepsilon_{13}] = \begin{bmatrix} -\frac{1}{a}(2\eta^3 - 3\eta^2) \\ 0 \\ -\frac{1}{b}\xi(6\eta^2 - 6\eta) \end{bmatrix}$$

$$[\varepsilon_{15}] = \begin{bmatrix} 0 \\ -\frac{1}{b}(2\xi^3 - 3\xi^2) \\ -\frac{1}{a}\eta\,(6\xi^2 - 6\xi) \end{bmatrix}$$

$$[\varepsilon_{17}] = -\begin{bmatrix} -\frac{b}{a}(\eta^3 - \eta^2) \\ \frac{a}{b}(\xi^3 - \xi^2) \\ -\xi(3\eta^2 - 2\eta) + \eta(3\xi^2 - 2\xi) \end{bmatrix}$$

$$[\varepsilon_{19}] = \begin{bmatrix} \frac{1}{a}(2\eta^3 - 3\eta^2) \\ 0 \\ -\frac{1}{b}(1 - \xi)(6\eta^2 - 6\eta) \end{bmatrix}$$

$$[\varepsilon_{21}] = \begin{bmatrix} 0 \\ \frac{1}{b}(2\xi^3 - 3\xi^2 + 1) \\ \frac{1}{a}\eta\,(6\xi^2 - 6\xi) \end{bmatrix}$$

$$[\varepsilon_{23}] = -\begin{bmatrix} \frac{b}{a}(\eta^3 - \eta^2) \\ \frac{a}{b}(\xi^3 - 2\xi^2 + \xi) \\ -(1 - \xi)(3\eta^2 - 2\eta) + \eta(3\xi^2 - 4\xi + 1) \end{bmatrix}$$

A.2 Stress Components

The corresponding stress components may be obtained by substitution of the above results into the following equation.

$$[\sigma_i] = \begin{bmatrix} \sigma_x \\ \sigma_z \\ \tau_{xz} \end{bmatrix}_i = \frac{E}{1-\nu^2} \begin{bmatrix} \varepsilon_x + \nu\varepsilon_z \\ \nu\varepsilon_x + \varepsilon_z \\ \lambda\gamma_{xz} \end{bmatrix}_i .$$

The results are (all terms on the right-hand side of the equations are to be multiplied by the factor $E/1-\nu^2$):

$$[\sigma_1] = \begin{bmatrix} -\frac{1}{a}(2\eta^3 - 3\eta^2 + 1) \\ -\frac{\nu}{a}(2\eta^3 - 3\eta^2 + 1) \\ \frac{\lambda}{b}(1 - \xi)(6\eta^2 - 6\eta) \end{bmatrix}$$

$$[\sigma_3] = \begin{bmatrix} -\frac{\nu}{b}(2\xi^3 - 3\xi^2 + 1) \\ -\frac{1}{b}(2\xi^3 - 3\xi^2 + 1) \\ \frac{\lambda}{a}(1 - \eta)(6\xi^2 - 6\xi) \end{bmatrix}$$

$$[\sigma_5] = -\begin{bmatrix} \frac{b}{a}(\eta^3 - 2\eta^2 + \eta) - \frac{a\nu}{b}(\xi^3 - 2\xi^2 + \xi) \\ \frac{b\nu}{a}(\eta^3 - 2\eta^2 + \eta) - \frac{a}{b}(\xi^3 - 2\xi^2 + \xi) \\ \lambda[-(1 - \xi)(3\eta^2 - 4\eta + 1) + (1 - \eta)(3\xi^2 - 4\xi + 1)] \end{bmatrix}$$

$$[\sigma_7] = \begin{bmatrix} \frac{1}{a}(2\eta^3 - 3\eta^2 + 1) \\ \frac{\nu}{a}(2\eta^3 - 3\eta^2 + 1) \\ \frac{\lambda}{b}\xi(6\eta^2 - 6\eta) \end{bmatrix}$$

$$[\sigma_9] = \begin{bmatrix} \frac{\nu}{b}(2\xi^3 - 3\xi^2) \\ \frac{1}{b}(2\xi^3 - 3\xi^2) \\ -\frac{\lambda}{a}(1 - \eta)(6\xi^2 - 6\xi) \end{bmatrix}$$

$$[\sigma_{11}] = -\begin{bmatrix} -\frac{b}{a}(\eta^3 - 2\eta^2 + \eta) - \frac{a\nu}{b}(\xi^3 - \xi^2) \\ -\frac{b\nu}{a}(\eta^3 - 2\eta^2 + \eta) - \frac{a}{b}(\xi^3 - \xi^2) \\ \lambda[-\xi(3\eta^2 - 4\eta + 1) + (1 - \eta)(3\xi^2 - 2\xi)] \end{bmatrix}$$

$$[\sigma_{13}] = \begin{bmatrix} -\frac{1}{a}(2\eta^3 - 3\eta^2) \\ -\frac{\nu}{b}(2\eta^3 - 3\eta^2) \\ -\frac{\lambda}{b}(6\eta^2 - 6\eta) \end{bmatrix}$$

$$[\sigma_{15}] = \begin{bmatrix} -\frac{\nu}{b}(2\xi^3 - 3\xi^2) \\ -\frac{1}{b}(2\xi^3 - 3\xi^2) \\ -\frac{\lambda}{a}\eta(6\xi^2 - 6\xi) \end{bmatrix}$$

$$[\sigma_{17}] = -\begin{bmatrix} -\frac{b}{a}(\eta^3 - \eta^2) + \frac{a\nu}{b}(\xi^3 - \xi^2) \\ -\frac{\nu b}{a}(\eta^3 - \eta^2) + \frac{a}{b}(\xi^3 - \xi^2) \\ \lambda[-\xi(3\eta^2 - 2\eta) + \eta(3\xi^2 - 2\xi)] \end{bmatrix}$$

$$[\sigma_{19}] = \begin{bmatrix} \frac{1}{a}(2\eta^3 - 3\eta^2) \\ \frac{\nu}{a}(2\eta^3 - 3\eta^2) \\ -\frac{\lambda}{b}(1 - \xi)(6\eta^2 - 6\eta) \end{bmatrix}$$

$$[\sigma_{21}] = \begin{bmatrix} \frac{\nu}{b}(2\xi^3 - 3\xi^2 + 1) \\ \frac{1}{b}(2\xi^3 - 3\xi^2 + 1) \\ \frac{\lambda}{a}\eta(6\xi^2 - 6\xi) \end{bmatrix}$$

$$[\sigma_{23}] = -\begin{bmatrix} \frac{b}{a}(\eta^3 - \eta^2) + \frac{\nu a}{b}(\xi^3 - 2\xi^2 + \xi) \\ \frac{\nu b}{a}(\eta^3 - \eta^2) + \frac{a}{b}(\xi^3 - 2\xi^2 + \xi) \\ \lambda[-(1 - \xi)(3\eta^2 - 2\eta) + \eta(3\xi^2 - 4\xi + 1)] \end{bmatrix}$$

APPENDIX B

SIMPLIFIED FLOWCHART OF THE MODIFIED GWU-FAP PROGRAM

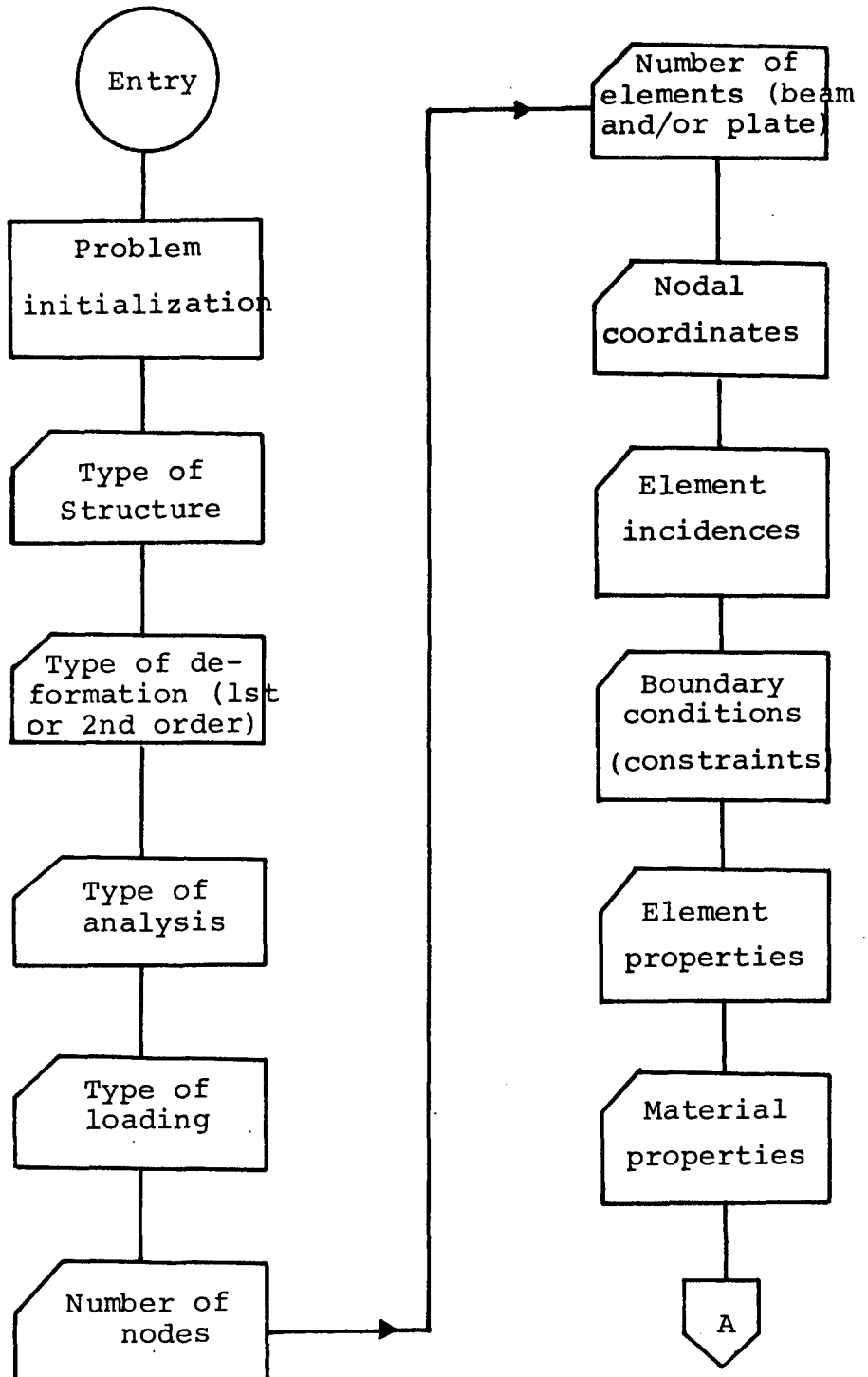

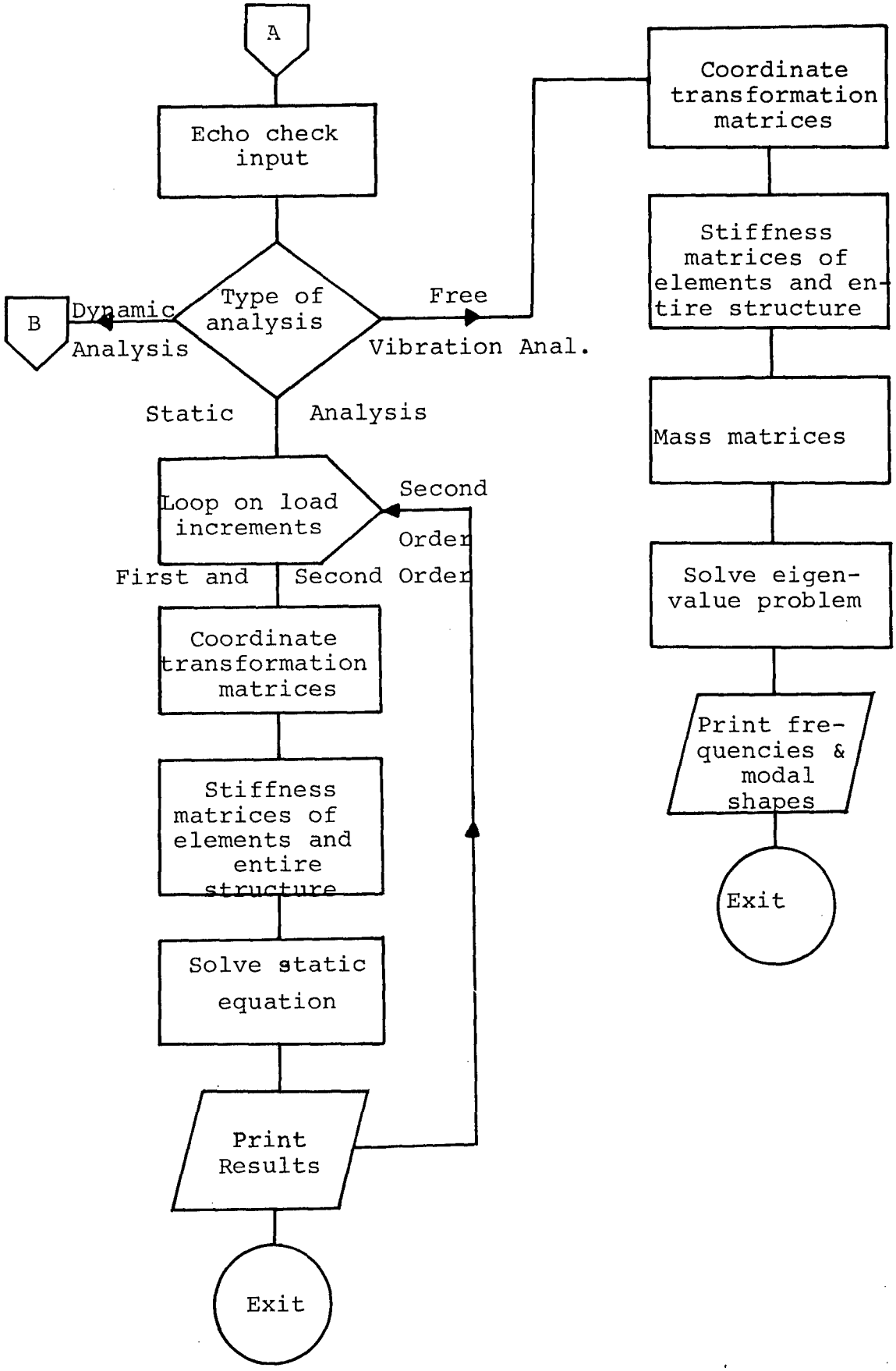
A
Echo check input
Type of analysis
B
Dynamic Analysis
Free Vibration Anal.
Static Analysis
Loop on load increments
Second Order
First and Second Order
Coordinate transformation matrices
Stiffness matrices of elements and entire structure
Solve static equation
Print Results
Exit
Coordinate transformation matrices
Stiffness matrices of elements and entire structure
Mass matrices
Solve eigen-value problem
Print frequencies & modal shapes
Exit

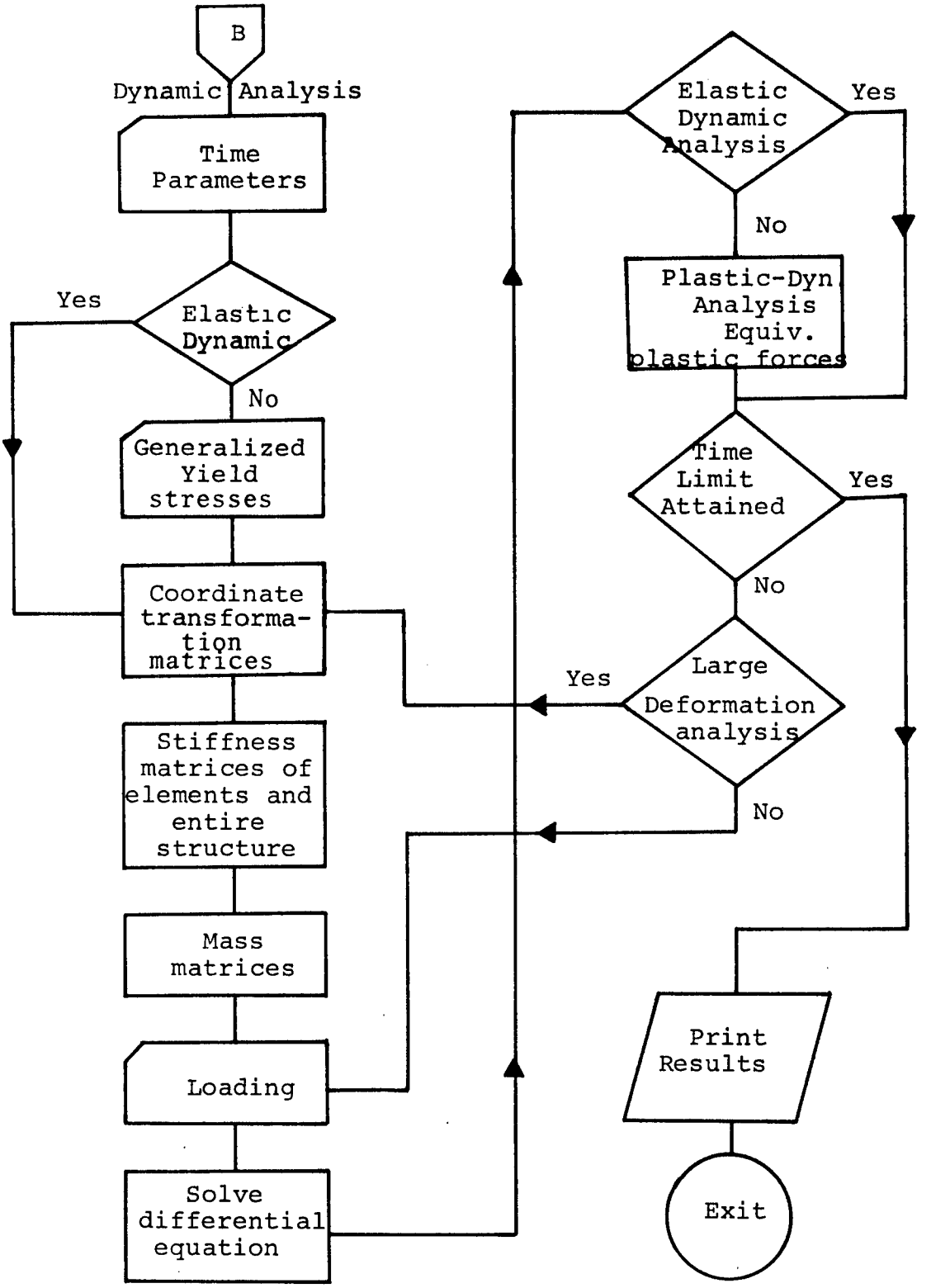
B
Dynamic Analysis
Time Parameters
Elastic Dynamic
Yes
No
Generalized Yield stresses
Coordinate transforma-tion matrices
Stiffness matrices of elements and entire structure
Mass matrices
Loading
Solve differential equation
Elastic Dynamic Analysis
Yes
No
Plastic-Dyn Analysis Equiv. plastic forces
Time Limit Attained
Yes
No
Large Deformation analysis
Yes
No
Print Results
Exit

APPENDIX C

TYPICAL INPUT FORMAT

C.1 STATIC ANALYSIS-FIRST ORDER
STRUCTURE ANALYZED IN SECTION 6.4 OF THIS REPORT

```
THIN PLATE ELASTICALLY SUPPORTED BY EDGE BEAMS-4 PLATE AND 8 BEAM ELEMENTS
STATIC ANALYSIS
SPACE FRAME FIRST ORDER
NUMBER OF JOINTS 8
NUMBER OF NODE POINTS 1
NUMBER OF BEAM ELEMENTS 8
NUMBER OF PLATE ELEMENTS 4
JOINT COORDINATES
    1       0.0         0.0         0.0
    2      15.0         0.0         0.0
    3      30.0         0.0         0.0
    4       0.0         0.0        15.0
    5      15.0         0.0        15.0
    6      30.0         0.0        15.0
    7       0.0         0.0        30.0
    8      15.0         0.0        30.0
NODAL COORDINATES
    9      30.0         0.0        30.0
MEMBER INCIDENCES
    1    1    2
    2    2    3
    3    3    6
    4    6    9
    5    9    8
    6    8    7
    7    4    7
    8    1    4
    1    1    2    5    4
    2    2    3    6    5
    3    4    5    8    7
    4    5    6    9    8
NUMBER OF CONSTRAINED VERTICES 9
    1111010
    2101010
    3111010
    4101010
    5101010
    6101010
    7111010
    8101010
    9111010
MEMBER PROPERTIES
    1    8    .212000E+01    .000000E+00    .440000E+00    .420000E-01 1.0
0000100004      0.25            1.0            3
MODULUS OF ELASTICITY   30.00
NU   0.30
LOADING
    1                    56.25
    2                   112.50
    3                    56.25
    4                   112.50
    5                   225.00
    6                   112.50
    7                    56.25
    8                   112.50
    9                    56.25
EJECT
```

C.2 STATIC ANALYSIS-SECOND ORDER
STRUCTURE ANALYZED IN SECTION 6.4 OF THIS REPORT

```
THIN PLATE ELASTICALLY SUPPORTED BY EDGE BEAMS-4 PLATE AND 8 BEAM ELEMENTS
STATIC ANALYSIS
SPACE FRAME SECOND ORDER
NUMBER OF JOINTS 8
NUMBER OF NODE POINTS 1
NUMBER OF BEAM ELEMENTS 8
NUMBER OF PLATE ELEMENTS 4
JOINT COORDINATES
    1       0.0         0.0         0.0
    2      15.0         0.0         0.0
    3      30.0         0.0         0.0
    4       0.0         0.0        15.0
    5      15.0         0.0        15.0
    6      30.0         0.0        15.0
    7       0.0         0.0        30.0
    8      15.0         0.0        30.0
NODAL COORDINATES
    9      30.0         0.0        30.0
MEMBER INCIDENCES
    1    1    2
    2    2    3
    3    3    6
    4    6    9
    5    9    8
    6    8    7
    7    4    7
    8    1    4
    1    1    2    5    4
    2    2    3    6    5
    3    4    5    8    7
    4    5    6    9    8
NUMBER OF CONSTRAINED VERTICES 9
    1111010
    2101010
    3111010
    4101010
    5101010
    6101010
    7111010
    8101010
    9111010
MEMBER PROPERTIES
    1    8    .212000E+01    .000000E+00    .440000E+00    .420000E-01 1.0
0000100004      0.25            1.0           5
MODULUS OF ELASTICITY   30.00
NU   0.30
LOADING
    1                   562.50
    2                  1125.00
    3                   562.50
    4                  1125.00
    5                  2250.00
    6                  1125.00
    7                   562.50
    8                  1125.00
    9                   562.50
EJECT
```

```
C3. ELASTIC DYNAMIC ANALYSIS-SECOND ORDER
    STRUCTURE ANALYZED IN SECTION 6.4 OF THIS REPORT

THIN PLATE ELASTICALLY SUPPORTED BY EDGE BEAMS-4 PLATE AND 8 BEAM ELEMENTS
ELASTIC DYNAMIC ANALYSIS LTYPE 1
SPACE FRAME SECOND ORDER
NUMBER OF JOINTS 8
NUMBER OF NODE POINTS 1
NUMBER OF BEAM ELEMENTS 8
NUMBER OF PLATE ELEMENTS 4
JOINT COORDINATES
    1       0.0         0.0         0.0
    2      15.0         0.0         0.0
    3      30.0         0.0         0.0
    4       0.0         0.0        15.0
    5      15.0         0.0        15.0
    6      30.0         0.0        15.0
    7       0.0         0.0        30.0
    8      15.0         0.0        30.0
NODAL COORDINATES
    9      30.0         0.0        30.0
MEMBER INCIDENCES
    1    1    2
    2    2    3
    3    3    6
    4    6    9
    5    9    8
    6    8    7
    7    4    7
    8    1    4
    1    1    2    5    4
    2    2    3    6    5
    3    4    5    8    7
    4    5    6    9    8
NUMBER OF CONSTRAINED VERTICES 9
    1111010
    2101010
    3111010
    4101010
    5101010
    6101010
    7111010
    8101010
    9111010
LUMPED MASSES AT VERTEX POINTS
    1    9    .101000E-02
MEMBER PROPERTIES
    1    8    .212000E+01    .000000E+00    .440000E+00    .420000E-01 1.0
0000100004      0.25           1.0            5
MODULUS OF ELASTICITY   30.00
NU   0.30
TIME PARAMETERS
  0.0        2.7        0.0001
LOADING
  0.0        2.7
    1                   562.50
    2                  1125.00
    3                   562.50
    4                  1125.00
    5                  2250.00
    6                  1125.00
    7                   562.50
    8                  1125.00
    9                   562.50
EJECT
```

REFERENCES

1. Turner, M. J., Dill, E. H., Martin, H. C., and Melosh, R. J., "Large Deflections of Structures Subjected to Heating and External Loads," Journal of Aerospace Sciences, Vol. 27, Feb. 1960, pp.97-102, 127.

2. Martin, H. C., "On the Derivation of Stiffness Matrices for the Analysis of Large Deflection and Stability Problems," Proceedings, Conf. on Matrix Methods in Structural Mechanics, (Edited by J. S. Przemieniecki et al), AFFDL-TR-66-80, Wright-Patterson Air Force Base, Ohio, 1966.

3. Oden, J. T., "Finite Element Applications in Nonlinear Structural Analysis," Proceedings of the Symposium on Application of Finite Element Methods in Civil Engineering, November 1969, Vanderbilt University, pp. 419-457.

4. Al-Mawsawi, Q. M., "General Second-Order and Stability Analysis of Rigid Frames," Ph. D. Thesis, University of Wisconsin, 1967.

5. Jennings, A., "Frame Analysis Including Change of Geometry," Journal of the Structural Division, ASCE, Vol. 94, No. ST 3, March 1968.

6. Przemieniecki, J. S., and Purdy, D. M., "Large Deflection and Stability Analysis of Two-Dimensional Truss and Frame Structures," Technical Report AFFDL-TR-68-38, Wright-Patterson Air Force Base, Dayton, Ohio, 1968.

7. Iverson, J. K., "Dynamic Analysis of Nonlinear Elastic Frames," Ph. D. Thesis, Department of Civil Engineering, Michigan State University, 1968.

8. Timoshenko, S., and Woinowsky-Krieger, S., Theory of Plates and Shells, Second Edition, McGraw-Hill Book Co., Inc., New York, 1959.

9. Greene, B. C., "Stiffness Matrix for Bending of a Rectangular Plate Element with Initial Membrane Stresses," Structural Analysis Research Memorandum No. 45, The Boeing Company, Seattle, Wash., August, 1962.

10. Kapur, K. K., "Buckling of Thin Plates Using the Matrix Stiffness Method," Ph. D. Thesis, Department of Civil Engineering, University of Washington, Seattle, Wash., June, 1965.

11. Murray, D. W., and Wilson, E. L., "Finite-Element Large Deflection Analysis of Plates," Journal of the Engineering Mechanics Division, ASCE., Vol. 95, No. EM1, Feb., 1969, pp. 143-165.

12. Brebbia, C., and Connor, J. M., "Geometrically Nonlinear Finite-Element Analysis," Journal of the Engineering Mechanics Division, ASCE., Vol. 95, No. EM 2, April, 1969, pp. 463-483.

13. Zienkiewicz, O. C., and Cheung, Y. K., "The Finite Element Method for Analysis of Elastic Isotropic and Orthotropic Slabs," Proc. Inst. Civ. Eng., 28, 1964, pp. 471-488.

14. McNeice, G. M., "An Elastic-Plastic Finite Element Analysis for Plate with Edge Beams," Proceedings of the Symposium on Application of Finite Element Methods in Civil Engineering, Nov. 1969, Vanderbilt University, pp. 529-566.

15. Weaver, Jr., W., and Oakberg, R. G., "Analysis of Frames with She r Walls by Finite Elements," Symposium on Application of Finite Element Methods in Civil Engineering, Nov. 1969, Vanderbilt University.

16. Timoshenko, S., Theory of Elastic Stability, McGraw-Hill Book Co., Inc., New York, 1936.

17. Argyris, J. H., "Continua and Discontinua," Proc. of the Conf. on Matrix Methods in Structural Mechanics," Dayton, Ohio, 26-28 Oct. 1965, AFFDL-TR-66-80, Nov. 1966.

18. Marcal, P. V., "Finite Element Analysis of Combined Problems of Nonlinear Material and Geometric Behavior," Proc. ASME Joint Computer Conference on Computational Approach to Applied Mechanics, Chicago, 1969.

19. Morris, G. A., and Fenves, S. J., "A General Procedure for the Analysis of Elastic and Plastic Frameworks," S. R. S. No. 305, Department of Civil Engineering, University of Illinois, August, 1967.

20. Khojasteh-Bakht, M., "Analysis of Elastic-Plastic Shells of Revolution under Axisymmetric Loading by the Finite Element Method," Ph. D. Dissertation, Universtiy of California at Berkeley, SESM 67-68, April, 1969.

21. Whang, B., "Elasto-Plastic Orthotropic Plates and Shells," Proceedings of the Symposium on Application of Finite Element Methods in Civil Engineering, Nov. 1969, Vanderbilt University, pp. 481-515.

22. Hill, R., The Mathematical Theory of Plasticity, Oxford University Press, London, 1956.

23. Farhoomand, J. K., Iverson, M., and Wen, R. K., "Dynamic Analysis of Nonlinear Space Frames," Journal of the Engineering Mechanics Division, ASCE, Vol. 96, EM5, Oct. 1970.

24. Toridis, T. G., and Khozeimeh, K., "Inelastic Response of Frames to Dynamic Loads," Journal of the Engineering Mechanics Division, ASCE, Vol. 97, No. EM3, June 1971, pp. 847-863.

25. Akkoush, E. A., Khozeimeh, K., and Toridis, T. G., "Inelastic Deformations of Geometrically Nonlinear Frames," Meeting Preprint 1405, ASCE National Structural Engineering Meeting, Baltimore, Maryland, April 19-23, 1971.

26. McNamara, J. F., and Marcal, P. V., "Incremental Stiffness Method for Finite Element Analysis of the Nonlinear Dynamic Problem," Paper presented at the International Symposium on Numerical and Computer Methods in Structural Mechanics, Urbana, Illinois, September, 1971.

27. Przemieniecki, J. S., Theory of Matrix Structural Analysis, McGraw-Hill Book Co., Inc., New York, 1968.

28. Bogner, F. K., Fox, R. L., and Schmit, L. A., "The Generation of Interelement-Compatible Stiffness and Mass Matrices by the Use of Interpolation Formulas," Proceedings, Conf. on Matrix Methods in Structural Mechanics, (Edited by J. S. Przemieniecki, et al), AFFDL-TR-66-80, Wright-Patterson Air Force Base, Ohio, 1966.

29. Przemieniecki, J. S., "Equivalent Mass Matrices for Rectangular Plates in Bending," AIAA Journal, Vol. 4, No. 5, May, 1966, pp. 949-950.

30. Gallagher, R. H., Gellatly, R. A., Padlog, J., and Mallett, R. H., "A Discrete Element Procedure for Thin-Shell Instability Analysis," AIAA Journal, Vol. 5, No. 1, Jan. 1967, pp. 138-145.

31. Toridis, T. G., and Khozeimeh, K., "Elastic-Plastic Analysis of Three-Dimensional Rigid Frames," Final Technical Report Volume II--Computer Program, NSRDC, Oct. 1970.

32. Volterra, E., and Zachmanoglou, E. C., Dynamics of Vibrations, Charles E. Merrill Books, Inc., Columbus, Ohio, 1965.

33. Adotte, G. D., "Second-Order Theory in Orthotropic Plates," Proceedings, Journal of the Structural Division, ASCE, Vol. 93, No. ST5, Oct., 1967, pp. 343-462.

INITIAL DISTRIBUTION

Copies	
1	DIR OF DEF R & E
2	DNA
2	DNA, FC
2	CNO (OP 75)
1	DIR, USNRL
6	NAVMAT (MAT 0331)
4	NAVSHIPSYSCOM 1 SHIPS 031 1 SHIPS 032 2 SHIPS 2052
1	CO & DIR, USNELC
1	CO, USNCEL
8	NAVSEC 1 SEC 6102 1 SEC 6105 1 SEC 6110 1 SEC 6120 1 SEC 6128 1 SEC 6140 2 SEC 6034B
12	DDC
1	Professor Pedro V. Marcal Division of Engineering Brown University Providence, Rhode Island
1	Professor Robert K. Wen Civil Engineering Dept Michigan State University East Lansing, Michigan

CENTER DISTRIBUTION

Copies	Code	
1	012	R. C. Allen
1	1721	E. G. Fishlowitz
1	1725	R. Jones
1	1727	T. N. Tinley
1	173	A. Stavovy
1	1735	J. C. Adamchak
1	174	R. Short
66	1745	
	3	E. T. Habib
	1	L. R. Hill, Jr.
	6	S. Wang
	1	B. Whang
	1	C. Ng
	1	W. E. Gilbert
	1	W. R. Conley
	1	H. P. Gray
	1	J. M. Ready
	50	T. G. Toridis
1	177	H. Schauer
1	18	G. H. Gleissner
1	1805	E. Cuthill

UNCLASSIFIED

Security Classification

DOCUMENT CONTROL DATA - R & D

(Security classification of title, body of abstract and indexing annotation must be entered when the overall report is classified)

1. ORIGINATING ACTIVITY (Corporate author)	2a. REPORT SECURITY CLASSIFICATION
Naval Ship Research and Development Center Bethesda, Maryland 20034	UNCLASSIFIED
	2b. GROUP

3. REPORT TITLE

Dynamic Analysis of Frame and Plate Structures with Geometric and Material Nonlinearities

4. DESCRIPTIVE NOTES *(Type of report and inclusive dates)*

5. AUTHOR(S) *(First name, middle initial, last name)*

Theodore G. Toridis

6. REPORT DATE	7a. TOTAL NO. OF PAGES	7b. NO. OF REFS
May 1973	133	33

8a. CONTRACT OR GRANT NO.	9a. ORIGINATOR'S REPORT NUMBER(S)
b. PROJECT NO. ZR 02301	Report 3988
c.	9b. OTHER REPORT NO(S) *(Any other numbers that may be assigned this report)*
d.	

10. DISTRIBUTION STATEMENT

APPROVED FOR PUBLIC RELEASE: DISTRIBUTION UNLIMITED

11. SUPPLEMENTARY NOTES	12. SPONSORING MILITARY ACTIVITY
	Naval Ship Research and Development Center

13. ABSTRACT

The objective of this study is the development of a procedure for determining the large dynamic response of structural systems consisting of beam and rectangular plate elements. The analysis takes into account both geometrical and material nonlinearities. The general approach to the problem is based on the finite element method and the use of displacement interpolation functions. The strain energy expressions for both the beam and plate elements are obtained and are used to generate the stiffness and mass matrices of the elements. Also, the geometric stiffness matrices are derived which account for the effect of geometric nonlinearities. Plastic deformations are taken into account by means of an incremental theory of plasticity coupled with the concept of initial strain.

A computer program is developed for the analysis of structures which consist of beam and rectangular plate elements. This program may be used to perform an elastic static, elastic dynamic or plastic dynamic analysis with or without the inclusion of geometric nonlinearity effects. It can also be used to perform a free vibration analysis of a structure, leading to the natural frequencies and modes of vibration. The computer program is used in this study to obtain the solution to several example structures subjected to static or dynamic loads. Results indicate that both geometric and material nonlinearities have an important effect in the deformation of structures composed of beam and plate elements.

14 KEY WORDS	LINK A		LINK B		LINK C	
	ROLE	WT	ROLE	WT	ROLE	WT
Frame and Plate Structures						
Dynamic Response						
Geometric Nonlinearities						
Material Nonlinearities						
Plastic Deformations						
Computer Analysis						